



User Meeting 2020

Book of Abstracts

Contents

"Twisted" Conjugated Molecules as Donor Materials for Efficient All-Small-Molecule Organic Solar Cells Processed with Tetrahydrofuran.....	6
A V δ 3+ subset of MR1 reactive $\gamma\delta$ T cells recognise the side of the MR1 molecule	8
A structural and functional investigation of the periplasmic arsenate-binding protein, ArrX from <i>Chrysiogenes arsenatis</i>	9
Adventures in Biomedical Research Through Synchrotron Science.....	10
An in situ spectro-electrochemical cell for the simultaneous collection of high quality XAS and electrochemical data at low sample loadings: New insights into water oxidation chemistry and quantification of electrochemical effects of X-rays.....	11
An investigation of the T cell response against viruses through a structural lens.....	12
Assessment of bone microarchitecture and mineralisation changes in an animal model of inflammatory bowel disease using high-resolution synchrotron-based microCT.....	13
Asymmetrical Geometrical Distortion Correction Implemented in Python to Correct Cam- era Distortion in High-Resolution X-ray Images.....	15
COVID-19 Research at the MX Beamlines.....	18
Capturing lung health in animal models of ventilator-induced lung injury and cystic fibrosis using 4D X-ray imaging.....	19
Characterization of SARS-CoV-2 peptides presented by Human Leukocyte Antigen molecules.....	22
Chemical Crystallography at the Australian Synchrotron Macromolecular Beamlines.....	23
Coexistence of orthorhombic and tetragonal phases of CuSb ₂ O ₆ over a 750 K temperature range.....	24
Complex fluids and simple experiments - What could we do?.....	25
Coordination crosslinking of helical oligoamide nanorods: controlling independent SSA.....	26
Coupling in vitro cell culture with synchrotron SAXS to understand the bio-interaction of lipid-based liquid crystalline nanoparticles with vascular endothelial cells.....	27
Cubosomes for the Delivery of Biopharmaceuticals.....	28
Data evaluation on the fly: Auto-Rickshaw at the MX beamlines of the Australian Synchrotron.....	29
Deciphering structural interactions between human Plasminogen and the Group A streptococcus PAM protein.....	30
Developing High Pressure Single Crystal Crystallography at MX.....	31
Developing XFM and Rb+ tracing protocols to assess the distribution of important macronutrient, K+, in diseased leaves.....	32
Dual sample analysis on the XFM beamline: a new approach to increase the throughput of analysis of large samples.....	33
Effect of Emulsifier Type on Interfacial Crystallisation.....	35
Effect of surfactant ionicity on critical micelle concentration in aqueous ionic liquid mixtures.....	36
End to end demonstration of an image guided microbeam radiation therapy protocol for in vivo brain tumour radiosurgery at the Australian Synchrotron.....	37
Energy Dispersive X-ray Diffraction for In-Situ and Operando Characterization of Electrochemical Energy Storage Systems.....	38
Experiments on the high-flux BioSAXS beamline: opportunities for dynamic studies of soft matter systems and advanced materials.....	39
Fast-scanning X-ray Diffraction Microscopy (SXDM) at the XFM beamline.....	40
Fluctuation x-ray scattering of self-assembled lipids, colloidal particles and liquids.....	41
Full-field tomography with scattered X-rays.....	42
Further insights into the effect of pH on the fluorescence and structure of green fluorescent protein.....	43
Future upgrade options for the Australian Synchrotron Light Source.....	45
Generalizing small angle scattering form factors for nanostructure characterization.....	46
Generalizing small angle scattering form factors with linear transformations.....	47
Hidden Text: Imaging and reading an ancient tablet in an envelope.....	48
High-pressure and high-temperature XRD and XAS measurements using the MQ D-DIA.....	49
Highly Active Gas Phase Organometallic Catalysis Supported Within Metal-organic Framework Pores.....	50

Hydrothermal design of rGO/TiO ₂ nanocomposite for supercapacitors.....	51
Internal liquid crystal structures in nanocarriers containing drug hydrophobic ion pairs dictate drug release.....	52
Investigation of a 3D-crosslinked nonconjugated Radical Polymer to Tune Electrical Conductivity.....	53
Investigation of etched ion-tracks in SiO ₂ membranes.....	54
Investigation of the Placental Metallome via X-Ray Fluorescence Microscopy: Potential Markers of Placental Health.....	56
Jumping molecular crystals: the role of molecular vibrations.....	58
Laboratory data for astronomical searches of the conformers of crotonaldehyde.....	59
Latest developments and capabilities at the Infrared Microspectroscopy Beamline.....	60
Light on the details: exploring the nano-silver behaviour at the plant-soil interface.....	62
Macrocyclic peptides as the novel chemical probes for modulating the function of the Retromer endosomal trafficking complex.....	64
Materials And Interfacial Design For Advanced Potassium Ion Storage.....	65
Mechanistic insights into functional Electrocatalysis from XAS: the story from Experimental Design to Insights into Electron Transfer Timescales important for Selectivity.....	66
Metal Nanoparticle Radiosensitization for Improving Radiotherapy.....	67
Micro-Computed Tomography (MCT): A BRIGHT new beamline at ANSTO/Australian Synchrotron.....	68
Micro-RNA Target Identification for COVID-19 Through Dynamic PERL Programming.....	69
Microbeams in a heart beat.....	70
Microstructure analysis of Sn/TiO ₂ based hybrid nanostructure material.....	71
Mineral Weathering and Organic Carbon Sequestration in Magnetite Fe Ore Tailings Driven by Organic Matter input and Plant Colonization.....	72
Miscibility Modulation Enables Highly Efficient Polythiophene:Nonfullerene Solar Cells.....	73
Molecular Interplay between SARS-CoV-2 and Human proteins for viral activation and entry, potential drugs and scope of new therapeutics.....	74
Molecular insights into the specificity and potency of metabolite-mediated T-cell immunity.....	75
Molybdenum ditelluride: A high rate anode for sodium-ion battery and full cell prototype study.....	76
Monodisperse Silver Clusters Stabilized by an Organic Network.....	77
New insights into the self-assembly of amphiphilic poly(ethylene glycol-b-caprolactone) diblock copolymers in aqueous solution.....	78
Non-invasive imaging of hydraulic function in leaves, stems and roots.....	80
Novel optics for optimizing the 3rd and 4th Generation Synchrotron Radiation Facility	81
Peering into Batteries: Electrochemical Insight through Operando Methods.....	82
Phase-contrast tomography for breast cancer imaging at Imaging and Medical Beamline of the Australian Synchrotron.....	83
Probing phase transitions of metal-organic frameworks by THz/Far-IR.....	85
Probing the cell wall response of Sphagnum moss to a changing aqueous chemical environment. A synchrotron infrared microscopy study.....	86
Protein-Lipid interactions and protein structures in multi-component systems.....	87
Pulling Milk Lipids Apart and Putting Them Back Together Again – A Self-assembly Approach.....	88
Quantification of Material Gradients in Nanocrystals.....	90
Quantitative Determination of Protein Solubility in Ionic Liquids.....	92
Resonant Tender X-ray Diffraction for Disclosing the Molecular Packing of Paracrystalline Conjugated Polymer Films.....	93
Robust Biomimetic Ti ₃ C ₂ T _x MXene Films for High Performance Applications.....	94
Role on Methylammonium Lead Bromide on Microstructure, Photophysics, and Device Performance in Triple Cation based Perovskite Solar Cells.....	95
Rotary Computed Laminography and Tomosynthesis geometries using ASTRA Toolbox.....	96
Separating Macro- and Nano-structural Effects in Intensity Correlation Measurements of Self-assembled Lipid Materials.....	97
Serial crystallography at the Australian Synchrotron.....	98

Side-reaction-free direct arylation polycondensation of chlorinated thiophene derivatives to high mobility conjugated polymers.....	99
Soft x-ray studies of molecular nanoarchitectures.....	100
Soil carbon research from past, present and future using synchrotron-based techniques.....	101
Solvent properties of protic ionic liquid-water mixtures, and their application to biological molecules.....	102
Speckle-Based Dark-Field Tomography of a Phase Object.....	103
Spectroscopic Studies of Brain Zinc Homeostasis and Its Role During Cognitive Decline and Ageing.....	105
Structural characterisation of influenza epitopes presented by dominant Indigenous Australian Human Leukocyte Antigens.....	107
Structural characterisation of mitochondrial complex IV assembly factors.....	108
Structural plasticity between homo and heterodimeric IRF4-DNA Interactions.....	110
Structural studies of G protein-coupled receptors – implications for drug discovery.....	111
Synchrotron Powder Diffraction to disclose effect of catalyst phase change on CO ₂ reduction.....	112
Synchrotron macro ATR-FTIR: where we are and what's next for live-cell measurement.....	113
Synchrotron-based X-ray diffraction and spectroscopy for metal-ion battery material studies.....	115
Synthesis and structure of ALaTiO ₄ and A ₂ La ₂ Ti ₃ O ₁₀ (A = Na ⁺ , K ⁺) Ruddlesden-Popper type photocatalysts.....	116
Synthesis of Single Atoms Metal Supported on Carbon Materials.....	118
Tableting of human milk and colostrum and its impact on digestion kinetics and lipid self- assembly during digestion.....	119
The Evolution of Electronic Complexity in Biology: 2p3d and 1s3p RIXS of Iron-Sulfur Clusters.....	121
The Structure and Air Stability of Calcium and Magnesium Intercalated Graphene on 6H- SiC(0001).....	122
The design of Metal-Organic Frameworks using flexible and extendable tetra-carboxylic acid linkers enriched with embedded cyclohexyldiamine.....	124
The effect of fat content on the solubilization of halofantrine in infant formula during in vitro intestinal digestion.....	125
The effect of surfactant type on the secondary crystallisation of milk fat at the oil-water interface.....	127
The impact of microbeam irradiation on spinal cord function.....	128
The use of synchrotron X-ray fluorescence microscopy to study the “battle for nutrients” between plant and pathogen.....	129
Towards Personalized Microbeam Radiation Therapy for Brain Cancer Treatment.....	130
Trace element distributions in Al-Zn based coating alloys on steel substrates investigated by synchrotron XFM.....	132
Tracks, Pores, Cylinders and Cones: SAXS as a tool to study high-energy ion modified materials.....	133
Trindex: A complimentary grain mapping technique using neutron imaging.....	134
Using Synchrotron Radiation to map the Metallo-maze to memory loss.....	136
Understanding disorder in the Y ₂ Sn ₂ -xZrxO ₇ pyrochlore oxides.....	137
Understanding the Mechanisms Bending in Flexible Crystals.....	139
Unexpected Structural Properties in 4d and 5d Metal Oxides.....	140
Using Synchrotron Sourced Microscopy to Explore Fingermark Chemistry.....	142
Using synchrotron XFM, LA-ICP-MS and stable isotopes to identify an intense wildfire event recorded in a speleothem.....	144
Using synchrotron infrared micro-spectroscopy to monitor the electrochemical processes of non-flammable electrolytes on the electrode surface.....	145
Using the Imaging and Medical Beamline (IMBL) as a novel method to investigate structures and processes of lead-acid batteries.....	146
Using the Pair Angle Distribution Function for Analysing Protein Structure.....	148

Visualisation of the rapid Cu ₆ Sn ₅ lithium-ion battery anode fabrication process via real- time X-ray imaging.....	149
X-ray absorption spectroscopy studies of mixed metal-antimony oxide water oxidation catalysts: Studies comparing Sb, Mn, Co, and Ru edges.....	150
XFM analysis of marsupial teeth - insights into life, growth and reproduction.....	151
“Wax On – Wax Off” Using Infrared Reflectance for minimally invasive in vivo monitoring of changes in leaf epicuticular waxes.....	152

"Twisted" Conjugated Molecules as Donor Materials for Efficient All-Small-Molecule Organic Solar Cells Processed with Tetrahydrofuran

Xiafei Cheng; Miaomiao Li; Yanhou Geng

Corresponding Author(s): chengxiafei@tju.edu.cn, yanhou.geng@tju.edu.cn, miaomiao.li@tju.edu.cn

High-performance organic semiconductors that can be processed with environmentally benign solvents are highly desirable for printable optoelectronics. Therefore, it is of critical importance to develop the photoactive materials that are readily soluble in "greener" solvents and meanwhile have appropriate aggregation behavior to ensure proper phase separation and ordered molecular packing in BHJ films. In principle, the solubility of conjugated molecules can be enhanced via twisting their conjugated backbones from planarity. However, "over-twist" is detrimental to the close intermolecular packing, resulting in poor charge transport properties in film state. The ideal case is that the molecules adopt twisted backbones in solution but ordered molecular packing in film state. Herein, four acceptor-donor-acceptor conjugated molecules, i.e., DRTT-T, DRTT-R, DRTT-OR and DRTT, with 3-ethylrhodanine as acceptor terminal units and 2,5-bis(4,8-di(5-(2-ethylhexyl)thiophen-2-yl)benzo[1,2-b:4,5-b']dithiophen-2-yl)thieno[3,2-b]thiophene derivatives as donor units were synthesized. 5-(2-Ethylhexyl)thiophen-2-yl, 2-ethylhexyl and 2-ethylhexyloxy were introduced to the β -positions of the central thieno[3,2-b]thiophene (TT) units in DRTT-T, DRTT-R and DRTT-OR, respectively, and unsubstituted TT was used as the central unit in DRTT. As revealed by density functional theory calculations, DRTT-OR and DRTT adopt almost planar geometry, while DRTT-T and DRTT-R have "twisted" backbones due to the introduction of bulky substituents on TT units. Differing from DRTT-OR and DRTT which are only well-soluble in chlorinated solvents such as chloroform, DRTT-T and DRTT-R also show high solubility in "greener" solvents, including toluene and tetrahydrofuran (THF). Packing structures of the molecules in thin films were investigated by X-ray diffraction (XRD). The molecules (DRTT and DRTT-OR) with relatively planar structures self-organized very fast in the film forming process. The introduction of bulky substituents on TT unit improves the solubility of the molecules but retards the formation of ordered films due to the steric hindrance caused by the substituents. However, ordered nanostructures in which the molecules adopt planar geometry could be formed facilitated by the strong intermolecular π - π interaction, once self-organization time is long enough (SVA gave enough time for the self-organization of the molecules).

Non-fullerene small molecule (NFSM) organic solar cells (OSCs) were fabricated with these molecules as donor materials. The power conversion efficiencies (PCEs) of DRTT-T and DRTT-R based devices processed with THF reached 9.37% and 10.45%, respectively.

A V δ 3+ subset of MR1 reactive $\gamma\delta$ T cells recognise the side of the MR1 molecule

Michael Rice¹ ; Wael Awad¹ ; Richard Berry¹ ; Jerome Le Nours¹ ; Nicholas Gherardin² ; Dale Godfrey² ; Benjamin Gully¹ ; Jamie Rossjohn¹

¹ Monash University

² Department of Microbiology and Immunology, Peter Doherty Institute for Infection and Immunity, University of Melbourne, Melbourne, Victoria 3000, Australia.

Corresponding Author(s): michael.rice@monash.edu

T cells are broadly categorised by their expression of either an $\alpha\beta$ or $\gamma\delta$ T cell receptor (TCR). Whilst $\alpha\beta$ T cells are comprehensively understood $\gamma\delta$ T cells are ill-defined but are increasingly realised to be an important T cell subset that display both innate- and adaptive-like immune functions. The MHC class 1 related protein (MR1), presents bacterial vitamin B metabolites to $\alpha\beta$ mucosal associated invariant T cells (MAIT). MAIT cell TCR' bind atop MR1 in a conventional fashion, contacting the α 1 and α 2 helices which comprise the MR1 antigen presenting pocket, as well as contacting the ligand directly. Recently, published in Science we identified that $\gamma\delta$ T cells recognised MR1 but did so irrespective of the ligand being presented. Analysis of a V δ 1+ $\gamma\delta$ TCR in complex with MR1 revealed, an unusual docking mode binding underneath the MR1 antigen presenting groove. This was in stark contrast to the conventional MAIT TCR-MR1 interactions and all other TCR complex structures to date. Here, we present biochemical and structural analysis of a V δ 3+ MR1 restricted TCR which bound along the side of MR1, adopting another novel TCR docking topology and making no contacts with the presented antigen. Ultimately, our results expand the knowledge of MR1 restricted $\gamma\delta$ TCR's shedding further light on the unusual docking modes that $\gamma\delta$ TCR's likely employ more broadly.

A structural and functional investigation of the periplasmic arsenate-binding protein, ArrX from *Chrysiogenes arsenatis*

Nilakhi Poddar ; Consuelo Badilla ; Shadi Maghoo ; Thomas H Osborne ; Joanne Santini ; Megan Maher¹

¹ A/Prof

Arsenic is a toxic metalloid found both naturally in the environment and as a harmful pollutant generated from industrial waste waters and gold mines. Arsenic can exist in both organic and inorganic forms and in four oxidation states: arsines and methyl arsines (As^3^-), elemental arsenic (As^0), arsenite (AsO_3^{3-}) and arsenate (AsO_4^{3-}). Although arsenic is toxic and hazardous to human health, some prokaryotes have developed unique mechanisms that utilise inorganic forms of arsenic, such as arsenite (AsO_3^{3-}) and arsenate (AsO_4^{3-}) for respiration [2].

Such prokaryotes include *Rhizobium* NT-26 and *Chrysiogenes arsenatis* which utilise the arsenite oxidase enzyme (Aio) and the arsenate reductase enzyme (Arr), respectively for their crucial respiratory activities. In these bacteria, the periplasmic binding proteins (PBPs) AioX and ArrX bind to arsenite (AsO_3^{3-}) and arsenate (AsO_4^{3-}), respectively and trigger, through sensor histidine kinase signalling, the expression of their respective respiratory enzymes [3]. The structure of the AioX protein has been previously reported in the presence and absence of arsenite (AsO_3^{3-}) [4]. In order to investigate the structural basis of arsenate (AsO_4^{3-}) binding to the ArrX protein, we determined its crystal structure in the presence and absence of substrate. This presentation will describe the structure of ArrX and a structural comparison between it and that of the AioX protein, in order to determine the molecular mechanisms by which these proteins discriminate between the chemically similar substrates arsenate (AsO_4^{3-}) and arsenite (AsO_3^{3-}).

Keywords: arsenate, *Chrysiogenes arsenatis*, periplasmic binding protein (PBP), X-ray crystallography.

References:

- [1] Brinkel, K.K. et al. (2009). Int. Journal of Environmental Research and Public Health 6: 1609- 1619.
- [2] Gadd et al. (2000). Current opinion in biotechnology 11: 271-279.
- [3] Stolz JF, Basu P, Oremland RS (2002) Microbial transformation of elements: the case of arsenic and selenium. Int Microbiol 5: 201-7
- [4] Badilla et al. (2018). Scientific reports 8: 6282.

Adventures in Biomedical Research Through Synchrotron Science

Peter Lay¹

¹ *The University of Sydney*

Corresponding Author(s): peter.lay@sydney.edu.au

Peter A. Lay

School of Chemistry and Sydney Analytical, the University of Sydney

With each decade of my research in synchrotron science that began in the mid 1990's came multiple new developments in beamline technologies that made experiments in biomedical research possible that could only be dreamed about a short time beforehand. This, in turn, opened up many new possibilities in groundbreaking biomedical research that have placed synchrotron science at the forefront of providing previously inaccessible information on mechanisms of both disease processes and drug treatments.

In this lecture, I will discuss key developments and applications of synchrotron science in areas such as: (i) the use of multiple scattering analysis of EXAFS for 3D structural information on un- stable proteins and species related to understanding protein structure, and mechanisms of disease processes; (ii) XANES for probing metaldrug speciation under biologically relevant conditions; (iii) XFM and micro-XANES for understanding the biodistributions and speciation of elements in cells and tissues related to the roles of metals in diseases and the development of new metallodrugs; and (iv) the use of infrared microscopy to understand changes in the biochemistry of cells and tissues to provide information on the mechanisms of disease processes (brain, cardiovascular, etc.) and their treatments.

An in situ spectro-electrochemical cell for the simultaneous collection of high quality XAS and electrochemical data at low sample loadings: New insights into water oxidation chemistry and quantification of electrochemical effects of X-rays

Hannah King¹; Maxime Fournier²; Shannon Bonke²; Bernt Johannesson³; Peter Kappen⁴; Alexandr Simonov²; Rosalie Hocking⁵

1 James Cook University

2 Monash University

3 Australian Synchrotron

4 Australian Nuclear Science and Technology Organisation, 800 Blackburn Road, Clayton, VIC 3168, Australia

5 Swinburne University of Technology

Corresponding Author(s): shannon.bonke@monash.edu, hannah.king1@my.jcu.edu.au, alexandr.simonov@monash.edu.au, rhocking@swin.edu.au, peter.kappen@ansto.gov.au

Herein, we report the development of a spectroelectrochemical in situ cell for the simultaneous collection of high quality XAS and high quality electrochemical data – even at low sample loadings. A cobalt oxide (CoOx) water oxidation ($2\text{H}_2\text{O} \rightleftharpoons 4\text{H}^+ + \text{O}_2 + 4\text{e}^-$) electrocatalysts and nickel oxide (NiOx) electrocatalyst were used to benchmark the cell. The cell was sufficiently sensitive to quantify the electrochemical effects of the beam, and to measure phenomenon such as beam photo-reduction and photo-oxidation. The effects of photo-damage only became apparent in the XAS data when sample concentration was very low ($<15 \text{ nM cm}^{-2}$). At higher sample loadings, the sensitivity of the electrochemical cell allowed the electrochemical effects of the beam (such as photo-damage) to be partially compensated for by measuring the electrical contribution of the beam using the electrochemical system. During the course of benchmarking the new spectroelectrochemical cell, new types of photo-damage effects relevant to in situ electrochemical studies were investigated, namely beam mediated photo-deposition. The spectral differences between thick and thin CoOx films taken as a function of applied potential were used to provide new insights into the timescales of electro-chemical processes important for water oxidation catalysis.

An investigation of the T cell response against viruses through a structural lens

Stephanie Gras¹

¹ *Monash University*

Corresponding Author(s): stephanie.gras@monash.edu

T cells are a critical part of the immune response, that would determine the fate of an infection and disease outcome. Our Lab is focused on understanding how T cell engage with viral particles, called peptide antigens, that are presented by highly polymorphic molecules called Human Leukocyte Antigens (HLA). T cells have receptors on their surface called T cell receptor (TCR) that allow them to recognise the composite surface of the peptide-HLA complex.

Using X-ray crystallography we are seeking to understand both peptide antigens presentation as well as TCR recognition, both important to determine the quality of the subsequent immune response. This allow us to understand the response towards influenza and HIV viruses, and more recently SARS-cov-2 virus. The molecular and biophysical features of the peptide antigens help us map the regions of the virus that are recognised by T cells, as well as determining the most stable and potent antigens that represent attractive target for therapeutics.

Assessment of bone microarchitecture and mineralisation changes in an animal model of inflammatory bowel disease using high-resolution synchrotron-based microCT

Damian Myers¹; Chris Hall²; Ahmed Al Saedi³; Ali Ghasem-Zadeh⁴; Shilpa Sharma³; Sara Vogrin⁴; Rhiannon Filippone⁵; Anton Maksimenko²; Daniel Hausermann²; Kulmira Nurgali⁶; Gustavo Duque³

1 The University of Melbourne and the Australian Institute for Musculoskeletal Science (AIMSS)

2 ANSTO, The Australian Synchrotron 3 University of Melbourne and AIMSS 4 University of Melbourne

5 Victoria University

6 Victoria University and AIMSS

Corresponding Author(s): ahmed.mohan@unimelb.edu.au,
anton.maksimenko@synchrotron.org.au, alihrpqct@gmail.com, rhiannon.filippone@live.vu.edu.au,
daniel.hausermann@synchrotron.org.au, kulmira.nurgali@vu.edu.au, damianem@unimelb.edu.au
chris.hall@synchrotron.org.au, gustavo.duque@unimelb.edu.au, shilpas@student.unimelb.edu.au

Background: The Winnie-muc2 mouse (C57BL/6 background) exhibits pathophysiology of inflammatory bowel disease and other organ system changes, providing an opportunity to study bone loss related to malabsorption and other factors. We hypothesised that both bone microstructure and mineralisation may differ in Winnie-muc2 mice so performed temporal studies using high-resolution synchrotron-based microCT (HR-S-uCT).

Aim: To characterise cortical and trabecular metrics in Winnie-muc2 vs C57BL/6 mice including bone volume, bone mineral density (BMD) and other ultrastructural parameters.

Methods: Male and female animals (4-7/group) were euthanised after cardiac perfusion (4% PFA) at 6, 14 and 24 wks and femurs harvested then stored in 10% formol saline. MicroCT images were acquired at the Australian Synchrotron (25keV beam, 1800 projections, 6.82 μ m isotropic volumes, at 2-3 mm below condyls). Volumes were reconstructed using X-TRACT (CSIRO), trimmed using Image-J and processed using the BMA module in Analyze14.0 (Mayo Clinic).

Results:

In Winnie-muc2 males (vs C57BL/6), whole Bone Volume (Ctx+Tb) was 26% lower at 24 wks (0.99mm³, IQR 0.82-1.155 vs 1.34 mm³, IQR 1.28-1.39 p=0.021) and in Winnie-muc2 females (vs C57BL/6 females), whole BV was less at 14 and 24wks (21% p=0.011, and 9% p=0.021, respectively) with both female groups decreasing over time.

Tb vBMD was sustained over time for all groups but Tb Tissue vBMD (Tb+IntraTb) was lower at 14 and 24wks in Winnie-muc2 males (vs C57BL/6 males p=0.047 and 0.021) and at 14 wks in females (vs C57BL/6 females; p=0.033).

Tb Tissue BMD in Winnie-muc2 males (vs C57BL/6 males) was 21% less at 14 wks (155 mg/cc, IQR 131-173 vs 203 mg/cc, IQR 175-215 $p=0.043$) and 32% less at 24wks (116 mg/cc, IQR 105-128 vs 174 mg/cc, IQR 168-175, $p=0.021$). In females, both C57BL/6 and Winnie-muc2 showed similar temporal decreases over 6 to 24wks (both $p=0.021$).

Whilst Tb BMD was sustained in Winnie-muc2 and C57BL/6 males, C57BL/6 females showed an increase from 6 to 24wks ($p=0.021$), however, the Winnie-muc2 group did not change over time ($p>0.05$), indicating compromised mineralisation of trabeculae in female Winnie-muc2.

Conclusion: HR-S-uCT analysis reveals microarchitectural and BMD changes in the Winnie-muc2 that highlight the value of this model to study bone microarchitecture. This model exhibits severe bone loss and altered mineralisation and, through the capabilities of the Australian Synchrotron, will enable the study of mechanisms and potential treatments for diverse bone lytic diseases.

Asymmetrical Geometrical Distortion Correction Implemented in Python to Correct Camera Distortion in High-Resolution X- ray Images.

Jayan Gunasekera¹ ; Marcus Kitchen² ; Kentaro Uesugi³ ; Greg Falzon⁴ ; Peter Quin⁵ ; Konstantin Pavlov¹

1 University of Canterbury

2 Monash University

3 Japan Synchrotron Radiation Research Institute

4 Flinders University

5 University of Tasmania

Corresponding Author(s): kag95@uclive.ac.nz, marcus.kitchen@monash.edu

X-ray detectors using CMOS or CCD sensors are commonly employed for imaging in synchrotron facilities around the world [1]. However, these sensors are typically smaller than the required field of view. Thus, lenses or Fibre Optic Tapers (FOTs) are commonly used to couple the sensor chip to the scintillator. While both coupling methods have advantages and disadvantages, their common characteristic is the geometrical distortion presented in the image. Image distortions observed in lens coupling systems are typically radially symmetric (barrel or pincushion distortions) due to the symmetry of the lens design [2]. However, the image distortion in FOT coupling systems are asymmetrical. While, there have been developments in software to correct symmetric distortions to a higher degree [2], there is a lack of open-source software for the correction of asymmetrical distortion. Here, we present a Python-based software, which is capable of correcting asymmetrical distortion with a high degree of accuracy.

Our primary aim is to reconstruct the Ultra Small Angle Scattering (USAXS) 3D image of a high- scatter sample (finely sieved soil) using Tilted Laue Analyser-Based Imaging (TLABI). TLABI enables the extraction of 2D information about the phase gradient [3] and USAXS. A FOT coupled detector was used for the acquisition of our images, requiring the correction of distortion before the USAXS image reconstruction. As a solution to asymmetrical distortion, Islam et al. (2010) [4] investigated global polynomial fitting, local polynomial fitting and triangulated interpolation. They concluded that triangulated interpolation, implemented using the Warp_tri function from the commercially available program Interactive Data Language (IDL; Harrison Geospatial Solutions), produced the best results. Previous studies have used the Warp_tri function successfully [3,5].

As Python is becoming the most widely used language for data analysis, we have developed a Python program which implements triangulated interpolation to correct the FOT distortion with an even higher accuracy than IDL's Warp_tri with similar processing speeds. Our method essentially implements piecewise affine transformation (PWA) using a set of control points (a map of the distortion) [6]. Delaunay triangulation is used to divide the image using the control points as vertices of each triangle. Then an affine transform matrix for each triangle is calculated between the distorted and undistorted triangle using the coordinates of the vertices of these triangles. Each pixel in each triangle is then mapped onto an empty image of the same size correcting the distortion. Scikit-image [7] have an implementation of this method. However, this implementation took one and half hours to correct the distortion of a single high resolution (4000×2672 pixel) X-ray image using a computer with intel core i7-9700 @3.00GHz processor and 32GB RAM. Also, its output was considerably less accurate compared to IDL's Warp_tri output. We then implemented PWA using Python's OpenCV

[8] computer vision library's inbuilt modules. OpenCV is written in C/C++, specifically for the purpose of computer vision. This allowed our implementation to correct the distortion in a 4000×2672 -pixel X-ray image under 8 seconds. For a corrected sample grid image, IDL's Warp_tri and our method gave average root mean square errors (of 1448-pixel rows) of 10.7×10^{-2} and 0.323×10^{-2} , respectively. Though PWA is not widely used for X-ray image distortion correction, it is commonly used in computer vision for image registration and facial warping [9,10]. This new software provides a highly accurate, high speed solution for correcting distortions in images of any type, which is of particular importance for image reconstruction in X-ray imaging and tomography.

References

- K. Uesugi, M. Hoshino, and N. Yagi, 'Comparison of lens- and fiber-coupled CCD detectors for X-ray computed tomography', *J. Synchr. Rad.*, vol. 18, pp. 217–23, Mar. 2011, doi: 10.1107/S0909049510044523.
- N. T. Vo, R. C. Atwood, and M. Drakopoulos, 'Radial lens distortion correction with sub-pixel accuracy for X-ray micro-tomography', *Opt. Express*, vol. 23, no. 25, p. 32859, Dec. 2015, doi: 10.1364/OE.23.032859.
- M. C. Chalmers, M. J. Kitchen, K. Uesugi, G. Falzon, P. Quin, and K. M. Pavlov, 'Tomographic Reconstruction using Tilted Laue Analyser Based X-ray Phase-Contrast Imaging', *J. Synchr. Rad* (in press) (arXiv:2007.10520), 2020.
- M. S. Islam, R. A. Lewis, K. Uesugi, and M. J. Kitchen, 'A high precision recipe for correcting images distorted by a tapered fiber optic', *J. Inst.*, vol. 5, no. 09, pp. P09008–P09008, Sep. 2010, doi: 10.1088/1748-0221/5/09/P09008.
- M. J. Kitchen et al., 'X-ray phase, absorption and scatter retrieval using two or more phase contrast images', *Opt. Express*, vol. 18, no. 19, p. 19994, Sep. 2010, doi: 10.1364/OE.18.019994.
- T. F. Cootes and C. Taylor, 'Statistical Models of Appearance for computer vision', Apr. 2004.
- S. van der Walt et al., 'scikit-image: image processing in Python', *PeerJ*, vol. 2, p. e453, Jun. 2014, doi: 10.7717/peerj.453.
- G. Bradski, 'The opencv library', *Dr Dobb's J. Software Tools*, vol. 25, pp. 120–125, 2000.
- A. Davison, W. Merghani, C. Lansley, C.-C. Ng, and M. H. Yap, 'Objective micro-facial movement detection using face-based regions and baseline evaluation', in *2018 13th IEEE international conference on automatic face & gesture recognition (FG 2018)*, 2018, pp. 642–649.

D. Chen, Q. Chen, J. Wu, X. Yu, and T. Jia, 'Face Swapping: Realistic Image Synthesis Based on Facial Landmarks Alignment', Mathematical Problems in Engineering, vol. 2019, p. 8902701, Mar. 2019, doi: 10.1155/2019/8902701.

COVID-19 Research at the MX Beamlines

Author(s): Eleanor Campbell¹

Co-author(s): All Australian Synchrotron Staff

¹ ANSTO

Corresponding Author(s): campbele@ansto.gov.au

From March 2020, the Australian Synchrotron joined the rest of Victoria in COVID-19 lockdown, severely limiting the access to beamlines by staff and users. The MX beamlines stayed operational under a COVID-19 Rapid Access scheme, developed to facilitate research into the SARS-Cov-2 virus. A number of user groups pivoted their research interests to include SARS-Cov-2 proteins, and human proteins involved in the virus's progression and transmission. In this talk, we present a general overview of the COVID-19 Rapid Access program, some examples of research carried out using this beamtime, and the plans for supporting COVID-19 research in an ongoing capacity.

Capturing lung health in animal models of ventilator-induced lung injury and cystic fibrosis using 4D X-ray imaging

Author(s): Melissa Preissner¹

Co-author(s): Martin Donnelley²; Freda Werdiger³; Yong Song⁴; Ella Smalley⁴; Patricia Cmielewski²; Darren Thompson⁵; Mitzi Klein⁶; Clare Scott⁶; Anton Maksimenko⁶; Chris Hall⁶; Daniel Hausermann⁶; David Parsons²; Graeme Zosky⁴; Stephen Dubsy¹; Kaye Morgan¹

1 Monash University

2 University of Adelaide 3 Melbourne Brain Centre 4 University of Tasmania 5 CSIRO

6 ANSTO

Corresponding Author(s): david.parsons@adelaide.edu.au, kaye.morgan@monash.edu, ella.smalley@utas.edu.au, mitzik@ansto.gov.au, graeme.zosky@utas.edu.au, stephen.dubsy@monash.edu, christoh@ansto.gov.au, antonm@ansto.gov.au, martin.donnelley@adelaide.edu.au, yong.song@utas.edu.au, freda.werdiger@unimelb.edu.au, danielh@ansto.gov.au, clares@ansto.gov.au, darren.thompson@csiro.au, melissa.preissner@monash.edu, patricia.l.cmielewski@adelaide.edu.au

Introduction:

Lung disease, including chronic respiratory conditions and thoracic cancers, is Australia's second leading cause of death [1]. Furthermore, the current COVID-19 pandemic has acutely highlighted the importance of understanding acute respiratory distress syndrome and mechanical ventilation. Lung health is typically measured in the clinic by functional measures such as spirometry and structural measures from CT images, but neither can identify regional changes in lung function. The regional manifestation of lung disease and the dynamic nature of the lung means that experimental in vivo 4D X-ray imaging is ideal for detailed analysis of the lung in health and disease. The imaging and medical beamline (IMBL) at the Australian Synchrotron provides a wide, monochromatic X-ray beam, with suitable flux for high-speed in vivo imaging of small animals such as mice and rats. Here, we demonstrate the methods and preliminary results from two studies of dynamic lung imaging and X-ray velocimetry (4DXV) [2] analysis of mouse models of ventilator-induced lung injury and rat models of cystic fibrosis-like lung disease.

Methods:

The X-ray beam was set to an energy of 25 - 30 keV, with exposure lengths of between 0.02 - 0.04 seconds, suitable for the imaging of lung tissue in either mice or rats (respectively). The sample- to-detector distance was 3 metres, for capturing propagation-based phase contrast images of the lungs. Animals were anaesthetised, surgically intubated (according to University of Tasmania and University of Adelaide animal ethics committee approvals), and attached to a small animal ventilator (4DMedical) to acquire breath-cycle gated images.

A four-dimensional computed tomography image acquisition was conducted with 12133 projection images of the lungs captured over a 182 degree rotation for one 4DCT scan.

This resulted in 15 phases (CT images) in the 4DCT sequence and took 3.5 - 11 minutes, depending on the mechanical ventilation rate. The Ruby X-ray detector was used with a pixel size of between 19 - 24 μ m. The X-ray beam width (field-of-view) was set to either 2.4 cm (for mouse lungs) or 4 cm (for rat lungs).

Projection images were captured as hierarchical data format version 5 (hdf5) and binned into the phases of the breath cycle on the Australian Synchrotron's computing infrastructure environment (ASCI). Customised code provided integration of the projection images with the CSIRO X-TRACT CT reconstruction software [3], whereby images were reconstructed using the transport-of-intensity equation (TIE) phase retrieval algorithm [4]. The reconstructed CTs from both studies were transferred to MASSIVE, a dedicated computing cluster environment for image processing and visualisation [5], and the 4DXV analysis [2] was applied to the data.

Results:

An example of a resulting CT of a mouse lung is shown as a slice image in panel (c) of the figure. 4DXV results are shown in the figure from a normal rat (a) before, and (b) after delivery of sterile agar beads into a single lobe of the lung. The colour bar represents the lung tissue expansion (in voxels), whereby the dark blue region indicates a region of low expansion, due to the agar beads blocking the airways, in a similar manner to the mucus obstructions that are a hallmark of cystic fibrosis disease. Panel (c) shows the lung detail from a CT slice of mouse lungs from the ventilator-induced lung injury study, taken at the beginning of mechanical ventilation, with a peak inspiratory pressure of 12 cmH₂O and zero positive end-expiratory pressure. The scale bar represents 2 mm. The anatomical detail of the lung can be seen as airways (1), blood vessels (2), lobe fissures (3) and fat and muscle layers (4).

Conclusions:

We have successfully performed dynamic in vivo CT imaging and 4DXV analysis of lungs on the Australian Synchrotron IMBL. We have investigated two pre-clinical models: a rat model of cystic fibrosis-like disease, and a mouse model of ventilator-induced lung injury. In addition to the on-going studies of ventilator-induced lung injury, new pre-clinical studies are planned for testing the efficacy of novel drugs for the treatment of antibiotic-resistant bacterial lung infections.

Acknowledgements: MASSIVE HPC facility (www.massive.org.au), ARC DECRA (SD), ARC Future Fellowship (KM), NHMRC APP1160774 (GZ, KM, SD), NHMRC APP1160011 (DP, MD, KM),

Australian Synchrotron beamtime grants (14690, 11727, 12061, 12926).

Keywords: 4DCT, X-ray velocimetry, small animal imaging, lung imaging, mechanical ventilation, ventilator-induced lung injury, cystic fibrosis.

References:

Australian Bureau of Statistics – Australia's leading causes of death, 2016.

Dubsky S, Hooper S, Siu KKW, and Fouras A, "Synchrotron-based dynamic computed tomography of tissue motion for regional lung function measurement". *J. R. Soc. Interface* 9, 2213-2224, 2012.

Gureyev TE, Nesterets Y, Ternovski D, Thompson D, Wilkins SW, Stevenson AW, Taylor JA, "Tool-box for advanced X-ray image processing. *Advances in Computational Methods for X-Ray Optics II*", 8141, 1-14, 2011.

Paganin, D, Mayo SC, Gureyev TE, Miller PR, and Wilkins SW. "Simultaneous phase and amplitude extraction from a single defocused image of a homogeneous object." *Journal of microscopy* 206, no. 1: 33-40, 2002.

Goscinski, WJ, Hines C, McIntosh P, Bambery K, Felzmann U, Hall C, Maksimenko A, Panjkar S, Paterson D, and Tobin M. "MASSIVE: An HPC Collaboration To Underpin Synchrotron Science." 15th International Conference on Accelerator and Large Experimental Control Systems (ICALEPCS 2015), Melbourne, 2015.

Characterization of SARS-CoV-2 peptides presented by Human Leukocyte Antigen molecules

Christopher Szeto¹ ; Demetra S. M. Chatzileontiadou¹ ; Emma J. Grant¹ ; Andrea Nguyen¹ ; Dhillshan Jayasinghe¹ ; Hanim Halim¹ ; Alan Riboldi-Tunnicliffe² ; Stephanie Gras³

1 Department of Biochemistry and Molecular Biology, Biomedicine Discovery Institute, Monash University, Clayton, VIC, Australia

2 Australian Synchrotron

3 Biomedicine Discovery Institute, Monash University. ARC Centre of Excellence in Advanced Molecular Imaging, Monash University.

Corresponding Author(s): chris.szeto@monash.edu, dimitra.chatzileontiadou@monash.edu, alan.riboldi@synchrotron.org.au, stephanie.gras@monash.edu, noor.halim@monash.edu, andrea.nguyen@monash.edu, dhillshan.jayasinghe@monash.edu, emma.grant@monash.edu

To date, the COVID-19 pandemic has claimed 970,000 lives and afflicted more than 31 million individuals. Although a global effort has been enacted for vaccines and drug discovery, our rudimentary understanding of SARS-CoV-2 infection and our own immune defense against this infection remains unclear. Our immune system can naturally overcome viral infection through the presentation of viral protein fragments or peptides (p) via human leukocyte antigen (HLA) molecules. These peptide-HLA complexes (pHLAs) are recognized by cytotoxic T cells that can activate, proliferate, and kill infected cells. T cells also retain memory of their encounter with the virus, and will respond faster during re-infection. How peptides are presented on the cell surface by HLA molecules impact T cell recognition and influence the outcome of viral clearance, and therefore, outcome of the disease. Although SARS and SARS-CoV2 cause severe acute respiratory syndrome, other coronavirus strains (229E, OCE43, HKU1, and NL63) only cause the common cold. These coronaviruses share similar peptide sequences that can be presented by HLAs, meaning that prior exposure to a less severe strain of coronavirus may infer immunity via memory T cells if similar peptides are presented in the same structural fashion. Using protein crystallography and X-ray diffraction at the Australian Synchrotron, we have characterized the presentation of SARS-CoV-2 peptides, which could influence vaccine strategies and provide a basis for research in T cell therapy.

Chemical Crystallography at the Australian Synchrotron Macro- molecular Beamlines

Jason Price

Corresponding Author(s): jason.price@ansto.gov.au

The macromolecular (MX) beamlines at the Australian Synchrotron are mixed use between the structural biology (PX) and chemical crystallography (CX) communities. Since commissioning the high throughput MX1 bending magnet and the MX2 microfocus undulator beamlines have proven very successful for both communities.

With the deployment of upgrades to the optics, endstation and detectors, the beamlines are able to produce data at an astounding rate with high throughput crystallography the norm. For the calendar year of 2019, 51 million Eiger 16M frames were collected on MX2 equating to ~5 Petabytes of uncompressed data.

This increase in throughput necessitates the development of tools to give rapid feedback on data quality. There has also been the opportunity to develop automated collection of multiple CX datasets. An overview of these new tools will be presented.

Coexistence of orthorhombic and tetragonal phases of CuSb₂O₆ over a 750 K temperature range

Author(s): Sneha Patel¹ ; Hyung-Been Kang²

Co-author(s): Ben Mallett ¹; Ross Piltz ³ ; Maxim Avdeev ⁴; Chris Ling ⁵; Trevor Finlayson ⁶; Tilo Soehnel ²

1 University of Auckland

2 The University of Auckland

3 ACNS, ANSTO

4 ANSTO

5 University of Sydney

6 University of Melbourne

Corresponding Author(s): spt796@aucklanduni.ac.nz, rop@ansto.gov.au, t.soehnel@auckland.ac.nz, chris.ling@sydney.edu.au, b.mallett@auckland.ac.nz, trevorf@unimelb.edu.au, hkan026@aucklanduni.ac.nz

CuSb₂O₆ is reported to undergo a second-order phase transition from its room-temperature monoclinic crystal structure to a tetragonal structure around 130°C. However, symmetry reduction rules encapsulated by the Bärnighausen trees require there to be an intermediate orthorhombic crystal structure which had previously not been observed. Presented here is high-resolution synchrotron X-ray and neutron powder diffraction data along with single-crystal Laue neutron diffraction data which together show clear evidence for an orthorhombic Pnnm phase in CuSb₂O₆ above 100 °C. The orthorhombic phase coexists with the tetragonal P 4₂/mm and represents an approximately

0.003 Å distortion of the a unit-cell length (~0.06%). Unusually, this coexistence persists over an exceptionally large temperature range up to the highest measured temperature of 900°C.

Complex fluids and simple experiments - What could we do?

Patrick Spicer

Corresponding Author(s): p.spicer@unsw.edu.au

Structural studies often aim to overcome the shortcomings of a sample without compromising on signal or accuracy. One critical aspect of studying rheologically complex liquids is flow, and a sample's deformation history and characteristic time scales can complicate interpretation. In this talk I will discuss some simple (and cheap) methods of avoiding unwanted flow, but also adjusting fluid time scales when flow is desirable. We will also examine new (cheap and easy) methods of imposing flow on unsuspecting samples to benefit structural insights and enhance understanding of commercially relevant processes and materials.

Coordination crosslinking of helical oligoamide nanorods: controlling independent SSA

Author(s): Norton West¹

Co-author(s): Rebecca Griffin ¹; Claire Buchanan ¹; Andrew Molino ¹; Dongchen Qi ²; Ljiljana Puskar ³; Jisheng Pan ⁴; Christopher Garvey ⁵; Adam Mechler ¹

1 La Trobe University

2 Queensland University of Technology

*3 Helmholtz-Zentrum Berlin für Materialien und Energie 4 A*STAR (Agency for Science, Technology and Research) 5 ANSTO*

Corresponding Author(s): ljiljana.puskar@helmholtz-berlin.de, a.mechler@latrobe.edu.au, 17770191@students.latrobe.edu.au, js-pan@imre.a-star.edu.sg, cebuchanan@students.latrobe.edu.au, chris@cigarvey.com, rebecca.griffin@latrobe.edu.au, ngwest@students.latrobe.edu.au, dongchen.qi@qut.edu.au

Organic building blocks offer a promising direction in the development of cooperative framework materials. While employing the processes of bottom up nanofabrication, oligoamide demonstrate supreme specificity, selectivity and geometric variability through supramolecular recognition.

The oligoamide's peptide backbone is unaffected by metal coordination, as shown by vibrational spectroscopy (FT-IR). Through X-ray photoelectron spectroscopy (XPS) studies it was found that the Cu²⁺ ions were reduced to +1 and 0 oxidation states and were coordinated to the histidine and carboxylate moieties.

Our work shows versatile tuneable one- to two-dimensional superstructures based on independent multi-tiered supramolecular self-assembly developed upon metal coordinated oligoamide nanorods.

Our work shows oligoamide nanorods that demonstrate a primary motif of self-assembly through hydrogen bonding. Furthermore, metal coordination was used as an independent secondary self-assembly motif. Hence signifying the versatile tuneability of our oligoamide one- to two-dimensional superstructures.

Coupling in vitro cell culture with synchrotron SAXS to understand the bio-interaction of lipid-based liquid crystalline nanoparticles with vascular endothelial cells

Author(s): Yuen Yuen Yi Lam

Co-author(s): Ben Ben Boyd ; Angel Angel Tan

Corresponding Author(s): angel.tan@monash.edu, yuen.lam1@monash.edu, ben.boyd@monash.edu

Nonlamellar lipid-based liquid crystalline (LLC) nanoparticles possessing different internal nanostructures, specifically the 3D-ordered cubosomes (V2 phase) and the 2D-ordered hexosomes (H2 phase), are of increasing interest as drug delivery systems. To facilitate their development, it is important that we understand their interactions with healthy human umbilical vein endothelial cells (HUVECs). To this end, a 3D cells-in-a-tube model that recapitulates the basic morphology (i.e. tubular lumen) and in vivo microenvironment (i.e. physiological shear stress) of blood vessels was employed as a biomimetic testing platform, and the bio-nanoparticle interactions were compared with that of the conventional 2D planar cell culture. Confocal microscopy imaging revealed internalisation of the nanoparticles into HUVECs within 2 h and that the nanoparticle-cell interactions of cubosomes and hexosomes were not significantly different from one another. Low fluid shear stress conditions (i.e. venous simulation at 0.8 dynes/cm²) were shown to impose subtle effects on the degree of nanoparticle-cell interactions as compared with the static 2D culture. The unexpected similarity of cellular interactions between cubosomes and hexosomes was clarified via a real-time phase behaviour analysis using the synchrotron-based small-angle X-ray scattering (SAXS) technique. When the nanoparticles came into contact with HUVECs under circulating conditions, the cubosomes gradually evolved into hexosomes (within 16 min). In contrast, the hexosomes retained their original internal structure with minimal changes to the lattice parameters. This study highlights the need to couple cellular studies with high-resolution analytics such as time-resolved SAXS analysis to ensure that particle structures are verified in situ, enabling accurate interpretation of the dynamics of cellular interactions and potential bio-induced changes of particles intended for biomedical applications.

Cubosomes for the Delivery of Biopharmaceuticals

Brendan Dyett¹; Calum Drummond²; Charlotte Conn¹; Jamie Strachan²; Tom Meikle¹

1 RMIT

2 RMIT University

Corresponding Author(s): calum.drummond@rmit.edu.au, jbstrachan2015@gmail.com, brendan.dyett@rmit.edu.au, charlotte.conn@rmit.edu.au, thomas.meikle@rmit.edu.au

Biopharmaceuticals, including therapeutic proteins and peptides, represent the fastest growing class of new pharmaceuticals with application as treatments for auto-immune disorders, cancer and cardiovascular disease. Significant efforts have converged towards the design and development of more sophisticated delivery systems for protein-based pharmaceuticals, able to ensure controlled release of these bioactive compounds as well as protect the encapsulated therapeutic from denaturing processes such as enzymatic or acidic hydrolysis. Lipid-based nanomaterials are particularly useful for the encapsulation of amphiphilic proteins and peptides, as their bilayer structure mimics the native cell membrane environment and may assist in retaining the protein in a functionally active form.¹ The research presented aims to elucidate the fundamental physicochemical interactions between lipidic nanomaterials, encapsulated proteins and peptides, and cells. In order to screen the large compositional space associated with the design of such materials, we focus on high-throughput methodologies, and the use of large national and international synchrotron facilities such as the Australian Synchrotron, the Bragg Institute and ASTRID2 synchrotron, Denmark. Uptake of cubosomes into eukaryotic cells was shown to be driven by a process of membrane fusion between the lipid bilayer that makes up the nanoparticle and the external cell membrane.² Synchrotron CD experiments demonstrated that the lipidic cubic phase was able to protect encapsulated insulin against enzymatic degradation by chymotrypsin, which is typically found in the small intestine, over a period of several hours. Finally, the use of lipid nanoparticles as effective delivery vehicles for anti-microbial compounds will be discussed.³

Conn, C. E.; Drummond, C. J., Nanostructured Bicontinuous Cubic Lipid Self-Assembly Materials as Matrices for Protein Encapsulation. *Soft Matter* 2013, 9 (13), 3449-3464.

Dyett, B. P.; Yu, H.; Strachan, J.; Drummond, C. J.; Conn, C. E., Fusion dynamics of cubosome nanocarriers with model cell membranes. *Nat Commun* 2019, 10 (1), 4492.

Meikle, T.G.; Dyett, B.; Strachan, J.B.; White, J.; Drummond, C.J. and Conn, C.E. Preparation, Characterization, and antimicrobial activity of cubosome encapsulated metal nanocrystals. *ACS Applied Materials & Interfaces* 2020, 12 (6), 6944-6954

Data evaluation on the fly: Auto-Rickshaw at the MX beamlines of the Australian Synchrotron

Santosh Panjikar¹; MX team

¹ Australian Synchrotron

Corresponding Author(s): santosh.panjikar@synchrotron.org.au

Auto-Rickshaw [1,2] is a system for automated crystal structure determination. It provides computer coded decision-makers for successive and automated execution of a number of existing macro- molecular crystallographic computer programs thus forming a software pipeline for automated and efficient crystal structure determination.

Auto-Rickshaw (AR) is freely available to the crystallography community through the EMBL-Hamburg AR Server (<http://www.embl-hamburg.de/Auto-Rickshaw>).

Recently, it has been installed at the ASCI cluster at the Australian Synchrotron. The AS-AR server is accessible from the MX beamline computers during the X-ray data collection.

AR at the MX beamlines can be invoked through command line or a web-based graphical user interface (GUI) for data and parameter input and for monitoring the progress of structure determination. It can be also invoked via automatic data processing if the parameter inputs have been pre set at the GUI during X-ray diffraction experiment.

A large number of possible structure solution paths are encoded in the system and the optimal path is selected by the decision-makers as the structure solution evolves. The platform can carry out experimental (SAD, SIRAS, RIP or various MAD) and MR phasing or combination of experimental and MR phasing. The system can be used in evaluation of multiple datasets for any phasing protocols as well as for evaluation of ligand binding or fragment screening.

The new implementation and features will be discussed during the presentation.

References

Panjikar, S., Parthasarathy, V., Lamzin, V. S., Weiss, M. S. & Tucker, P. A. (2005). Auto-Rickshaw

- An automated crystal structure determination platform as an efficient tool for the validation of an X-ray diffraction experiment. *Acta Cryst. D61*, 449-457.

Panjikar, S., Parthasarathy, V., Lamzin, V. S., Weiss, M. S. & Tucker, P. A. (2009). On the combination of molecular replacement and single-wavelength anomalous diffraction phasing for automated structure determination *Acta Cryst. D65*, 1089-1097.

Deciphering structural interactions between human Plasminogen and the Group A streptococcus PAM protein

Author(s): Hui Li¹

Co-author(s): Adam Quek²; Ruby Law²; James Whisstock³

1 Monash University

2 Monash University

3 ARC Centre of Excellence in Advanced Molecular Imaging, Department of Biochemistry and Molecular Biology, Biomedical Discovery Institute, Monash University

Corresponding Author(s): ruby.law@monash.edu, juinn.quek@monash.edu, hui.li1@monash.edu

Plasminogen is an abundant protein that circulates in the blood as the inactive precursor of Plasmin. The Plasminogen/Plasmin system plays a fundamental role in the regulation of fibrinolysis by degrading an insoluble fibrin network to result in the resolution of the blood clot. Perceivably, the tight regulation of the Plasminogen/Plasmin activity is crucial in achieving homeostasis. However, the Plasminogen/Plasmin system is often hijacked by bacterial species to enhance their virulence and pathogenesis.

Group A Streptococcal (GAS) infections represent a global disease burden with more than 220 identified strains differentially distributed around the world, causing a myriad of non-invasive to invasive diseases. Many skin-tropic strains of GAS express a Plasminogen-binding group A streptococcal M-like protein, PAM, which is embedded throughout the GAS cell surface. The recruitment of Plasminogen to the GAS cell surface, followed by its sequential activation by the GAS-secreted streptokinase protein, facilitates GAS invasion and dissemination from the human host. Deciphering the interactions between Plasminogen and PAM is therefore crucial in gaining a better understanding of the virulence of GAS.

We aim to investigate the structural interactions between Plasminogen and various PAM serotypes with different pathogenic potential and sequence variation at the Plasminogen-binding domain. Here, we present an X-ray crystal structure of a complex between the Kringle 2 domain of Plasminogen and a short internal peptide of the NS455 GAS serotype that harbours the Plasminogen-binding motif. The crystal diffracted to 2.5 Å and it revealed several unique intermolecular interactions that may explain the differential Plasminogen-binding and activation potential in comparison to another well-studied PAM serotype. This work has provided insight into the structural interactions between Plasminogen and PAM and may facilitate the development of novel therapeutics targeting GAS infections.

Developing High Pressure Single Crystal Crystallography at MX

Author(s): Stephanie Boer¹

Co-author(s): Stephen Moggach²

1 Australian Synchrotron

2 University of Western Australia

Corresponding Author(s): stephen.moggach@uwa.edu.au, boers@ansto.gov.au

Pressure is an important thermodynamic variable, but its effects on chemical systems have been explored to a much smaller extent than that of temperature. High pressure has been shown to induce significant geometrical, configurational and conformation changes within chemical systems.

The development of diamond anvil cells (DACs) in recent years has allowed the study of chemical systems under high pressure by single crystal X-ray crystallography. This has enabled the analysis of the molecular structure of materials at high pressure, which is invaluable for an increased understanding of their properties. Pressure has been shown to be an important tool in the characterisation of structure-property relationships in porous materials, such as metal organic frameworks (MOFs). High pressure has been used as a useful tool for investigating the stability of MOFs, as well as their mechanical properties such as elasticity, stiffness, and hardness.

A diamond anvil cell contains two opposing diamonds which between them create a sample chamber which can reach pressures of up to 10 GPa. The macromolecular crystallography (MX) beamlines at the Synchrotron are a pair of dual-purpose beamlines serving the needs of the Australasian structural biology and chemical crystallography community. The development of small DACs which can be easily mounted on a goniometer has opened the possibility to conduct high pressure crystallography on the MX beamlines, without major changes to the beamline setup. This development of beamline capability will enable users to study chemical systems at high pressure in order to better understand their properties and study the geometric changes which occur at high pressure.

Developing XFM and Rb⁺ tracing protocols to assess the distribution of important macronutrient, K⁺, in diseased leaves

Author(s): Karina Khambatta¹

Co-author(s): Mark J. Hackett ²; Fatima Naim ¹

1 Curtin University

2 School of Molecular and Life Sciences, Curtin University

Corresponding Author(s): fatima.naim@curtin.edu.au, markjhackett.curtin@gmail.com, karina.khambatta@student.curtin.edu.au

Plants require a number of different elemental macro and micro-nutrients, such as K, Ca, Fe, Mn, Cu, and Zn, to name a few. These nutrients are an essential part of plant development and growth. Plant fungal diseases (such as yellow spot, powdery mildew and leaf rust) are major biotic threats affecting wheat production and resulting in yield losses of up to 50%. Understanding how plant physiology changes in response to the fungal infections, may reveal important information on disease pathology. Potassium in particular, which exists as the K⁺ ion in biology, one of the most abundant elemental nutrients seen throughout a plant, and is crucial to numerous physiological pathways that regulate plant health, and fitness. However imaging K⁺ distribution has been an unmet challenge due its low emission energy (~3300 eV), making it difficult to obtain sufficient signal response from internal leaf structures. One potential strategy to reveal K⁺ distribution in situ within plant leaves is to image the distribution of a surrogate element, which has a higher energy emission. Such an opportunity is presented by Rb, which displays remarkably similar chemical and physiological function to K⁺ in living cells.

I will present my initial work on the development of protocols that will eventually aim to use confocal X-ray fluorescence microscopy (confocal XFM) to reveal Rb⁺ distribution in 3D, as a marker of K⁺ distribution. Such information may be essential in studying the physiological interactions between important agricultural crops (e.g., wheat and barley) and fungal diseases such as yellow spot, which can devastate crop yield and negatively impact the agriculture economy.

Dual sample analysis on the XFM beamline: a new approach to increase the throughput of analysis of large samples

Casey Doolette¹

1 University of South Australia

Corresponding Author(s): casey.doolette@unisa.edu.au

Casey L. Doolette¹, Daryl L. Howard², David, J. Paterson², Cameron M. Kewish², Nader Afshar², Peter M. Kopittke³, Enzo Lombi¹

1University of South Australia, Future Industries Institute, Mawson Lakes, South Australia 5095, Australia

2Australian Synchrotron, ANSTO Clayton, Victoria, 3168, Australia

3The University of Queensland, School of Agriculture and Food Sciences, St. Lucia, Queensland 4072, Australia

X-ray fluorescence microscopy (XFM) is a powerful mapping technique that can be used to determine the distribution of elements and chemical species at a range of spatial resolutions. Synchrotron radiation is commonly used as the X-ray source over conventional benchtop XFM as the photon flux is orders of magnitude greater, meaning that speed of analysis is also orders of magnitude faster.¹ However, there is extremely high demand for synchrotron-based X-ray fluorescence mapping due to its wide range of applications including biomedical, geological, environmental, agricultural and cultural heritage fields of research.² Therefore, user access to the Australian Synchrotron XFM beamline is very competitive and the beamline is oversubscribed. In this study, we developed a dual scanning approach that allows for simultaneous data collection from two samples. More specifically, we performed milliprobe analysis of an upstream sample concurrently with microprobe analysis of a downstream sample. The motivation behind this work was driven by the need to map large samples (>100 cm²) without sacrificing the throughput of the XFM beamline. For this study, our upstream samples were large (10 cm x 17 cm) diffusive gradient in thin-film devices (DGT); a DGT is a hydrogel embedded with a binding agent that acts as a sink for labile soil nutrients. After deployment on the soil surface, the DGT can then be mapped to visualise the distribution of available soil nutrients. We investigated the effect of DGT composition on the quality of analysis of two contrasting highly heterogeneous downstream samples (mineral and wheat thin-sections). Overall, gel composition did not affect the quality of analysis of highly heterogeneous downstream. For the first time, we demonstrated that data collection from large DGT devices can be performed in the background of other experiments on the Kirkpatrick Baez mirror (KB) end-station.

This dual-scanning approach has the potential to translate to an increased throughput of analysis for XFM, as large DGTs (or other gels e.g. those used for metalloprotein separation) can be scanned at virtually no beamtime cost.

Kopittke, P. M.; Punshon, T.; Paterson, D. J.; Tappero, R. V.; Wang, P.; Blamey, F. P. C.; van der Ent, A.; Lombi, E. *Plant physiology* 2018, 178, 507-523.

Paterson, D.; Jonge, M. D. d.; Howard, D. L.; Lewis, W.; McKinlay, J.; Starritt, A.; Kusel, M.; Ryan, C. G.; Kirkham, R.; Moorhead, G.; Siddons, D. P. *AIP Conference Proceedings* 2011, 1365, 219- 222.

Effect of Emulsifier Type on Interfacial Crystallisation

Stephanie Macwilliams¹; Andrew Clulow²; David Beattie¹ ; Marta Krasowska¹

1 University of South Australia

2 Monash University

The study of interfacial crystallisation with SAXS/WAXS is commonly conducted using both water- in-oil and oil-in-water and emulsions. The former case can be compared to that of a continuous lipid system, where impurities in the bulk lipid catalyse the formation of a lipid crystal network. In the latter case, the dispersion of the lipid phase into emulsion droplets means the division of crystal-promoting impurities amongst these droplets, with the number of droplets likely to exceed the number of impurities, hence lowering the temperature required to form crystals. The inability to distinguish bulk lipid crystals from those at an interface is also made challenging in an emulsion system due to the size of the droplets relative to the size of the x-ray beam. We have used a different approach to study interfacial crystallisation, whereby a model lipid layer (medium-chain triglyceride, MCT) containing a mono-diglyceride mixture was added on top of a water layer inside a capillary. Synchrotron SAXS/WAXS was then used to study crystallisation occurring at the oil- water interface. Surfactant molecules are present in emulsions as stabilising agents and they may also influence crystallisation and the lipid crystal structure. The effect of stabilising agents on the structure and properties of lipid crystals was also investigated. The interfacial activity of fat crystals was also assessed in a complementary series of experiments using Profile Analysis Tensiometry by monitoring the kinetics of interfacial tension in response to temperature changes. Both the addition of stabiliser and the stabiliser type alter the interfacial tension profiles for heating and cooling cycles compared to the lipid-water system in the absence of stabiliser.

Effect of surfactant ionicity on critical micelle concentration in aqueous ionic liquid mixtures

Sachini Kadaoluwa Pathirannahalage¹; Tamar Greaves¹; Michael Hassett¹; Andrew Christofferson¹; Tu Le¹; Margarida Costa Gomes²

1 RMIT University

2 ENS de Lyon

Corresponding Author(s): tamar.greaves@rmit.edu.au, s3544991@student.rmit.edu.au

Protic ionic liquids are the largest known solvent class capable of promoting surfactant self-assembly. However, ILs are increasingly used as mixtures with molecular solvents, such as water, to reduce their cost, viscosity and melting point, and the self-assembly promoting properties of these mixtures are largely unknown. Here we investigated the critical micelle concentration (CMC) of ionic and non-ionic amphiphiles in ethylammonium nitrate (EAN)-water mixtures to gain insight into the role of solvent species, and effect of solvent ionicity on the self-assembly process. The amphiphiles used were the cationic cetyltrimethylammonium bromide (CTAB), anionic sodium octanoate sulfate (SOS), and the non-ionic surfactant tetraethylene glycol monododecyl ether (C12E4). Surface tensiometry was used to obtain the CMCs and free energy parameters of micelle formation, and Small angle x-ray scattering (SAXS) was used to characterise the micelle shape and size.

The EAN-water solvents displayed self-assembly results consistent with a salt in water for EAN proportions below 5 mol% across all three surfactants, leading to CMC values lower than the CMC observed in water. A steep incline in the CMC was observed for concentrations between 5 mol% to 50 mol% of EAN for SOS and C12E4. However, CTAB displayed more complex behaviour where the CMC remained below the CMC of water until 33 mol% EAN. Across all surfactants, a plateau in CMC values were observed at very high EAN concentrations, which could indicate that there is a shift in the dominant solvent beyond EAN concentrations of 50 mol%. This study furthers our understanding of PIL solvent behaviour in ternary mixtures with amphiphiles.

End to end demonstration of an image guided microbeam radiation therapy protocol for in vivo brain tumour radiosurgery at the Australian Synchrotron

Author(s): Jason Paino¹

Co-author(s): Micah Barnes ² ; Elette Engels ³ ; Jeremy Davis ³ ; Chris Hall ⁴ ; Daniel Hausermann ⁴ ; Moeava Tehei ⁵ ; Stephanie Corde ⁶ ; Michael Lerch ³

1 UOW

2 Royal Melbourne Institute of Technology, Applied Physics, Melbourne, Australia

3 University of Wollongong

4 Australian Synchrotron

5 University of Wollongong, Centre for Medical Radiation Physics, Wollongong, Australia

6 Prince of Wales Hospital, Radiation Oncology Department, Randwick, Australia

Corresponding Author(s): mlech@uow.edu.au, micah.barnes@student.rmit.edu.au, christoh@ansto.gov.au, elette@uow.edu.au, moeava@uow.edu.au, jeremyd@uow.edu.au, stephanie.cordetehei@health.nsw.gov.au, jrp933@uowmail.edu.au, daniel.hausermann@synchrotron.org.au

The Imaging and Medical Beamline (IMBL) at the Australian Synchrotron has seen increasing use for the irradiation of healthy and tumour-bearing live animals. This has been facilitated with great improvements in the image guidance capability available to users. In this paper, we present an end- to-end demonstration of an image-guided microbeam radiation therapy protocol for in vivo brain tumour radiosurgery performed on the Imaging and Medical Beamline at the Australian Synchrotron. The protocol utilises CT scanners at the adjoining Monash Biomedical Imaging facility for tumour identification and the recently developed SYNCMRT for image guidance. End-to-end accuracy is first demonstrated first on an anatomical rat phantom and finally on the treatment of a tumour bearing rat, using histology slides for verification 14 days after treatment. To date, 35 tumour-bearing rats have been treated with this technique.

Energy Dispersive X-ray Diffraction for In-Situ and Operando Characterization of Electrochemical Energy Storage Systems

Amy Marschilok

Corresponding Author(s): amy.marschilok@stonybrook.edu

Electrochemical energy storage systems can be challenging to characterize as they function far from equilibrium, dominated by kinetics. Heterogeneity of the ion distribution and phase transformations within the electrode can have a significant impact on the electrochemistry of the system, but is not discernable by conventional methods. The benefits of energy dispersive x-ray diffraction as a tool for in-situ and operando characterization of electrochemical energy storage systems will be highlighted in this presentation, including examples from both conversion and insertion based electrodes.

Experiments on the high-flux BioSAXS beamline: opportunities for dynamic studies of soft matter systems and advanced materials

Author(s): Lester Barnsley¹

Co-author(s): Christina Kamma-Lorger²

1 ANSTO

2 Lead Scientist BioSAXS

Corresponding Author(s): ckamma@ansto.gov.au, barnslel@ansto.gov.au

The BioSAXS beamline is one of the new beamlines to be constructed at the Australian Synchrotron within the BRIGHT program. BioSAXS will be dedicated to perform solution small-angle X-ray scattering (SAXS) experiments, offering access to a variety of researchers from Australia and New Zealand. Solution SAXS experiments continue to be a growing area of the current Australian Synchrotron SAXS/WAXS operations, particularly in regard to protein and DNA/RNA structure, polymer solutions, nanoparticles and liquid crystal phases. Highly radiation-sensitive samples will be studied on the BioSAXS beamline with unprecedented levels of flux, using the CoFlow sample environment, a pioneering development of the Australian Synchrotron. A highly-automated end-station combined with a versatile detector system will allow the BioSAXS beamline to accommodate most solution SAXS experiments, covering a q -range of $\sim 0.001 - 3 \text{ \AA}^{-1}$, with low instrument background. The optical design is optimized for high flux ($>5 \times 10^{14} \text{ ph/s}$) x-rays and a focused beam size of $0.3 \text{ mm (H)} \times 0.03 \text{ mm (V)}$.

Along with the CoFlow, a wide range of automated, in-situ sample environments are planned for users studying soft matter and nanoparticulate systems, with a focus on high throughput measurements and real-time dynamics to take advantage of the high flux beam and fast detector response time. These will include a stopped-flow and rheometer for dispersed polymer solutions, along with a novel, versatile magnetic-array system, optimized for small-angle scattering experiments on magnetic nanoparticles used in biomedical applications. The BioSAXS beamline will be developed as a highly-automated and versatile beamline that can accommodate a wide-range of solution scattering experiments, complementing the existing SAXS/WAXS beamline to ensure the world-leading capabilities of the SAXS offering at the Australian Synchrotron.

Fast-scanning X-ray Diffraction Microscopy (SXDM) at the XFM beamline

Michael Jones¹; Christoph Schrank²; Nicholas Phillips³; Cameron Kewish⁴

1 QUT

2 Queensland University of Technology

3 Oxford University

4 Australian Nuclear Science and Technology Organisation, 800 Blackburn Road, Clayton, VIC 3168, Australia

Corresponding Author(s): cameronk@ansto.gov.au, nicholas.phillips@eng.ox.ac.uk, christoph.schrank@qut.edu.au, mw.jones@qut.edu.au

Scanning X-ray Diffraction Microscopy (SXDM, aka ptychography) produces phase and absorption contrast images at high spatial resolution, well below the incident beam size(1). The experimental conditions for SXDM are close enough to X-ray Fluorescence Microscopy (XFM) that they are readily combined into a single simultaneous measurement(2-5). However, SXDM has additional coherence and positioning precision requirements compared to XFM and therefore has tended to slow down the whole data collection process(3). Here we present recent advances in fast “flyscan” SXDM data collection, and processing strategies implemented at the XFM beamline that reduce the time taken to collect the data, and produce artefact-free images. These advances provide a pathway to nanoscale imaging of millimetre-sized samples, in the gigapixels per hour regime.

Fluctuation x-ray scattering of self-assembled lipids, colloidal particles and liquids

Author(s): Andrew Martin¹

Co-author(s): Jack Binns ¹; Patrick Adams ¹; Tamar Greaves ¹; Connie Darmanin ²

¹ RMIT University

² La Trobe

Corresponding Author(s): cdcoeltu@gmail.com, s3826109@student.rmit.edu.au, jack.binns@rmit.edu.au, tamar.greaves@rmit.edu.au, andrew.martin@rmit.edu.au

Fluctuation x-ray scattering studies how the x-ray diffraction pattern changes as a small x-ray beam is scanned relative to the sample. The ensemble of diffraction patterns from different sample positions can reveal information about the local 3D structure in disordered materials. We have developed a fluctuation scattering technique called the pair-angle distribution function (PADF) method that recovers three- and four-body correlations in the sample, including local angular structure[1,2]. This is a natural generalisation of the pair-distribution function obtained from small-angle x-ray scattering (SAXS). Here we present recent applications of the PADF technique to self-assembled lipids[3] to reveal distortions of the water channel shape with lipid composition. We discuss the potential application to disordered, dense packings of colloidal particles to distinguish dominant icosahedral, face-centred cubic, body-centred cubic or hexagonal packings[4]. Looking further into future, we discuss the potential applications to liquid structure with x-ray free-electron lasers.

[1] A.V. Martin, IUCrJ, 2017, 4, 24-36.

A.V. Martin, E.D. Bøjesen, T.C. Petersen, C. Hu, M.J. Biggs, M. Weyland, A.C.Y. Liu, Small 2020, 16, 2000828.

A.V. Martin, A. Kozlov, P. Berntsen, F.G. Roque, L. Flueckiger, S. Saha, T.L. Greaves, C.E. Conn, A.M. Hawley, T.M. Ryan, B. Abbey, C. Darmanin, Commun. Mater. 2020, 1, 40.

E. Bøjesen, T.C. Petersen, A.V. Martin, M. Weyland, A. Liu, Journal of Physics: Materials, 2020, 3 044002.

Full-field tomography with scattered X-rays

Gary Ruben¹ ; Isaac Pina¹ ; Florian Schaff² ; James Pollock¹ ; Marcus Kitchen¹

1 Monash University

2 Technical University Munich

Corresponding Author(s): gary.ruben@monash.edu, isaac.pinar@monash.edu,
james.pollock@monash.edu, florian.schaff@tum.de, marcus.kitchen@monash.edu

X-ray absorption imaging relies on transmitted photons being absorbed by the subject. As a natural consequence, X-rays are also scattered in significant quantities in all directions. This makes it potentially feasible to do tomography and obtain 3D volumetric information by capturing photons using detectors placed around the subject. Scatter tomography has previously been attempted with pencil and sheet beam illumination, in order to limit the multiple-scattering of photons, which generates an unwanted background signal. At energies suitable for preclinical imaging, multiple-scattering is less problematic, making it possible to imagine doing tomography even with full-field X-ray illumination. With the aim of augmenting our existing full-field 2D imaging experiments with additional scatter detectors, we pursued this possibility. Here we present what we believe are the first successful X-ray Scatter Tomography experiments using full-field illumination, performed in 2019 at the Imaging & Medical Beamline, of the chest of a juvenile rat, achieving sufficient resolution for segmentation of the lung and major airways.

Further insights into the effect of pH on the fluorescence and structure of green fluorescent protein (GFP)

Nathalia V. dos Santos¹ ; Carolina F. Saponi² ; Timothy M. Ryan³ ; Fernando L. Primo² ; Tamar L. Greaves⁴ ; Jorge F. B. Pereira⁵

1 São Paulo State University, Brazil / RMIT University, Australia

2 São Paulo State University, Brazil

3 The Australian Synchrotron, Australia

4 RMIT University, Australia

5 University of Coimbra, Portugal / São Paulo State University, Brazil

Corresponding Author(s): carolina.saponi@gmail.com, fernando.primo@unesp.br, jfbpereira@eq.uc.pt, nathalia.v.santos@unesp.br, tamar.greaves@rmit.edu.au, tim.ryan@synchrotron.org.au

The Enhanced Green Fluorescent Protein (EGFP) has intense and natural fluorescence, and is biocompatible with a diversity of biological systems, which makes it promising for use in the development of biosensors. However, this commercial application is limited, mainly due to the high cost and lack of knowledge about EGFP stability under stress conditions. Although studies have been done into EGFP stability at different pH, they mostly only show the presence or lack of fluorescence, with no in-depth structural evaluations or analysis of the reversibility of the process. Bridging this knowledge gap can allow the development of novel biocompatible pH-biosensors for medical use, which can help in monitoring different diseases that are known for altering the pH of the affected areas, such as certain tumors and synovial diseases. Hence, the objective of this work was to evaluate the effect of pH on the fluorescence activity and structure of EGFP to assist in the development of biosensors.

In this study, EGFP was exposed to different pH for 30 min and evaluated by circular dichroism, fluorescence spectroscopy (2D and 3D), intrinsic fluorescence, small-angle X-ray scattering (SAXS) in well-plates, and with size-exclusion chromatography (SEC-SAXS). Then, the pH of each sample was adjusted until the solution reached neutrality (pH 7.4), and after 60 min, EGFP was again evaluated by the same techniques. It was determined that EGFP is highly stable at neutral-alkaline pH (7.4 to 13.0), has a small fluorescence quenching at slightly acidic pH (6.0 and 5.0) and total quenching at pH

≤ 4.0 . At pH 6.0, the fluorescence was almost completely recovered with the return of the pH to neutral, however, from pH values of 5.0 to 2.0, the fluorescence was only partially recovered.

In addition, at pH 6.0 there was no change in the secondary and tertiary structure of EGFP (as observed by CD, SAXS, and SEC-SAXS) because the fluorescence quenching was only the result of reversible changes caused by protonation, considering the isoelectric point of the protein is 6.2. Between pH 5.0 to 2.0, the results indicate that there were structural changes at tertiary and secondary levels, hence EGFP recovery was only partial. Therefore, it is possible to conclude EGFP fluorescence is highly dependent on pH, exhibiting reversible changes in conformation between pH 6.0 and 7.0, and irreversible structural changes at $\text{pH} \leq 5.0$. These properties make EGFP a very promising biomolecule for the development of novel acidic-to-basic pH-biosensors.

Keywords: Green Fluorescent Protein, pH Stability, Biosensors, Circular Dichroism, SAXS.

Financial support: FAPESP (2014/16424-7; 2014/19793-3; 2018/50009-8; 2018/01858-2; 2016/07529-5; 2018/20833-0), CAPES 001, CNPq and RMIT University.

Future upgrade options for the Australian Synchrotron Light Source

Rohan Dowd¹; Eugene Tan¹; Rebecca Auchettl¹; Karl Zingre¹; Jonathan Chi¹; Mark Atkinson¹; David Zhu¹

1 Australian Synchrotron - ANSTO

Corresponding Author(s): rebecca@ansto.gov.au, rohand@ansto.gov.au, yawrent@ansto.gov.au, davidz@ansto.gov.au, chij@ansto.gov.au, zingrek@ansto.gov.au, marka@ansto.gov.au

The Australian Synchrotron is a 3rd generation Light source and has been operating since 2007. It is expected to reach the end of its operational life in 2035. Since it was commissioned, there have been significant advances in light source lattice design that has led to order of magnitude brightness increases, enabling new beamline techniques taking advantage of higher coherence and diffraction limited optics. Many 3rd Generation light sources around the world are currently undertaking of planning upgrade paths to convert their rings into these 4th generation light sources to stay at the forefront of photon science and meet the needs of future users.

This poster will present some design options for upgrading the Australia synchrotron as it reaches its end of life. We present both the options of upgrading the existing ring and building a new, larger ring on-site. The details of the proposed new storage ring lattice are shown, as well as a summary of the main engineering advantages and challenges of each option.

Generalizing small angle scattering form factors for nanostructure characterization

Matt Thompson¹

1 Australian National University

Corresponding Author(s): matt.a.thompson@anu.edu.au

Diffraction based techniques, such as small angle scattering (SAS) are widely used to characterize the morphology of nanoscale materials such as quantum dots and thin films. These techniques typically involve the iterative fitting of a model of the diffraction pattern of the system under investigation. Analytical solutions for diffraction patterns are only available for features with special symmetries. These so-called “form factors” are widely available for simple structures such as spheres, parallelograms, and cylinders. Other low-symmetry structures instead require numerical integration which can require several orders of magnitude more computational time to determine the scattering pattern. Although the number of analytically derived form factors is limited, it is possible to generalize each to describe a much greater range of structures via the application of a linear transformation on these structures. Here we illustrate how this methodology can be applied to any arbitrary combination of linear transformations, including rotation, shear, stretch, and translation operations in order to significantly expand the range of structures that can be fitted using exact analytical models. This approach has the potential to significantly reduce the computational cost associated with determining the size and shape of many common structures encountered by the small angle scattering community, which in turn should enable greater precision and robustness in nanostructure form factor determination.

This approach also enables rapid computation of form factors for which there are no analytic solutions by calculating the form factor of a “standard” structure (say, a cone) then fitting the data to this standard structure by iteratively modifying a transformation that maps between the two structures.

Generalizing small angle scattering form factors with linear transformations

Matt Thompson¹

1 Australian National University

Corresponding Author(s): matt.a.thompson@anu.edu.au

Nanostructure characterization using small angle scattering is often performed by iteratively fitting a scattering model to experimental data. These scattering models are usually derived in part from the form factors of the expected shapes of the particles. Most small angle scattering pattern fitting software is well-equipped with form factor libraries for high-symmetry models, yet have more limited support for distortions to these ideals that are more typically found in nature. Here, we introduce a means of generalizing high-symmetry form factors to these lower-symmetry cases via linear transformations, significantly expanding the range of form factors available to researchers. These linear transformations are composed of a series of scaling, shear, rotation and inversion operations, enabling particle distortions to be understood in a straightforward and intuitive way. This approach is expected to be especially useful for in-situ studies of nanostructure growth where anisotropic structures change continuously and large datasets must be analyzed.

Hidden Text: Imaging and reading an ancient tablet in an envelope

Christopher Davey¹; Joseph Bevitt²; Carla Raymond³; Luis Siddall¹

1 Australian Institute of Archaeology

2 ANSTO

3 Macquarie University

Corresponding Author(s): cdavey@aiarch.org.au

The poster as presented at the Annual Meeting of the American Schools of Oriental Research is attached. The poster presentation will be largely the same with some additions to the Method section.

High-pressure and high-temperature XRD and XAS measurements using the MQ D-DIA

Nicholas Farmer¹; Tracy Rushmer¹; Jeremy Wykes²

1 Macquarie University

2 Australian Synchrotron

Corresponding Author(s): tracy.rushmer@mq.edu.au, jeremyw@ansto.gov.au, nick.farmer@mq.edu.au

The Macquarie University Deformation-DIA (MQ D-DIA) multi-anvil press enables in situ experimentation at the Australian Synchrotron under high-temperature and high-pressure conditions up to ~ 1500 °C and 6 GPa. The MQ D-DIA can be deployed at suitable beamlines or used 'offline' on the experiment floor. Several online experiments have been conducted at the X-ray absorption spectroscopy (XAS) beamline, where we have developed a detector and optical setup at the XAS beamline that allows both XAS and energy-scanning X-ray diffraction (ES-XRD) measurements to be collected during high-pressure and high-temperature experiments.

A fundamental prerequisite for in situ high pressure experimentation is accurate determination of the P-T conditions experienced by the sample as a function of control variables such as heater power and hydraulic oil pressure. Sample pressure and temperature in the MQ D-DIA has been calibrated by near-simultaneous diffraction of two dissimilar phases (NaCl and Au), and a new Markov chain Monte Carlo method. We have also measured the thermal profile through the sample region using a new technique for mapping compositional variations in electron probe microanalyzer (EPMA) maps of fine-grained polyphase assemblages.

This characterization of sample conditions in the MQ D-DIA facilitates in situ XAS measurements at precisely known pressure and temperature conditions. Preliminary in situ XAS measurements of the speciation of Zr present as a trace component in silicate melt under conditions corresponding to the Earth's mantle show an increase in coordination number with increasing pressure.

Highly Active Gas Phase Organometallic Catalysis Supported Within Metal-organic Framework Pores

Ricardo Peralta¹

¹ University of Adelaide

Corresponding Author(s): ricardo.peralta@adelaide.edu.au

Metal-organic Frameworks (MOFs) possess a set of unique attributes including permanent porosity, large internal surface areas and robust crystallinity which has motivated extensive interest in the field of gas-phase catalysis. In particular, MOFs can act as a platform for the heterogenization of molecular catalysts, allowing easy catalyst recovery and a route towards structural elucidation of the active centres immobilised in a crystalline host. We have developed a unique MOF, MnMOF-1 which features vacant N,N-chelation sites which are accessible via the porous channels that penetrate the structure^{1,2}. In the present work, cationic Rhodium(I) norbornadiene (NBD), cyclooctadiene (COD) and bis(ethylene) complexes have been incorporated into the vacant N,N-chelation sites of MnMOF-1 via post-synthetic metalation and facile anion exchange. Exploiting the crystallinity of the host framework, the immobilised Rh(I) centres were structurally characterised using X-ray crystallography.

The activity of the Rh(I) bisethylene complexes MnMOF-1·[Rh(C₂H₄)₂]BF₄ and MnMOF-1·[Rh(C₂H₄)₂]Cl in gas phase butene isomerisation was studied using gas-phase NMR spectroscopy. Under one atmosphere of butene at 46 °C, MnMOF-1·[Rh(C₂H₄)₂]BF₄ rapidly catalyses the conversion of 1-butene

References

Peralta, R.A.; Huxley, M.; Young, R.; Linder-Patton, O. M.; Evans, J. D.; Doonan, C. J.; Sumby, C. J. *Faraday Discussions* 2020.

Peralta R. A.; Huxley, M. T.; Evans, J. D.; Fallon, T.; Cao, H.; He, M.; Zhao, X. S.; Agnoli, S.; Sumby, C. J.; Doonan, C. J. *J. Am. Chem. Soc.*, 2020.

Hydrothermal design of rGO/TiO₂ nanocomposite for supercapacitors

Author(s): Syeda Wishal Bokhari¹

Co-author(s): Ahmad Hassan Siddique ²; Wei Gao ¹

¹ University of Auckland

² Chinese Academy of Science

Corresponding Author(s): w.gao@auckland.ac.nz, ahmad@nimte.ac.nz, sbok703@aucklanduni.ac.nz

Supercapacitors (SCs) have gained tremendous interest due to their comparatively higher electrochemical performance than batteries, fuel cells, and electrocatalytic capacitors. Talking about the SC device components, electrodes make a major component as they are the sites for the chemical reactions to occur and charge storage during the electrochemical cycles. Henceforth, many materials have been so far explored as the active/support materials for SC electrodes.

There is an increased interest in designing hybrid electrode materials for all different types of energy storage and conversion devices as the hybrid materials offer improved electrochemical charge storage. One of the key parameters for hybrid materials is that they are designed in a way to incorporate advantageous traits of the parent materials. E.g. carbon-transition metal oxides (TMO) hybrid composites (HCs) are said to demonstrate a high conductance and specific capacitance, long life cycle, and good capacitance retention which is far better than their parent materials.

Reduced graphene oxide (rGO) has unique properties that can revolutionize the performance of the functional devices. rGO hybrids can be designed with TMO for improved energy storage applications.

Herein, a hybrid composite of conductive rGO with titanium dioxide, designed by a simple hydrothermal method, is reported to demonstrate a high double-layer capacitance in aqueous electrolyte systems. The mesoporous structure of the composite provides short ion diffusion pathways and the resultant capacitance of the material is 334 F/g with ~77% capacitance retention after 7000 charge- discharge cycles. The HC has also shown a low contact resistance (CR) of only Ω 3.8 and charge transfer resistance (CT) of Ω ~9.8 and capacitance retention of ~77% after 7,000 cycles, which demonstrate the potential of G-TiO₂ HC as SC electrode material.

Internal liquid crystal structures in nanocarriers containing drug hydrophobic ion pairs dictate drug release

Kurt Ristroph; Malinda Salim¹; Brian Wilson; Andrew Clulow¹; Ben Boyd²; Robert K Prud'homme³

¹ Monash University

² Monash Institute of Pharmaceutical Sciences

³ Department of Chemical and Biological Engineering, Princeton University, Princeton

Corresponding Author(s): ben.boyd@monash.edu, andrew.clulow@monash.edu, ristroph@princeton.edu, ma-linda.salim@gmail.com

Hypothesis: Hydrophobic ion pairing (HIP), a solubility engineering technique in which ionic hydrophilic molecules are paired with a hydrophobic counterion, is an attractive strategy for encapsulating ionic water-soluble species into nanocarriers (NC). Drug release from NCs containing HIP complexes is sensitive to ionic strength, pH, and drug:counterion charge ratio, but the exact mechanism for this was unknown, as was the underlying microstructure inside the NC. We hypothesize that HIP complexes arrange into liquid crystalline structures in NC cores and that these structures are responsible for salt- and pH-dependent release.

Experiment: A model hydrophobic ion pair from the cationic antimicrobial peptide polymyxin B sulfate and the anionic counterion sodium oleate is encapsulated into ~100nm NCs formed using Flash NanoPrecipitation (FNP) and stabilized with an amphiphilic diblock copolymer, poly(caprolactone)-b-poly(ethylene glycol). Internal structures are observed by synchrotron small-angle X-ray scattering (SAXS) and transmission electron microscopy (TEM) following NC formulation and are found to vary with polymyxin:oleate charge ratio. In vitro drug release is also measured at two pHs and two charge ratios.

Findings: For a formulation containing a four-fold charge excess of oleate relative to polymyxin, internal structures rearranged from a lamellar phase into an inverse hexagonal phase. The hexagonal phase formation corresponds to a greatly reduced rate of polymyxin release, suggesting that the polymyxin was incorporated into the center of hexagonally-packed rods. When release tests are repeated using phosphate-buffered saline (PBS) at pH 2.0 to ensure protonation of the oleic acid, all internal structures are eliminated and release occurs much faster than at neutral pH, regardless of charge ratio. These findings shed light on the mechanism behind stimulus-responsive drug release from systems containing hydrophobic ion pairs and enable the rational design of controlled-release formulations by manipulating the formation and dynamics of liquid crystalline phases inside NCs.

Investigation of a 3D-crosslinked nonconjugated Radical Polymer to Tune Electrical Conductivity

Ahmed Al-Qatatsheh¹; Jawroski Capricho²; Saulius Juodkazis¹; Nishar Hameed²

1 Swinburne University of Technology

2 Swinburne University of Technology

Corresponding Author(s): saulius.juodkazis@gmail.com, nisharhameed@swin.edu.au, jcapricho@swin.edu.au, aalqatatsheh@swin.edu.au

Organic-based high-performance semiconductor research has attracted significant attention not long ago because of their promising performance. Since the morphology of the solution-processed conductive polymers, used in organic semiconductors, affects the intrinsic charge transport characteristics and mechanical properties, several strategies have been searched to control molecular ordering and alignment enhancing performance. Also, improving performance requires using a measurement technique for molecular orientation and a molecular dynamics simulation approach to predict electrical and mechanical properties.

Our work presents a protocol that adopts the four angles technique to provide an accurate measurement of molecular orientation and a Hamiltonian Monte Carlo simulation to investigate charge transport characteristics. The four angle technique offers precise information on the molecular orientation of selected molecules utilizing the alignment of the electric vector of the Polarised Infrared probing beam with the dipole oscillation corresponding to the absorbing frequency of a specific functional group. In contrast, the Monte Carlo simulation algorithm can generate polymeric molecular chains following a standard random walk controlled by Hamiltonian parametrized utilizing Ab Initio calculations. This simulation will depend on radical concentration, the distance between radicals, and radical orientation to the polymer backbone, allowing to investigate the effect of radical and defect densities on the formation of the percolation network, which supports designing conductive polymers with high conductivity.

Key Words:

Four Angle Approach, Organic-based high-performance semiconductor, Nonconjugated radical polymer, Monte Carlo Simulation, Hamiltonian parametrized utilizing Ab Initio calculations.

Investigation of etched ion-tracks in SiO₂ membranes

Author(s): Shankar Dutt¹

Co-author(s): Christian Notthoff ²; Andrea Hadley ³; Alexander Kiy ⁴; Nigel Kirby ⁵; M.E. Toimil-Molares ⁶; C. Trautmann ⁶; Patrick Kluth ¹

1 Australian National University

2 The Australian National University

3 ANU

4 Australian Nation University

5 Australian Synchrotron

6 GSI Helmholtz Center for Heavy Ion Research, Plankstraße, Darmstadt, Germany

Corresponding Author(s): shankar.dutt@anu.edu.au, christian.notthoff@anu.edu.au, andrea.hadley@anu.edu.au, patrick.kluth@anu.edu.au, nigel.kirby@synchrotron.org.au, alexander.kiy@anu.edu.au

Nano-pore membranes have been investigated for over two decades for different applications. Solid- state nano-pore membranes are in particular interesting due to their chemical and mechanical robustness and their easy integration into silicon-based microelectronics. These membranes have been investigated for many applications in the fields of chemical- and bio-sensing, nano-electronics, nano-fluidics, and filtration. To realize these applications, we need excellent control over the shape and size of the pores in the membranes. In the present study, we report on single and double conical nano-pores in silicon dioxide (SiO₂) membranes fabricated using the 'track-etch technology'. The membranes were characterized using Small Angle X-ray Scattering (SAXS), Scanning Electron Microscopy (SEM) and Atomic Force Microscopy (AFM).

The free-standing membranes were fabricated using standard Micro-Electro-Mechanical Systems processing and selective removal of the silicon substrate using optical lithography in an area of size

0.55 mm x 0.55 mm. Plasma-enhanced chemical vapor deposition (PECVD) SiO₂ was used to fabricate the membranes, allowing control over the film's properties, including stoichiometry, density, reflective index, thickness as well as the resultant stress. The fabricated membranes were then tested using nano-indentation for mechanical properties. The membranes thus fabricated show elastic behavior and can bend up to 5000 nm before deformation.

For the fabrication of nano-pores in the membranes, they were irradiated with 185 MeV and 1.6 GeV Au ions at the 14UD Pelletron Accelerator at the Australian National University and the UNILAC Linear Accelerator at GSI Helmholtzzentrum für Schwerionenforschung, respectively. Irradiation at low fluences of 10⁸ and 5 x 10⁸ ions/cm² was used to avoid overlap of the resulting nano-pores.

The irradiation leads to the formation of ion tracks in the SiO₂ membrane, which was subsequently etched for different times using hydrofluoric acid in a custom-built etching cell to form nano-pores. The ion tracks are etched from one side to form single cones and from both the sides to form double-sided cones. The conical pores are then characterized using different techniques to understand and control the etching process. SAXS is a non-destructive powerful technique to determine ion track and nano-pore morphologies with high precision. It was found that etching from both sides result in asymmetric cones. Python and C based fitting models were developed to fit the complex 2D scattering patterns. From the fitting, both axial and radial ion track etch rates and the cone opening angles, were determined with unprecedented accuracy.

Investigation of the Placental Metallome via X-Ray Fluorescence Microscopy: Potential Markers of Placental Health

Vladimira Foteva¹; Roger Smith¹; Michael Jones²; David Paterson³; Kaushik Maiti¹

1 Mothers and Babies Research Centre, Hunter Medical Research Institute; Faculty of Health and Medicine, School of Medicine and Public Health, University of Newcastle

2 X-ray Fluorescence Microscopy Beamline, Australian Synchrotron; Institute for Future Environments, Queensland University of Technology

3 X-ray Fluorescence Microscopy Beamline, Australian Synchrotron

Corresponding Author(s): roger.smith@newcastle.edu.au, mw.jones@qut.edu.au, davidp@ansto.gov.au, kaushik.maiti@newcastle.edu.au, vladimira.vladimirova@uon.edu.au

Background: Intrauterine growth restriction (IUGR), preterm birth, prolonged pregnancy, and still- birth are associated with placental dysfunction and have long-term pathological consequences for the offspring, with some evidence that placental health is dependent upon appropriate metal homeostasis. Synchrotron technology is an unambiguous method for the identification and quantification of metal ions in biological tissue which, combined with molecular biology techniques, forms a novel, multi-disciplinary approach to investigation of the placental metallome, and therefore the aetiology of gestational morbidities.

Study Aims: 1) Elucidate the changes in concentration and distribution of metals in early term, late term, IUGR and stillbirth placentas by Synchrotron X-Ray Fluorescence Microscopy (XFM) analysis.

2) Corroborate findings, and further investigate the variation in the metallome environment between placental groups, by examining the mRNA levels of specific zinc and calcium metal transporters in term and pathologic placentas.

Methods: Experimental groups consisted of 7 early term (37-39 wks), 7 late term (41+ wks), 5 IUGR, and 5 stillbirth pregnancies. X-Ray Fluorescence Microscopy imaging was used to spatially resolve the distribution and concentration of metals in 24 frozen, unfixed, 60µm placental tissue sections. Metal concentrations (ppm, parts per million) were measured via GeoPIXE software. RNA transcript levels of specific metal transporter proteins were consequently assessed using RT PCR, with results normalised to 18s RNA.

Results: Statistically significant differences in elemental concentrations (ppm) were found between different placental sets. Ca ($p < 0.01$), Zn ($p < 0.01$) and Mn ($p < 0.05$) concentrations were elevated in stillbirth placentas in comparison to term controls.

Likewise, transcript levels of both calcium membrane transporters tested, ATP2B1 ($p<0.05$), and ATP2B4 ($p<0.01$), were significantly elevated in stillbirth placentas in comparison to term, as was SLC39A3 ($p<0.01$), the only zinc transporter of the nine tested, to show significant expression change.

Conversely, elemental concentrations of Ca ($p<0.01$), Zn ($p<0.01$) and Mo ($p<0.01$) were lower in IUGR placental tissue. Fe ($p<0.05$) and Mn ($p<0.05$) concentrations were both elevated in late term placentas, while Mo ($p<0.01$) was decreased in both late term and stillbirth placentas. Cu did not change significantly across placental sets.

Conclusions: XFM is a unique, powerful tool in the field of placental physiology, and has opened numerous avenues for nucleic acid and protein-based research. In this study, statistically significant differences can be observed in the placental metallome between pathological conditions, which are further reflected in transcript analyses. It is as yet unclear whether this represents differences in the uptake of metals from the maternal circulation or differences in the transport of metals to the fetus, or a combination of these mechanisms. However, the overall increase in mineralization noted in stillbirth placentas indicates ageing of the tissues, which has previously been associated with placental dysfunction and as a possible cause for stillbirth. Further research is required to determine whether changes observed are causative or consequential.

Jumping molecular crystals: the role of molecular vibrations

Annette Dowd

Corresponding Author(s): annette.dowd@uts.edu.au

Authors: A. Dowd, C. Ellis, A. Angeloski.

Affiliations: Faculty of Science, University of Technology Sydney; Department of Chemistry, University of Otago.

While we are familiar with the concept of the conversion of thermal energy to mechanical work, there is a little known class of materials known as thermosalient or jumping crystals which can spectacularly turn a small temperature change into a high speed leap, many times their own length. These materials might lead to some exciting new options for the creation of microscopic machines. The jumping and other movement is usually associated with a rapid single crystal-single crystal phase transition. Unfortunately the confusing mix of explanations in the literature shows that this phenomenon is poorly understood, which hinders the crystal engineering required to explore technical applications.

The classic approach in studying such materials is to use diffraction to determine the crystal structure, however vibrational spectroscopy can be used to complement this information particularly from a dynamical aspect, revealing more about the nature of the phase transition.

In this presentation I will present a case study on the newly discovered jumping crystal, nickel dithiocarbamate (Ni:DTC). I will briefly outline the current thinking on SCSC phase transitions in molecular crystals. Measurements of phonon and intramolecular vibrational modes from the THz – Far Infrared beamline using the variable temperature cryostat will be presented. Interpretation was guided with Crystal17 modelling using periodic density functional theory so lattice modes could be calculated. Calculations were based on structures determined by single crystal diffraction.

Laboratory data for astronomical searches of the conformers of crotonaldehyde

Chris Medcraft¹

¹ UNSW

Corresponding Author(s): c.medcraft@unsw.edu.au

The search for complex organic molecules in space provides insights into the chemistry and dynamics of their formation and the availability of biological precursors in prebiotic environments. Enantiomer and stereoselectivity is a fundamental property of the chemistry life on Earth. The detection and quantification of molecular isomers, conformers, or enantiomers in space may show an origin of abiotic stereoselectivity. Crotonaldehyde (2-butenal) is simple, 4-carbon, unsaturated aldehyde that has four conformational isomers. Crotonaldehyde is used in synthetic chemistry for stereoselectivity and the conformers have been shown interact with surfaces differentially.

All aldehydes with three carbons have been detected in space - towards SgrB2(N) - these do not have any conformational flexibility. It is reasonable to assume that crotonaldehyde may also be present in similar environments however no positive detections have been reported. This is partially due to the lack of quality laboratory data, here the three lowest energy conformations of crotonaldehyde have been measured by pure rotational spectroscopy from 7 GHz (4 cm) up to 110 GHz (2.7 mm) this could be extended into the terahertz region at the Australian Synchrotron. These data are used for searches in astronomical observations.

Latest developments and capabilities at the Infrared Microspectroscopy Beamline

Author(s): Mark J. Tobin¹

Co-author(s): Jitraporn (Pimm) Vongsvivut¹ ; Annaleise Klein² ; Keith Bambery²

1 Australian Synchrotron

2 ANSTO

Corresponding Author(s): jitrapov@ansto.gov.au, tobinm@ansto.gov.au, kleina@ansto.gov.au, keithb@ansto.gov.au

The Infrared Microspectroscopy (IRM) beamline has been in operation for user experiments since 2007 and continues to provide access to cutting edge Fourier transform infrared (FTIR) microscope instrumentation with a bright, diffraction limited infrared beam for the analysis of diverse materials from single cells to cultural artefacts, and composite materials to food products. This presentation will provide an update on the current status and capabilities of the IRM beamline, illustrated with relevant case studies.

Operation of the microscope in transmission mode provides a lateral resolution of between 4 μ m and 10 μ m, depending on wavelength, and is suitable for the analysis of thin films, single biological cells and microtomed thin sections of materials from biological tissues to polymer composites. The IRM beamline is equipped with a range of sample chambers for use in transmission mode, including a diamond compression cell for the flattening of materials, a Linkam heated stage for analysis at temperatures between -195°C and 600°C, and a set of custom liquid chambers for the analysis of live biological samples.

Reflection and grazing incidence capabilities enable the analysis of certain materials that either have a polished surface, or are presented as a thin film coating on the surface of a reflective metal substrate.

Enhanced lateral resolution, and the ability to map materials that are otherwise not suited to transmission IR microanalysis, are achieved by the Attenuated Total Reflection (ATR) method. The ATR approach has been developed as a key capability of the IRM beamline, and a separate presentation on this will be given at this meeting.

The standard operating spectral range for the IRM microscope is from 4000 cm^{-1} to 750 cm^{-1} , using a high sensitivity narrow band detector.

This range can be extended on request using a wide band detector with a lower limit of around 500 cm^{-1} , but with an overall loss of sensitivity across the full mid-IR range. A further extension of the range is possible through the use of a far-IR Si:B photodetector, or a Bolometer detector, with a lower limit of 250 cm^{-1} set by the IRM beamline infrared window.

A focal plane array detector can be made available for certain experiments requiring snap-shot images of small regions of around 30 μm .

Rapid scan IR measurements at a microscopic scale are possible on the IRM beamline, with the ability to collect 65 spectra per second at 16 cm^{-1} spectral resolution.

Future developments at the IRM beamline include the use of higher numerical aperture optics for improved beam collection in the reflection analysis of materials, a liquid ATR flow cell for the study of live biological samples at high spatial resolution, full piezo control of all adjustable mirrors and pinholes within the IR microscope, and improved capabilities for mail-in experiments.

Light on the details: exploring the nano-silver behaviour at the plant-soil interface

Author(s): Ryo Sekine¹ ; Elma Lahive² ; Amaia Green-Etxabe² ; Sam Harrison² ; Marianne Matzke² ; Carolin Schultz² ; Steve Lofts² ; David Spurgeon² ; Claus Svendsen²

Co-author(s): Enzo Lombi³ ; William Bennett⁴

1 USC

2 UK Centre for Ecology & Hydrology

3 University of South Australia

4 Griffith University

Corresponding Author(s): rsekine@usc.edu.au, elmhiv@ceh.ac.uk, carsch@ceh.ac.uk, amagre@ceh.ac.uk, enzo.lombi@unisa.edu.au, martzk@ceh.ac.uk, stlo@ceh.ac.uk, csv@ceh.ac.uk, w.bennett@griffith.edu.au, sharrison@ceh.ac.uk, dasp@ceh.ac.uk

Over the past decade, significant advances have been made towards understanding the fate and impact of engineered nanomaterials (ENMs) in the environment, driven by concerns over their unique nanoscale properties and their increasing abundance in the market [1]. Synchrotron-based X-ray Absorption Spectroscopy (XAS) has played a key role in these advances, giving insights to the chemical speciation of common ENMs in environmental matrices, a key determinant of the potential fate and effects in the environment. The speciation of commonly studied metal-based ENMs (Zn, Cu and Ag) determined by XAS in the environmental matrices to which they are likely to be released, often resemble their non-nano (ionic) counterparts (for example [2-4]). In these cases, understanding the transformation from nanomaterial to dissolved form helped to predict impacts. However, this is not always the case, for example sulfidation of Ag in waste streams results in different speciation which have been shown to alter environmental fate and toxicity. XAS has been vital in demonstrating this and has consequently, together with an array of analytical and predictive tools on their behaviour, transport and fate, have greatly advanced our understanding of ENMs and their potential impact on the environment.

However, while our general understanding has greatly advanced, the exponential rate at which nanotechnology is expanding precludes the case-by-case experimental assessment of every nano-enabled product. Therefore, there is a need for predictive tools that enable stakeholders, such as manufacturers, regulators and consumers, to assess the potential fate and impact of their ENM products in the environment. Furthermore, an understanding of how ENMs interact with the environment to which they are released (e.g. varying soil characteristics, interactions with biota) needs to be improved [5].

Recently, as part of a purposely designed experiment towards the development of such tools within the European NanoFASE project [6], we examined the speciation, kinetics and the distribution of silver nanomaterials (nano-Ag) in three different soils cropped with wheat. In particular, there was a focus on resolving the nano-Ag behaviour at the soil-plant interface via operationally defined regions of proximity and interplay with the plant roots. We will present the key results from these experiments, demonstrate how XAS was used at two different facilities to provide complementary insights, and finally give some consideration to how the results improve our understanding towards future exposure assessment tools.

References: [1] The Nanodatabase. 2011-2019, <https://nanodb.dk/>. [2] Sekine, R. et al. 2014. Environ. Sci. Tech. 49: 897-905. [3] Wang P, et al. 2016. Environ. Sci. Tech. 50: 8274-8281. [4] R. Sekine et al. J. Environ. Qual. 46: 1198-1205 (2017). [5] Pradas del Real, A.E. et al. 2017. Environ Sci. Tech. 51: 5774-5782. [6] NanoFASE: Nanomaterial Fate and Speciation in the Environment, 2015-2019, <http://nanofase.eu>.

Macrocytic peptides as the novel chemical probes for modulating the function of the Retromer endosomal trafficking complex

Kai-En Chen¹ ; Qian Guo¹ ; Yi Cui² ; Amy Kendall³ ; Zhe Yang² ; Timothy Hill¹ ; Hiroaki Suga⁴ ; David Fairlie¹ ; Lauren Jackson⁵ ; Rohan Teasdale² ; Toby Passioura⁶ ; Brett Collins¹

1 The University of Queensland, Institute for Molecular Bioscience

2 The University of Queensland, School of Biomedical Sciences

3 Department of Biological Sciences Center for Structural Biology, Vanderbilt University,

4 Department of Chemistry, Graduate School of Science, the University of Tokyo

5 Department of Biological Sciences Center for Structural Biology, Vanderbilt University

6 Sydney Analytical, the University of Sydney

Corresponding Author(s): z.yang3@uq.edu.au, b.collins@imb.uq.edu.au, t.hill@imb.uq.edu.au, k.chen@imb.uq.edu.au, amy.k.kendall@vanderbilt.edu, qian.guo@uq.edu.au, y.cui@uq.edu.au

Maintenance of appropriate levels of endocytic trafficking and subsequent sorting in endosomes is essential for every aspect of cellular life. The evolutionarily conserved Retromer complex (composed of VPS35-VPS26-VPS29) is a central hub responsible for this process in endosomal compartments in all eukaryotes. It is known that mutations in Retromer complex can cause late-onset Parkinson's disease, and can also be hijacked by viral and bacterial pathogens during cellular infection. Seeking tools to modulate Retromer function would provide new avenues in understanding Retromer function and the associated diseases. Here we employed the random nonstandard peptides integrated discovery (RaPID) approach to identify a group of macrocyclic peptides capable of binding to Retromer with high affinity and specificity. Our crystal structures show that five of the macrocyclic peptides bind to Vps29 via a di-peptide Pro-Leu sequence. Interestingly, these peptides structurally mimic known interacting proteins including TBC1D5, VARP, and the bacterial effector RidL, and potentially inhibit their interaction with Retromer in vitro and in cells. Further analysis using cryo- electron microscopy (CryoEM) and mutagenesis showed that a unique macrocyclic peptide binds Retromer at the interface between Vps35 and Vps26 subunits and can act as a molecular chaperone to stabilise the complex with minimal disruptive effects on Retromer's ability to interact with its accessory proteins. Finally, using reversible cell permeabilization approach, we demonstrate that both the Retromer inhibiting and stabilizing macrocyclic peptides can specifically co-label Vps35-positive endosomal structures, and can be used as baits for purifying Retromer from cells and subsequent proteomic analyses. We believe these macrocyclic peptides can be used as a novel toolbox for the study of Retromer-mediated endosomal trafficking, and sheds light on developing novel therapeutic modifiers of Retromer function.

Materials And Interfacial Design For Advanced Potassium Ion Storage

Wenchao Zhang¹

¹ University of Wollongong

Corresponding Author(s): wz990@uowmail.edu.au

Developing new renewable energy storage devices is vital for regulating the energy output of intermittent solar and wind energy, which have been expected to occupy increasing proportions of energy sources in light of the environmental issues caused by fossil fuel energy. Amid staggering advances on grid-scale devices and electric vehicles, there has been great interest in exploring potassium ion batteries (PIBs). The motivations triggering the study of PIBs relate to the benefits of their relatively high energy density resulting from the low standard redox potential of potassium (-2.93 V vs. E₀), which is close to that of lithium (-3.04 V vs. E₀), their low cost, which is ascribed to the abundance of potassium (1.5 wt. %) in the Earth's crust, and also their fast ion transport kinetics in electrolyte. In terms of electrode materials, alloy-based materials have been considered as good candidates for high-energy-density devices due to their relatively high theoretical capacity. However, the huge volume variations and sluggish ionic diffusion hinder their cycle life and fast charge/discharge capability. Through the optimization of materials processing, the introduction of carbon matrix and the selection of electrolytes, the high-energy-density and long cycle life alloy-based anodes have been obtained. In addition, to further increase the energy density, we successfully fabricate the K-CO₂ batteries by employing three-dimensional carbon-based metal-free electrocatalysts. We hope the relevant work will promote the developments of K ion chemistry in energy storage fields.

Mechanistic insights into functional Electrocatalysis from XAS: the story from Experimental Design to Insights into Electron Transfer Timescales important for Selectivity

Rosalie Hocking¹

1 Swinburne University of Technology

Corresponding Author(s): rhocking@swin.edu.au

¹Department of Chemistry and Biotechnology and Centre for Translational Atomaterials, Faculty of Science, Engineering and Technology, Swinburne University of Technology

One of the greatest challenges of the 21st century will be securing cheap and renewable sources of energy. One of the most promising approaches to this challenge is to design catalysts from earth abundant materials capable of implementing key chemical reactions including splitting water into hydrogen and oxygen ($\text{H}_2\text{O} \rightarrow 2\text{H}^+ + \text{O}_2$); and both the oxidation ($\text{H}_2 \rightarrow 2\text{H}^+$) and reduction ($2\text{H}^+ \rightarrow \text{H}_2$) of hydrogen among many others. Structural type and disorder have become important questions in catalyst design- it is often noted in studies of functional materials that the most active catalysts are “disordered” or “amorphous” in nature. But the impact of this “disorder” on catalysis and other material properties has been hard to quantify- in part because of the challenges of characterising disordered materials. X-ray Absorption Spectroscopy offers an important solution to this problem enabling us to study materials in their “functional active state” even when highly disordered and amorphous. In this talk I will examine some of the things we have learnt about functional electro-catalysts from X-ray Absorption Spectroscopy- from catalyst identification to understanding timescale effects in electron transfer important for catalyst design.

Metal Nanoparticle Radiosensitization for Improving Radiotherapy

Ivan Kempson

Corresponding Author(s): ivan.kempson@unisa.edu.au

Ivan Kempson¹, Douglass Howard¹, Tyron Turnbull¹

¹ Future Industries Institute, University of South Australia, SA, 5095 Corresponding Author:
Ivan.Kempson@unisa.edu.au

Metal nanoparticles have gained market approval for enhancing the effects of ionizing radiation in radiotherapy treatment of cancer. However the mechanism of action of metal nanoparticles exerting their effect remain controversial and poorly elucidated. We have developed a methodology inspired by Quality-by-Design principals to investigate the structure-function relationship of nanoparticle parameters with radiobiological effect.

A cross-correlative methodology was developed to measure biological parameters such as the number of DNA breaks in single cells after irradiation with clinical X-ray sources coupled with quantitative analysis of the number nanoparticles in the same individual cells with XRF. A major challenge in identifying mechanisms is the massive degree of heterogeneity between cells.¹

Sub-cellular populations were identified and radiobiological response was determined for individual cells as a function of the number of nanoparticles in the same cells. The data is continuing to reveal many insightful aspects of nanoparticle-cell interactions and the consequence these have on radiobiological response of cancer cells. Importantly, a number of biological mechanisms exist that not only sensitize cells but can actually de-sensitize cells. These mechanisms contravene the physical concepts of radiosensitization. Nanoparticle uptake is highly heterogeneous and the observations made in our research cannot be deduced by conventional bulk assays. Biological mechanisms, such as down regulating proteins involved in DNA damage repair, lead to preferential sensitization of the most radio-resistant S-phase cells which act as a negative prognostic factor for many indications.² Despite metal nanoparticles entering clinical use, we highlight many questions that remain in how they exert their function. Our research is revealing these mechanisms and will enable optimization of radiosensitizer formulations.

References

- T Turnbull, B Thierry, I Kempson. A Quantitative Study of Intercellular Heterogeneity in Gold Nanoparticle Uptake across Multiple Cell Lines, *Analytical Bioanalytical Chemistry*, 411(28), 7529- 7538, 2019.
- T Turnbull, M Douglass, N Williamson, D Howard, R Bhardwaj, M Lawrence, D Paterson, E Bezak, B Thierry, I Kempson, Cross-Correlative Single-Cell Analysis Reveals Biological Mechanisms of Nanoparticle Radiosensitization, *ACS Nano*, 13(5), 5077-5090, 2019.

Micro-Computed Tomography (MCT): A BRIGHT new beamline at ANSTO/Australian Synchrotron

Andrew Stevenson¹; Benedicta Arhatari¹; Rahul Banerjee¹; Ron Bosworth¹; Tom Fiala¹; Emily Griffin¹; Jonathan McKinlay²; Christina Magoulas¹; Tony Mazonowicz¹; Stephen Oelofse¹; Sinem Ozbilgen³; Azizi Rakman¹; Nick Sarris¹; Prithi Tissainayagam¹; Adam Walsh³

1 Australian Synchrotron

2 ANSTO - Australian Synchrotron

3 ANSTO/Australian Synchrotron

Corresponding Author(s): sarrisn@ansto.gov.au, ozbilges@ansto.gov.au, rahulb@ansto.gov.au, oelofses@ansto.gov.au, prithitt@ansto.gov.au, tomf@ansto.gov.au, ron.bosworth@synchrotron.org.au, azizia@ansto.gov.au, tonym@ansto.gov.au, christim@ansto.gov.au, adamw@ansto.gov.au, stevensa@ansto.gov.au, griffine@ansto.gov.au, jonathan.mckinlay@ansto.gov.au, arhatarb@ansto.gov.au

Micro-Computed Tomography (MCT) has been announced as one of the first new beamlines to be constructed at the Australian Synchrotron as part of the BRIGHT program. MCT will complement the existing X-ray imaging/tomography capability provided by the Imaging and Medical Beamline (IMBL), and will target applications requiring higher (sub-micron) spatial resolution and involving smaller samples. MCT will be a bending-magnet beamline, operating in the 8 to 40 keV range, based on a double-multilayer monochromator. This monochromator will be able to be removed from the X-ray beam path, enabling studies with a filtered white beam when required. The photon-delivery system will also house a single-(vertical)bounce mirror, capable of suppressing harmonic contamination in low-energy monochromatic beams and providing the means to shape the spectrum of filtered white beams on the high-energy side. MCT will benefit from X-ray phase-contrast modalities (such as propagation-based, grating-based and speckle) in addition to conventional absorption contrast, and be equipped with a robotic stage for rapid sample exchange. A higher-resolution CT configuration based on the use of a Fresnel zone plate system will also be available. A number of sample environmental stages, such as for high temperature and the application of loads, are planned in collaboration with certain groups in the user community.

Anticipated application areas for non-destructive 3D sample characterization include biomedical/ health science, food, materials science, and palaeontology. This presentation will provide an up- date on the progress of the MCT project, detailing the current design, planning and procurement effort.

Micro-RNA Target Identification for COVID-19 Through Dynamic PERL Programming

Subhojyoti Chatterjee¹ ; Jagriti Chatterjee²

1 Department of Biotechnology, Brindavan College,

2 Karunya Institute of Technology and Sciences

Corresponding Author(s): jagritichatterjee@outlook.com, subhojyotichatterjee@outlook.com

The functioning of gene expression or ribonucleic acid (RNA) silencing is governed by microRNA also known as miRNA is a small non-coding RNA molecule which finds its existence in animals, viruses, or plants. The large part of miRNAs is found to be transcribed from DNA sequences to form primary miRNAs followed by the processing of the precursor miRNAs and mature miRNAs. The miRNAs interconnect with their target genes in an effective manner and is dependent on factors like sub-cellular location of miRNAs, the availability of miRNAs and target miRNAs and their interaction affinities. Along with its involvement in normal functioning of eukaryotic cells, microRNA deregulation is associated with cancer, i.e., chronic lymphocytic leukemia. Therefore, microRNA target identification becomes important to unwind the relationship between microRNA deregulation and human diseases. Towards that direction, we have attempted to use the platform of PERL programming (a user-friendly and dynamic language to easily process and manipulate long sequences), to detect the microRNA target sites in genomic sequences, thereby trying to suppress the expression level for prognosis as well as potential drug target for COVID-19.

Microbeams in a heart beat

Jason Paino¹; Elisabeth Schultke; Timo Kirschstein; Katrin Porath ; Falko Lange; Stefan Fiedler; Jeremy Davis; Elette Engels; Michael Lerch

1 University of Wollongong

Corresponding Author(s): jeremyd@uow.edu.au, elisabeth.schultke@med.uni-rostock.de, timo.kirschstein@uni-rostock.de, stefan.fiedler@embl-hamburg.de, ee215@uowmail.edu.au, falko.lange@uni-rostock.de, katrin.porath@uni-rostock.de, jrp933@uowmail.edu.au, mlerch@uow.edu.au

Synchrotron generated X-ray microbeam radiotherapy (MRT) continues to develop around the globe and at the Australian Synchrotron. Before advancing MRT into the phase of clinical studies, the normal tissue response in organs potentially at risk for adverse effects needs to be tested. In the treatment of malignant tumours in the thoracic cavity, the heart is one of the most important organs at risk. Combining X-Tream dosimetry; one of the leading approaches to dosimetry in small volumes, with the Langendorff model of the beating heart, we have established a suitable ex vivo alternative to short-term in vivo studies. In this work ex vivo spontaneously beating hearts were irradiated with broad beam doses up-to 400 Gy and microbeam peak doses up-to 4,000 Gy while recording ECG activity, coronary perfusion pressure and left ventricular pressure in real time. γ H2AX immunostains of the heart tissue after MRT irradiation confirm spatial fractionation of microbeams is preserved despite the motion of the heart beating.

Prior to this study, it was not known how the electric impulse conducting system of the heart would respond to such high peak doses. To understand the acute impact of MRT on heart function, we conducted a first pilot study in an ex vivo model of the beating rodent heart. Results place the functionally limiting exposure of the heart between 40-400 Gy for broad-beam irradiation and between 400-4,000 Gy for MRT.

Microstructure analysis of Sn/TiO₂ based hybrid nanostructure material

Author(s): Mahmood Jamil¹

Co-author(s): Shanghai Wei¹ ; Mark Taylor¹ ; John Kennedy²

1 The University of Auckland

2 National Isotope Centre, GNS Science.

Corresponding Author(s): s.wei@auckland.ac.nz, mjam790@aucklanduni.ac.nz

Hybrid nanostructured materials address the challenges of low energy and power density, and poor cyclic life of electrochemical energy storage systems. Nanostructured TiO₂ is one such promising candidate because of its comparable capacity to graphite electrode (335 vs 372 mAhg⁻¹). Tin (Sn) is a low cost, abundantly available material possessing a theoretical capacity of 994 mAhg⁻¹ and an excellent electrical conductivity (91.7*10³/cm Ω). However, the Sn insertion/deinsertion process causes massive volume expansion (~300%), resulting in severe pulverization.

This study focuses on the development of Sn/TiO₂ based hybrid nanostructure material that will have advantages of both materials resulting in high electrochemical performance. A two-step electrochemical anodization process was applied to synthesize TiO₂ nanotubes. It was found that altering the anodic conditions affected the morphology and arrays of nanotubes. Concurrently, Sn was deposited by ion beam sputtering and heat-treated at 350°C. XRD, SEM, TEM were employed for morphological analysis of Sn/TiO₂ and cyclic voltammetry (CV) was applied to evaluate the electro- chemical performance. TEM results confirmed the formation of core-shell structure-TiO₂ as a core, and Sn as a shell.

Key words: Hybrid nanostructures, Titanium dioxide (TiO₂), Sn ion beam sputtering, microstructure analysis, electrochemical performance.

Mineral Weathering and Organic Carbon Sequestration in Magnetite Fe Ore Tailings Driven by Organic Matter input and Plant Colonization

Author(s): Songlin Wu¹

Co-author(s): Yunjia Liu ¹ ; Longbin Huang ¹

¹ The University of Queensland

Corresponding Author(s): l.huang@uq.edu.au, songlin.wu@uq.edu.au

Eco-engineering tailings into soil-like substrates is an emerging technology to rehabilitate the tailings landscapes. The formation of water-stable aggregates in finely textured and polymineral magnetite- Fe ore tailings is one of critical processes in the eco-engineering processes. Organic matter (OM) amendment and plant colonization are considered to be effective in enhancing water stable aggregation, but the underlying mechanisms have yet been elucidated. The present study aimed

to characterise detailed changes in physicochemistry, Fe-bearing mineralogy, and organo-mineral interactions in magnetite Fe-ore tailings subject to the combined treatments of OM amendment and plant colonization, by employing various micro-spectroscopic methods, including synchrotron based X-ray absorption fine spectroscopy (XAFS) and nanoscale secondary ion mass spectroscopy (NanoSIMS). The results indicated that OM amendment and plant colonization neutralized the tailings' alkaline pH and facilitated water stable aggregate formation. The resultant aggregates were consequences of ligand promoted bioweathering of primary Fe bearing minerals (mainly biotite- like minerals) and the formation of secondary Fe rich mineral gels. Especially, the sequestration of organic matter (rich in carboxyl and aromatic C) by Fe rich minerals via ligand exchange and/or hydrophobic interactions contributed to the aggregation [1]. These findings have uncovered the role of extra OM and plant driven initial primary Fe bearing mineral weathering and organic carbon sequestration in water-stable aggregate formation in alkaline Fe ore tailings, providing fundamental basis for eco-engineering pedogenesis in the tailings.

References:

[1] Wu et al. (2019) Environ Sci Technol 53, 13720-13731

Miscibility Modulation Enables Highly Efficient Polythiophene: Nonfullerene Solar Cells

Author(s): Zhongxiang Peng¹

Co-author(s): Qi Wang ¹ ; Miaomiao Li ¹ ; Nigel Kirby ² ; Long Ye ¹ ; Yanhou Geng ¹

¹ *Tianjin University*

² *Australian Synchrotron*

Corresponding Author(s): yelong@tju.edu.cn, nigel.kirby@synchrotron.org.au, zxpeng@tju.edu.cn

Polythiophenes have received growing interest in organic solar cells due to the merits of low cost and high scalability of synthesis. However, the power conversion efficiencies (PCEs) of polythiophene:nonfullerene solar cells (10%~12%) is lower than those employing star polymers (>17%). The inferior performance is mostly limited by the unmatched miscibility between polythiophene and acceptors. Herein, the miscibility of polythiophene:nonfullerene blend system was finely tuned by varying the ratios of siloxane-terminated chains and alkyl chains in ester-substituted polythiophenes (Figure 1a) through random copolymerization. Based on a series of the polythiophene and non- fullerene acceptors, the detailed analysis of blend miscibility and performance reveals a surprising anticorrelation between the Flory-Huggins interaction parameter (χ_{aa}) and the optimal time of solvent vapor annealing for device performance across these systems. Primarily due to the slightly higher χ_{aa} , the blend of PDCBT-Cl-Si5 and ITIC-Th1 results in a record-high PCE of 12.85% in polythiophene:nonfullerene solar cells. In addition, GIWAXS analysis (Figure 1b) was also performed to exclude the effect of solvent vapor annealing on crystallinity. Our results not only provide a calculation-guided approach for molecular design but also prove that precise control of the miscibility is an effective way to design high-performance polythiophene:nonfullerene blends and beyond.

Molecular Interplay between SARS-CoV-2 and Human proteins for viral activation and entry, potential drugs and scope of new therapeutics

Naveen Vankadari¹

¹ Monash University

Corresponding Author(s): naveen.vankadari@monash.edu

The pandemic Coronavirus Disease 2019 (COVID19) caused by SARS-CoV-2 is a serious public health concern with global mortality reaching 1 million. Whilst the search for a vaccine is underway, there are several antiviral and antibody treatments being clinically evaluated to fill the “therapeutic gap”. The development of potential drugs requires an understanding of SARS-CoV-2 pathogenicity and mechanism of action. Thus, it is essential to understand the full repertoire of viral proteins and their interplay with host factors. Here, we show how the SARS-CoV-2 spike protein undergoes 3 stages of processing to allow virion activation and host cell infection. We also conduct pre-clinical and cohort studies and found effective viral clearance by Arbores drug treatment in patients. Our comprehensive structural studies reveal why COVID19 is hypervirulent and the reason for the failure of several antibody treatments to date. We demonstrate via molecular dynamics and functional studies how the host proteins CD26, Furin and TMPRSS2 process the viral spike glycoprotein and assist in the viral entry in addition to ACE2. These results recognize the detailed mechanism of spike glycoprotein and reveal new avenues for potential therapeutics to block different stages of viral entry and new pathways for vaccine development.

Molecular insights into the specificity and potency of metabolite-mediated T-cell immunity

Wael Awad¹ ; Geraldine Ler² ; Andrew Keller³ ; Jeffrey Y. W. Mak² ; Xin Yi Lim⁴ ; Jérôme Le Nours³ ; Ligong Liu² ; James McCluskey⁴ ; Alexandra J. Corbett⁴ ; David P. Fairlie² ; Jamie Rossjohn³

1 Monash University

2 Institute for Molecular Bioscience, The University of Queensland, Australia.

3 Infection and Immunity Program and Department of Biochemistry and Molecular Biology, Biomedicine Discovery Institute, Monash University, Australia.

4 Department of Microbiology and Immunology, Peter Doherty Institute for Infection and Immunity, University of Melbourne, Australia.

Corresponding Author(s): wael.awad@monash.edu

Mucosal associated invariant T (MAIT) cells are an abundant human T cells subset that are variably activated by small-molecule metabolites presented by the MHC class 1 related molecule, MR1. During infection with riboflavin-producing microorganisms, the microbial metabolite 5-amino-6-D-ribitylaminouracil (5-A-RU) reacts with glycolysis byproducts of glyoxal/methylglyoxal forming highly potent ribityl pyrimidine ligands. These pyrimidine intermediates are trapped by MR1 and presented on the surface of the antigen-presenting cells encountering the MAIT T cell receptor (TCR) leading to the activation of the MAIT cells. These riboflavin-based MAIT cell agonists are unique for a wide range of microbes and accordingly represent a molecular signature of microbial infection. The most potent MAIT agonist is 5-(2-oxopropylideneamino)-6-D-ribitylaminouracil (5-OP-RU), but the mechanism that underpins this potency remains unclear.

To explore the molecular basis for the high potency of 5-OP-RU as a MAIT agonist, we chemically synthesized and characterized a large panel of 5-OP-RU analogues, termed “altered metabolite ligands” (AMLs), and investigated functionally and structurally their impact on MAIT TCR recognition. Here, modification of the 5-OP-RU ribityl moiety impacted differentially on MAIT TCR binding affinity, consistent with the ability of AMLs to stimulate MAIT cells. Through an analysis of 13 high-resolution (~ 1.9 Å) MAIT TCR-MR1-AML crystal structures, we show that the propensity of MR1 upregulation on the cell surface was related to the nature of MR1-AML interactions. Further, MR1-AML adaptability and a dynamic compensatory interplay at the MAIT TCR-AML-MR1 interface impacted on the affinity of the MAIT TCR-MR1-AML interaction, which ultimately underscored the ability of the AMLs to activate MAIT cells. Therefore, we determined the molecular basis underlying MR1 antigen capture, MAIT TCR recognition and thereby provide insights into MAIT cell antigen specificity and potency.

Awad, W.#, Ler, G.J.M.# et al. (2020). The molecular basis underpinning the potency and specificity of MAIT cell antigens. *Nature Immunology* 21, 400-411.

Salio, M.#, Awad, W.# et al. (2020). Ligand-dependent downregulation of MR1 cell surface expression. *PNAS*, 202003136.

Awad W., et al. (2020). Atypical TRAV1-2- T cell receptor recognition of the antigen-presenting molecule MR1. *J. Biol. Chem.*, in press.

Molybdenum ditelluride: A high rate anode for sodium-ion battery and full cell prototype study

Author(s): Manas Ranjan Panda¹

Co-author(s): Mainak Majumder²; Sagar Mitra²

¹ PhD student, Dept. of Material Sc. and Engineering, Monash University.

² Professor

Corresponding Author(s): manas.panda@monash.edu, mainak.majumder@monash.edu

Two-dimensional (2D) transition metal dichalcogenides (TMDs) with good electronic conductivity and weak interlayer interaction have been intensively studied in the electrochemical processes involving ion migrations. In particular, molybdenum ditelluride (MoTe₂) has emerged as a new material for energy storage applications. We demonstrated a new class of 2D layered structured molybdenum di-telluride (MoTe₂) as anode material in sodium-ion batteries (SIBs) through this work. Synchrotron X-ray diffraction (SXRD) and high-resolution scanning transmission electron microscopy (HRSTEM) confirm the hexagonal structure of MoTe₂, which has the space group, P6₃/mmc. In a half-cell configuration (with respect to sodium metal), the MoTe₂ electrode exhibits an initial specific capacity of 320 mA h g⁻¹ at a current density of 1.0 A g⁻¹, and it retains a high capacity of 270 mA h g⁻¹ after 200 cycles. To detect the phase changes during sodiation/desodiation process and to explore the underlying sodium storage mechanism, SXRD, HRTEM with SAD, X-ray photoelectron spectroscopy (XPS), X-ray absorption near edge structure (XANES) in ex situ mode have been used. Further, a sodium-ion full cell is constructed by coupling the MoTe₂ as anode and sodium vanadium phosphate Na₃V₂(PO₄)₃ (NVP) as cathode. The sodium-ion full cell retains 88 % of its initial capacity after 150 cycles at a current density of 0.5 A g⁻¹. Operating at an average potential of ~2 V, the full cell delivers a high energy density of 414 Wh kg⁻¹. The present study opens up a new direction to the anode materials for rechargeable sodium-ion batteries.

Monodisperse Silver Clusters Stabilized by an Organic Network

Vishkaya Jayalatharachchi¹ ; Jennifer MacLeod² ; Josh Lipton-Duffin¹

1 Queensland University of Technology

2 QUT

Corresponding Author(s): josh.liptonduffin@qut.edu.au, jennifer.macleod@qut.edu.au, vishakya.jayalatharachchi@hdr.qut.edu.au

In this study, we investigate 7-atom metal clusters coordinated by deprotonated 1,3,5-benzenetricarboxylic acid (TMA) molecules on Ag(111). The chemical and spatial precision of these types of monodisperse clusters of atoms has important implications for catalysis and energy production. Deprotonation was examined by X-ray photoemission spectroscopy (XPS) and scanning tunnelling microscopy (STM). The evolution of HOMO-LUMO levels has been studied using a combination of Valence band spectra and Resonant photoemission spectroscopy (RESPES) and compared with the calculated density of states with corresponding charge distribution of intact TMA and deprotonated TMA molecules.

A careful study of the chemical and electronic structure of these clusters will allow us to better understand how to use organic molecules to engineer arrays of single-atom catalysts on surfaces, with the goal of tailoring these 2D materials systems for reactivity and selectivity in targeted catalysed reaction.

New insights into the self-assembly of amphiphilic poly(ethylene glycol-b-caprolactone) diblock copolymers in aqueous solution

Author(s): Khandokar Sadique Faisal¹

Co-author(s): Andrew Clulow²; Marta Krasowska³; Todd Gillam¹; Stanley J. Miklavacic³; Nathan H. Williamson⁴; Anton Blencowe¹

1 University of South Australia, Applied Chemistry and Translational Biomaterials Group

2 Monash University

3 University of South Australia

4 Eunice Kennedy Shriver National Institute of Child Health and Human Development

Corresponding Author(s): anton.blencowe@unisa.edu.au, andrew.clulow@monash.edu, khandokar.faisal@unisa.edu.au, marta.krasowska@unisa.edu.au

The ability to self-assemble into nanostructures is a fundamental phenomenon in many living and non-living systems. The design of polymeric systems that assemble into hierarchically structured nanomaterials requires careful consideration of the microstructure and molecular interactions. For many applications, such as micellar drug delivery systems, precise control over the self-assembly process is required. However, the relationship between molecular structural characteristics of block polymers and their micellar self-assembly mechanisms vary with different block types. In this study, the effect of polymer molecular weight and copolymer block ratio on the micellization of poly(ethylene glycol-b-caprolactone) (PEG-b-PCL) block copolymers was investigated. The stealth properties of PEG and biodegradable nature of PEG-b-PCL makes it a suitable choice for biomedical applications, including tissue engineering and drug delivery. Nuclear magnetic resonance (NMR) and dynamic light scattering (DLS) were used to measure the diffusion of block copolymers in water, from which the hydrodynamic diameters and dispersity of the polymer aggregates were determined; three aggregation scenarios were inferred from the data, including unimers (no self-assembly), large metastable aggregates, and monodisperse micelles. Small-angle x-ray scattering (SAXS) from polymer solutions provided morphological information on the shape of the micelles and their relationship to the polymers microstructure. The PEG molecular weight and PCL:PEG ratio was the primary factor affecting micelle shape. A clear transition from unimers to large aggregates to cylindrical and ellipsoid micelles was observed as the PEG molecular weight and PCL:PEG ratio increased, with an increase in the micelle hydrodynamic radii. We therefore propose a self-assembly phase diagram for the PEG-b-PCL system in aqueous media by combining NMR, DLS and SAXS data.

Block copolymer composition with larger PEG molecular weights and larger PEG-b-PCL block ratios formed more monodisperse micelles, whereas copolymer compositions with smaller PEG molecular weights and smaller PEG-b-PCL block ratios formed large metastable aggregates.

Non-invasive imaging of hydraulic function in leaves, stems and roots

Brendan Choat

Corresponding Author(s): b.choat@westernsydney.edu.au

Plants have evolved a water transport system that relies on water sustaining a tensile force. Counter intuitively, this means water moves through the plant as a liquid under negative absolute pressures. This mechanism is made possible by the intricate plumbing system that constitutes the xylem tissue of plants. However, water under tension is prone to cavitation, which results in the formation of a gas bubble (embolism). Embolism reduces the capacity of the xylem tissue to deliver water to the canopy, eventually causing dieback and whole plant mortality. Xylem embolism is exacerbated by environmental stresses and is now considered one of the leading causes of plant mortality resulting from drought stress. Non-invasive imaging techniques offer the potential to make direct observations on intact plants at high resolution and in real time. In this presentation, I discuss recent exciting developments in the application of non-invasive imaging technologies such as X-ray Micro Computed Tomography (microCT) and optical imaging to studies of plant vascular function. This includes visualisation of xylem networks during drought stress and recovery in leaves, stems and roots. MicroCT imaging of stems and roots indicated that significant embolism formation occurs at similar time points and levels of water stress in dehydrating plants. This result was observed in herbaceous and woody species, and is surprising given previous hydraulic measurements indicating that, within a plant, roots were more vulnerable to drought-induced embolism than stems. A newly developed optical technique indicates that leaf vasculature is also similar in vulnerability to stems and roots. The overlap in vulnerability suggests that induction of embolism occurs at the same time in different organs or is propagated rapidly through the plant. In examining recovery from drought stress, we saw little evidence of embolism refilling in the xylem of woody plants, except in cases where substantial root pressure is produced. These results suggest that embolism refilling is less widespread than previously thought.

Novel optics for optimizing the 3rd and 4th Generation Synchrotron Radiation Facility

Author(s): Yoshio Ichi¹

Co-author(s): Masahiko Kanaoka ; Bui Van Pho ; Hiromi Okada

1 JTEC Corporation

Corresponding Author(s): yoshio.ichii@j-tec.co.jp

We, JTEC Corporation, have manufactured various High-Precision X-ray Mirrors by using EEM, nano-figuring, and RADSI and MSI, nano-measurements [1] derived from Osaka University. So far, we have fabricated over 890 mirrors in worldwide synchrotron facility, and XFEL. We give an overview of our production examples such as super flat mirror for M1(pv 1~2nm), KB mirror (for nano-focusing) [2,3] Advanced KB Mirror (for imaging and nano-focusing) [4], Ellipsoidal /Paraboloidal Mirror (micro focusing/ collimating)[5] that have a possibility to contribute the best use of the Australian synchrotron. Advanced KB Mirrors can increase the stability of imaging/focusing while maintaining the conventional brilliance and the focal size. Ellipsoidal / Paraboloidal Mirrors can decrease the number of reflections to keep the brightness.

Kazuto Yamauchi et al., Rev. Sci. Instrum. 73, 4028 (2002)

Haruhiko Ohashi et al., J. Phys.: Conf. 425, 052018 (2013)

Hirokatsu Yumoto et al., Nature Photon. 7, 43 (2013)

Satoshi Matsuyama, et.al., Scientific Reports, 7:46358 (2017)

Valentina Bisogni, et.al., the 11th International Conference on Inelastic X-ray Scattering, June 23-28 (2019)

Peering into Batteries: Electrochemical Insight through Operando Methods

Esther Takeuchi

Corresponding Author(s): esther.takeuchi@stonybrook.edu

Esther S. Takeuchi

William and Jane Knapp Chair of Energy and the Environment Stony Brook University

Chief Scientist and Chair Brookhaven National Laboratory

Emerging new applications such as electric vehicles and integration of renewable energy demand expanded function of batteries. However, complex phase transitions of electroactive materials, kinetics of ion transport, and electrode-electrolyte interfacial reactions, still limit the full understanding of functional and degradation mechanisms. To date, many interrogation approaches of batteries are static, unable to track mechanisms arising from dynamic battery (dis)charge behavior. Emerging in situ and operando characterization methodologies focused on multiple size domains and time scales are becoming a powerful approach to resolve existing limitations of material and battery design and provide insights for future directions. A series of illustrative examples of in situ and operando characterization over atomic, crystallite/particle, electrode, and battery system length scales will be provided for lithium based batteries as well as those beyond lithium ion. The use of multiple synergistic methods to gain further insight will also be highlighted.

Phase-contrast tomography for breast cancer imaging at Imaging and Medical Beamline of the Australian Synchrotron

Timur Gureyev¹

1 the University of Melbourne

Corresponding Author(s): timur.gureyev@unimelb.edu.au

T. E. Gureyev^{1,2,3,4}, B. Arhatari^{5,6}, A. Aminzadeh¹, Ya. I. Nesterets^{7,4}, S. T. Taba², E. Vafa², S.

C. Mayo⁷, D. Thompson^{7,4}, D. Lockie⁸, J. Fox³, B. Kumar³, Z. Prodanovic³, D. Hausermann⁵, A. Maksimenko⁵, C. Hall⁵, A. G. Peele^{5,6}, M. Dimmock³, K. M. Pavlov^{9,3,4}, S. Lewis², G. Tromba¹⁰, H.M. Quiney¹ and P. C. Brennan²

1 The University of Melbourne, Parkville 3010, Australia

2 The University of Sydney, Lidcombe 2141, Australia

3 Monash University, Clayton 3800, Australia

4 University of New England, Armidale 2351, Australia

5 Australian Synchrotron, ANSTO, Clayton 3168, Australia

6 La Trobe University, Bundoora 3086, Australia

7 Commonwealth Scientific and Industrial Research Organisation, Clayton 3168, Australia

8 Maroondah BreastScreen, Ringwood East 3135, Australia

9 University of Canterbury, Christchurch 8041, New Zealand 10 Elettra Sincrotrone, 34149 Basovizza, Trieste, Italy

Electronic mail: timur.gureyev@unimelb.edu.au

Breast cancer is one of the two leading causes of cancer fatalities among women in most industrialized countries. This type of cancer is very aggressive, with success of the treatment depending heavily on early detection. Health authorities in most countries recommend regular screening of women over a particular age, with 2D X-ray mammography being the main screening and diagnostic technique. Unfortunately, mammography produces a relatively high percentage of both false- positive and false-negative results. In this research, we aim at defining and developing a practical imaging setup for whole breast imaging using propagation-based phase-contrast computed tomography (PB-CT) in such a way that, compared to the best presently utilised medical X-ray imaging techniques: (a) the quality and the diagnostic value of the obtained 3D images are higher, (b) the delivered radiation dose is lower and (c) the need for painful breast compression is removed. To date, we have imaged 95 unfixed complete mastectomy samples with and without breast cancer lesions using absorption-only CT and PB-CT techniques at the Imaging and Medical Beamline (IMBL) of the Australian Synchrotron. The radiation doses delivered to the mastectomy samples during the scans were comparable to those approved for mammographic screening. Physical characteristics of the re- constructed images, such as spatial resolution and signal-to-noise ratio, and radiologic quality were assessed and compared to conventional absorption-based CT.

Our results demonstrate that PB-CT holds a high potential for improving on the quality and diagnostic value of images obtained using existing medical X-ray technologies, such as mammography and digital breast tomosynthesis.

When implemented at IMBL in 2021, PB-CT will be used to complement existing medical breast imaging modalities, leading to more accurate breast cancer diagnosis [1, 2].

[1] S.T. Taba et al., *Am.J.Roentgen.*, 211, 133-145 (2018).

[2] T.E. Gureyev et al., *Med.Phys.*, 46, 5478-5487 (2019).

Probing phase transitions of metal-organic frameworks by THz/Far- IR

JINGWEI HOU¹ ; VICKI CHEN¹ ; THOMAS BENNETT²

1 University of Queensland

2 University of Cambridge

Corresponding Author(s): tdb35@cam.ac.uk, v.chen@uq.edu.au, jingwei.hou@uq.edu.au

Current research on metal–organic frameworks (MOFs) has concentrated predominantly on the properties of ordered crystalline phases. However, there is growing recognition of the importance of the physical properties of MOFs. In particular, the role of disorder, defects, and structural flexibility in installing beneficial physical behaviour is now widely studied. We synthesised four novel crystalline zeolitic imidazolate framework (ZIF) structures using a mixed-ligand approach. The inclusion of both imidazolate and halogenated benzimidazolate-derived linkers leads to glass-forming behaviour by all four structures. Melting temperatures are observed to depend on both electronic and steric effects. In situ THz/far-IR spectroscopic techniques reveal the dynamic structural properties of crystal, glass, and liquid phases of the halogenated ZIFs, linking the melting behaviour of ZIFs to the propensity of the ZnN₄ tetrahedra to undergo thermally induced deformation.

Probing the cell wall response of Sphagnum moss to a changing aqueous chemical environment. A synchrotron infrared microscopy study.

Author(s): Annaleise Klein¹

Co-author(s): Ewen Silvester²

¹ ANSTO

² La Trobe University

Corresponding Author(s): kleina@ansto.gov.au, e.silvester@latrobe.edu.au

Sphagnum is an important species of moss in peatland ecosystems and subsequently plays a vital role in carbon sequestration. Understanding its physiology is essential for predicting the possible impacts of a changing climate. In particular, the cell wall tissue of Sphagnum is composed of a high proportion of carboxylated polysaccharides, acting as ion exchangers, and is therefore sensitive to changes such as pH and metal ion concentrations in the surrounding environment. Using synchrotron infrared microscopy coupled with a flow-through liquid cell, the influence of pH and metal ions (Na⁺ and Ca²⁺) on the cell wall chemistry of freshly sectioned Sphagnum cristatum stems was investigated. The carboxylate functional groups in the cell wall were shown to behave as a monoprotic aliphatic acid with an acid dissociation constant (pK_a) of 4.976.04. Furthermore, the cell wall material showed a high affinity for calcium, with the binding constant (K) determined to be 103.9104.7 for a 1:1 complex. These results allow for the prediction of environmental chemical conditions for which calcium uptake in Sphagnum can occur, and improves our ability to understand the patterns of distribution of Sphagnum in the environment.¹

¹Silvester et al. (2018) Environ. Chem. 15, 513.

Protein-Lipid interactions and protein structures in multi-component systems

Leonie van 't Hag¹

¹ Monash University

Corresponding Author(s): leonie.vanthag@monash.edu

Understanding protein-lipid interactions and the resulting protein structures is crucial for evolving food technology, biological and biomedical applications of nanomaterials. Knowledge regarding the effect of the multiple components in the system on the nanostructure, within the context of the application, is needed. Lyotropic liquid crystal design rules¹ were developed and the effect of protein encapsulation on lipid self-assembly materials was extensively studied by us in recent years. We used this to obtain a protein-eye view of the in meso crystallisation method of integral membrane proteins from the bicontinuous cubic phase over time.² Recently there has been a shift towards using biomimetic cubic phases,^{1,3,4} and SAXS studies at the Australian Synchrotron were used to investigate encapsulation of biologically relevant proteins and peptides.

Pulling Milk Lipids Apart and Putting Them Back Together Again—A Self-assembly Approach

Andrew Clulow¹; Malinda Salim²; Anna Pham³; Syaza Binte Abu Bakar; Adrian Hawley⁴; Ben Boyd²

1 Monash University

3 Monash Institute of Pharmaceutical Sciences/ Monash University

4 Australian Synchrotron

Corresponding Author(s): ben.boyd@monash.edu, malinda.salim@monash.edu, anna.pham@monash.edu, syaza.binteabubakar@m andrew.clulow@monash.edu, adrianh@ansto.gov.au

Introduction: Digestion of the milk lipids in our intestines yields monoglycerides and fatty acids that self-assemble into a variety of liquid crystalline structures. This self-assembly process is species dependent,[1,2] suggesting an important role for these structures in infant nutrition. Our recent work on the SAXS/WAXS beamline has focussed on studying how the lipid compositions of different milks generates different self-assembled structures both by digesting milk and analysing the by-products and assembling lipid mixtures that replicate the milk of different species from readily available fats and oils.

Methods: Small angle X-ray scattering (SAXS) with in situ lipolysis was used to measure the lipid self-assembly in various types of milk and infant formulae during digestion.[3] The structures observed were correlated with the resulting digestion products using a combination of liquid chromatography coupled to mass spectrometry (LCMS) and principle component analysis (PCA).[4] Lipid mixtures were prepared in the lab by mixing either homotriglycerides or natural fats and oils. These lipid mixtures were dispersed to form milk-like emulsions and their lipid self-assembly during digestion was compared with the milks and infant formulae.

Results & Discussion: This presentation will discuss the lipid liquid crystalline structures formed in a variety of milks and milk-like emulsions during digestion and how they can be mimicked. The lipid self-assembly in cow and human milk was shown to be replicated when the right balance of emulsified lipids was prepared by mixing homotriglycerides or blending milk fat with natural oils.[5] These emulsions provide representative digestive colloid structures through which to analyse the impact of lipid composition on self-assembly and bioactive delivery.

References

Clulow, A. J.; Salim, M.; Hawley, A.; Boyd, B. J. A closer look at the behaviour of milk lipids during digestion. *Chem. Phys. Lipids* 2018, 211, 107-116.

S. Salentinig, S. Phan, A. Hawley, B. J. Boyd, *Angew. Chem. Int. Ed.* 2015, 54, 1600-1603.

Warren, D. B.; Anby, M. U.; Hawley, A.; Boyd, B. J. Real Time Evolution of Liquid Crystalline Nanostructure during the Digestion of Formulation Lipids Using Synchrotron Small-Angle X-ray Scattering. *Langmuir* 2011, 27 (15), 9528-9534.

Pham, A. C.; Peng, K.-Y.; Salim, M.; Ramirez, G.; Hawley, A.; Clulow, A. J.; Boyd, B. J. Correlating Digestion-Driven Self-Assembly in Milk and Infant Formulas with Changes in Lipid Composition. *ACS Appl. Bio Mater.* 2020, 3 (5), 3087-3098.

Clulow, A. J.; Salim, M.; Hawley, A.; Boyd, B. J. Milk mimicry – Triglyceride mixtures that mimic lipid structuring during the digestion of bovine and human milk. *Food Hydrocolloids* 2021, 110, 106126.

Quantification of Material Gradients in Nanocrystals

Author(s): Boldt Klaus^{s1}

Co-author(s): Stuart Bartlett²; Nicholas Kirkwood³; Bernt Johannessen⁴

1 University of Konstanz

2 Diamond Light Source

3 The University of Melbourne

4 Australian Synchrotron

Corresponding Author(s): klaus.boldt@uni-konstanz.de, bernt.j@synchrotron.org.au

Core/shell nanocrystals in which the materials change gradually from core to shell are very, very promising structures to optimise the opto-electronic properties and quantum efficiencies of nanoscale semiconductors. Gradients are able to minimise crystal defects, lattice mismatch, and can be used to engineer the envelope wave function of excitons in order to suppress non-radiative Auger processes. However, due to the small size of the particles, so far no reliable method exists to quantify the extent of such a gradient.

In this work we have measured the material gradient of ZnSe/CdS core/shell nanocrystals, which were synthesised at elevated temperatures (260 and 290 °C), which controls the rate of radial ion migration. We used EXAFS spectroscopy to determine the average coordination of selenium ions, which were fitted to a continuum model for the radial distribution of cations and anions [2].

It could be shown that for the 260 °C sample the data shows strong cation migration, which transports significant amounts (> 50%) of cadmium into the core, while the anion gradient is consistent with negligible ion migration beyond the interfacial monolayer. This is significant, because many shell growth protocols that are assumed to produce sharp interfaces are performed at similar temperatures. At higher temperatures of 290 °C the data deviates strongly from the model, with effectively less cation migration. This is explained by the formation of an ordered Zn_{0.5}Cd_{0.5}Se superlattice in the core in order to mitigate the lattice mismatch due to the increasing CdSe content of the core [3]. Raman spectroscopy shows selective resonant enhancement of the core LO phonon overtones, which indicates that the exciton is primarily localized in the core and at interfacial traps, and that the electronic structure flips from a type-II to a type-I system.

Hence, the combination of X-ray and Raman spectroscopy is able to identify both the chemical and electronic structure of core/shell particles and produces an accurate gradient model that can be employed in more precise and predictive structural calculations. The high-temperature product sheds light on why some highly emissive nanocrystals still blink and struggle to reach unity quantum yield [4].

References:

Boldt, K.; Bartlett, S.; Kirkwood, N.; Johannessen, B. Quantification of Material Gradients in Core/Shell Nanocrystals Using EXAFS Spectroscopy. *Nano Lett.* 2020, 20, 1009-1017.

Cragg, G. E.; Efros, A. L. Suppression of Auger Processes in Confined Structures. *Nano Lett.* 2010, 10, 313-317.

Wei, S. H.; Ferreira, L. G.; Zunger, A. First-Principles calculation of Temperature-Composition Phase of Semiconductor Alloys. *Phys. Rev. B* 1990, 41, 8240-8269.

Boldt, K.; Kirkwood, N.; Beane, G. A.; Mulvaney, P. Synthesis of Highly Luminescent and Photo- Stable, Graded Shell CdSe/CdxZn1-xS Nanoparticles by In Situ Alloying. *Chem. Mater.* 2013, 25, 4731-4738.

Quantitative Determination of Protein Solubility in Ionic Liquids

Author(s): Stuart Brown¹

Co-author(s): Tamar Greaves²; Calum Drummond²

¹ RMIT

² RMIT University

Corresponding Author(s): tamar.greaves@rmit.edu.au, s3399895@student.rmit.edu.au, calum.drummond@rmit.edu.au

Proteins are often utilised for a range of applications in the pharmaceutical, biological, chemical and food industries[1-2]. The ideal solvent for hydrophilic proteins is usually buffered water due to its minimal cost, and ability to mimic the native environment of proteins, however many proteins are hydrophobic and have poor solubility in water. Because of this, organic solvents have been investigated as an alternative solvent for biocatalysis[3] and protein extraction[4], but often have detrimental effects on the protein stability and structure. We propose to use ionic liquids (ILs) as an alternative solvent, or as an additive in aqueous solutions, to quantify the solubility and stability of proteins. Initially the model protein lysozyme will be tested in ILs from highly dilute to neat. A novel, high throughput method has been developed to quantitatively determine the solubility of lysozyme. The aim is to explore specific-ion effects and how these differ for concentrated IL solutions compared to conventional dilute salts. A variety of techniques including UV/vis spectroscopy, Fourier-transformation infrared spectroscopy, circular dichroism and small angle x-ray scattering will be used to describe the stability and structure of the protein, and to gain insight into its interactions with ILs. It is hoped that any solubility trends present for lysozyme or specific ions can then be extrapolated to other proteins. Further studies will be done to compare any variations in the specific ion effects on different proteins and to begin building a database of quantified protein solubility and stability in ILs.

Egorova, K. S.; Gordeev, E. G.; Ananikov, V. P., Biological Activity of Ionic Liquids and Their Application in Pharmaceuticals and Medicine. *Chemical Reviews* 2017, 117 (10), 7132-7189.

van Rantwijk, F.; Sheldon, R. A., Biocatalysis in Ionic Liquids. *Chemical Reviews* 2007, 107 (6), 2757-2785.

Klibanov, A. M., Improving enzymes by using them in organic solvents. *Nature* 2001, 409 (6817), 241-246.

Hyde, A. M.; Zultanski, S. L.; Waldman, J. H.; Zhong, Y.-L.; Shevlin, M.; Peng, F., General Principles and Strategies for Salting-Out Informed by the Hofmeister Series. *Organic Process Research & Development* 2017, 21 (9), 1355-1370.

Resonant Tender X-ray Diffraction for Disclosing the Molecular Packing of Paracrystalline Conjugated Polymer Films

Chris McNeill¹

¹ Monash University

Corresponding Author(s): christopher.mcneill@monash.edu

The performance of optoelectronic devices based on conjugated polymers is critically dependent upon molecular packing; however the paracrystalline nature of these materials limits the amount of information that can be extracted from conventional X-ray diffraction. Resonant diffraction (also known as anomalous diffraction) occurs when the X-ray energy used coincides with an X-ray absorption edge in one of the constituent elements in the sample. The rapid changes in diffraction intensity that occur as the X-ray energy is varied across an absorption edge provide additional information that is lost in a conventional nonresonant experiment. Taking advantage of the fact that many conjugated polymers contain sulfur as heteroatoms, this work reveals pronounced resonant diffraction effects at the sulfur K-edge with a particular focus on the well-studied electron transporting polymer poly([N,N'-bis(2-octyldodecyl)-naphthalene-1,4,5,8-bis(dicarboximide)-2,6-diyl]-alt-5,5'-(2,2'-bithiophene)), P(NDI2ODT2). The observed behavior is found to be consistent with the theory of resonant diffraction, and by simulating the energy-dependent peak intensity based on proposed crystal structures for P(NDI2OD-T2) it is shown that resonant diffraction can discriminate between different crystalline packing structures. The utilization of resonant diffraction opens up a new way to unlock important microstructural information about conjugated polymers for which only a handful of diffraction peaks are typically available.

Robust Biomimetic Ti₃C₂T_x MXene Films for High Performance Applications

KEN ALDREN USMAN¹; Jizhen Zhang²; Peter Lynch²; Pablo Mota-Santiago³; Dylan Hegh⁴; Si Qin⁴; Joselito Razal⁵

1 Institute for Frontier Materials, Deakin University

2 Institute for Frontier Materials, Deakin University, Geelong, VIC 3216, Australia

3 Australia Australian Synchrotron, Clayton, VIC 3168, Australia

4 Institute for Frontier Materials, Deakin University, Geelong, VIC 3216

5 Deakin Univeristy, Insitute for Frontier Materials

Corresponding Author(s): joselito.razal@deakin.edu.au, peter.lynch@deakin.edu.au, kausman@deakin.edu.au, pablom@ansto.gov.au, dylan.hegh@deakin.edu, zja@deakin.edu.au, si.qin@deakin.edu.au

The remarkable electrical conductivity, high specific capacitance, and excellent colloidal stability of two-dimensional Ti₃C₂T_x MXene nanosheets (referred to as MXene) have made them promising candidates for a wide variety of applications including in wearable electronics, energy storage, sensors, and electromagnetic interference shielding. However, MXene architectures with high conductivity and electrochemical capacitance exhibit poor tensile properties (i.e. tensile strength and toughness of ~34 MPa and ~0.6 MJ m⁻³, respectively). Here, we report that sequential bridging (SB) of MXene sheets significantly enhances the mechanical properties of its free-standing films, with improvements in strength and toughness of up to ~339 MPa and ~12.0 MJ m⁻³, respectively, while simultaneously retaining both high conductivity (~4,850 S cm⁻¹) and volumetric capacitance (~1,125 F cm⁻³). It was found that through this method, highly aligned framework with consistent inter-layer spacing between MXene sheets can be achieved. In contrast to the conventional biomimetic methods of fabricating MXene architectures, this strategy was able to restrict the increase in interlayer spacing in MXene films, thereby minimizing structural voids and resulting in retained electrical contact. Based on our results, the SB method provides a versatile modification strategy towards the processing of robust and multi-functional MXene-based materials without the compromise in electrical conductivity and electrochemical performance.

Role on Methylammonium Lead Bromide on Microstructure, Photophysics, and Device Performance in Triple Cation based Perovskite Solar Cells

Author(s): Naresh Chandrasekaran¹

Co-author(s): Jacek Jasieniak²

¹ Monash University

² ARC Centre of Excellence in Exciton Science, Monash University, Clayton, Victoria 3800, Australia

Corresponding Author(s): jacek.jasieniak@monash.edu, naresh.chandrasekaran@monash.edu

Role on Methylammonium Lead Bromide on Microstructure, Photophysics, and Device Performance in Triple Cation based Perovskite Solar Cells

Solution processable hybrid perovskite materials have gained significant interest in recent years owing to the ability to control the optical and electrical properties via compositional engineering. But the influence of compositional engineering on microstructure formation and charge carrier dynamics in the solar cell device is poorly understood. [1,2]

Here, we fabricated Cs-FAPbI₃-MAPbBr₃ triple cation mixed cation perovskite solar cells by systematically varying the concentration of MAPbBr₃. Using in-situ temperature-dependent XRD and grazing incidence wide-angle X-ray scattering techniques, the evolution of microstructure with a change in the MABr₃ concentration is revealed. A combination of advanced transient characterisation is then used to correlate the microstructure evolution and perovskite solar cell device performance. GIWAXS results reveal that an optimum concentration (0.15 mol%) of MAPbBr₃ is required to achieve mixed perovskite film without any secondary phase. We also found that the perovskite crystals have a preferential orientation about 45° with respect to the substrate for films with an optimal concentration of MABr.

The absence of secondary phase and oriented crystals helps in improving the charge transport inside the device and increasing the solar cell performance. The findings presented here elucidate the microstructure evolution process in different mixed cation perovskites and their role on the charge carrier dynamics and device performance which helps to develop new perovskite materials for high- performance solar cells.

References

- Jeon, N. J.; Noh, J. H.; Yang, W. S.; Kim, Y. C.; Ryu, S.; Seo, J.; Seok, S. I. Compositional Engineering of Perovskite Materials for High-Performance Solar Cells. *Nature* 2015, 517 (7535), 476-480.
- Xu, Z.; Liu, Z.; Li, N.; Tang, G.; Zheng, G.; Zhu, C.; Chen, Y.; Wang, L.; Huang, Y.; Li, L.; Zhou, N.; Hong, J.; Chen, Q.; Zhou, H. A Thermodynamically Favored Crystal Orientation in Mixed Formamidinium/Methylammonium Perovskite for Efficient Solar Cells. *Adv. Mater.* 2019, 31 (24), 1900390.

Rotary Computed Laminography and Tomosynthesis geometries using ASTRA Toolbox

Benedicta Arhatari¹; Chris Hall¹ ; Sinem Ozbilgen¹; Christina Magoulas¹ ; Andrew Stevenson¹

1 ANSTO/Australian Synchrotron

Corresponding Author(s): stevensa@ansto.gov.au, ozbilges@ansto.gov.au, christim@ansto.gov.au, arhatarb@ansto.gov.au, christoh@ansto.gov.au

The ideal form for X-ray Computed Tomography (CT) is cylindrical geometry. However, for large flat, laterally extended objects such as circuit boards or paintings, the object may not physically fit longitudinally when it is being scanned using a conventional CT geometry. In some cases, the total X-ray transmission may be too low in the direction of the longitudinally extended object. In this case, we need to use Laminography or Tomosynthesis geometries. The new MCT beamline as part of the BRIGHT program at the Australian Synchrotron will use these Laminography and Tomosynthesis geometries for large flat, longitudinally extended samples. In Tomosynthesis, projection images are acquired over a limited angular range to prevent the essentially zero transmission from the thickest part of the sample. In Laminography, the rotation axis is no longer perpendicular to the plane defined by the beam direction and the rows of detector pixels. Instead, it is deliberately tilted with respect to that plane. Neither Tomosynthesis nor Laminography data can be reconstructed using conventional CT algorithms. In this study, we will use open source ASTRA toolbox [1] in creating (simulating) projections (images) and doing reconstruction for Laminography and Tomosynthesis geometries. This study is part of the preparation for developing a comprehensive reconstruction pipeline for the MCT beamline.

1. Wim van Aarle, W.J.P., Jeroen Cant, Eline Janssens, Folkert Bleichrodt, Andrei Dabrovolski, Jan De Beenhouwer, K. Joost Batenburg, and Jan Sijbers, Fast and flexible X-ray tomography using the ASTRA toolbox. Optics Express 2016. 24(22): p. 25129-25147.

Separating Macro- and Nano-structural Effects in Intensity Correlation Measurements of Self-assembled Lipid Materials

Author(s): Jack Binns¹

Co-author(s): Tamar Greaves¹; Connie Darmanin²; Brian Abbey³; Peter Berntsen³; Sachini Kadaoluwa Pathirannahalge¹; Francisco Gian Roque³; Andrew Martin¹

¹ RMIT University

² La Trobe

³ La Trobe University

Corresponding Author(s): cdcoeltu@gmail.com, tamar.greaves@rmit.edu.au, p.berntsen@latrobe.edu.au, andrew.martin@rmit.edu.au, jack.binns@rmit.edu.au

By correlating large ensembles of X-ray scattering data, fluctuation X-ray scattering can extract atomic and nanoscale structural information from a range of systems including colloidal glasses and crystals, liquid-crystal membranes, nanoparticles, and magnetic domains [1-4]. Real-space pair-angle distribution functions are higher order analogues of the basic pair-distribution functions and are rich in information about orientation and bond angles. This method maps fluctuations of scattered intensity into three- and four-atom correlation functions which encode two pairwise distances and one relative angle [5-7].

Here we present results of fluctuation scattering experiments on the inverted hexagonal phase of a model self-assembled lipid system (cetyltrimethylammonium bromide-water). Using newly developed semiautomated algorithms for big datasets (>1000 patterns) we uncover a macroscopic preferred orientation effect which masks the nano-structural signal due to intensity fluctuations. Texture phenomena such as a preferred orientation, strain and peak broadening are commonly encountered throughout materials science. By simulating distorted datasets, we explore how correlation plots are altered by macroscale effects and present methods for disentangling structural information at these two length scales, broadening the range of materials and phase transitions amenable to fluctuation scattering analysis.

P. Wochner, C. Gutt, T. Autenrieth, T. Demmer, V. Bugaev, A. D. Ortiz, A. Duri, F. Zontone, G. Grübel, and H. Dosch, *Proceedings of the National Academy of Sciences of the United States of America* 106, 11511–11514 (2009).

I. A. Zaluzhnyy, R. P. Kurta, N. Mukharamova, Y. Y. Kim, R. M. Khubbutdinov, D. Dzhigaev, V.

V. Lebedev, E. S. Pikina, E. I. Kats, N. A. Clark, M. Sprung, B. I. Ostrovskii, and I. A. Vartanyants, *Physical Review E* 98, 1–8 (2018).

R. P. Kurta, L. Wiegart, A. Flueraşu, and A. Madsen, *IUCrJ* 6, 635–648 (2019).

R. Su, K. A. Seu, D. Parks, J. J. Kan, E. E. Fullerton, S. Roy, and S. D. Kevan, *Physical Review Letters* 107, 16–19 (2011).

[5] A. V. Martin, *IUCrJ* 4, 24–36 (2017)

Martin, A. V., et al., *Communications Materials*, 1(40), 1–8 (2020)

Martin, A. V., Bøjesen, E. D., Petersen, T. C., Hu, C., Biggs, M. J., Weyland, M., & Liu, A. C. Y., Small, 200828, 1–6. (2020)

Serial crystallography at the Australian Synchrotron

Author(s): Connie Darmanin¹

Co-author(s): Marjan Hadian-Jazi ² ; Peter Berntsen ³ ; Hugh Marman ³ ; Brian Abbey ³

1 La Trobe

2 La Trobe University and ANSTO

3 La Trobe University

Corresponding Author(s): p.berntsen@latrobe.edu.au, m.hadianjazi@latrobe.edu.au, cdcoeltu@gmail.com

Serial Synchrotron Crystallography (SSX) is rapidly emerging as a promising technique for collecting data for time-resolved structural studies or for performing room temperature micro-crystallography measurements using micro-focused beamlines. SSX is often performed using high frame rate detectors in combination with continuous sample scanning or high-viscous or liquid jet injectors. When performed using ultra-bright X-ray Free Electron Laser (XFEL) sources serial crystallography typically involves a process known as 'diffract-and-destroy' where each crystal is measured just once before it is destroyed by the intense XFEL pulse. In SSX, however, particularly when using high- viscous injectors (HVIs) such as Lipidico, the crystal can be intercepted multiple times by the X-ray beam prior to exiting the interaction region. This has a number of important consequences for SSX including whether these multiple-hits can be incorporated into the data analysis or whether they need to be excluded due to the potential impact of radiation damage. Here we investigate the occurrence and characteristics of multiple hits on single crystals using SSX with Lipidico.

Side-reaction-free direct arylation polycondensation of chlorinated thiophene derivatives to high mobility conjugated polymers

Ying Sui¹ ; Yunfeng Deng¹ ; Yanhou Geng¹

¹ Tianjin University

Corresponding Author(s): yunfeng.deng@tju.edu.cn, [syinq@tju.edu.cn](mailto:sying@tju.edu.cn), yanhou.geng@tju.edu.cn

High mobility conjugated polymers (CPs) are highly desired for printable electronics. Direct arylation polycondensation (DAP) offers a straightforward, atomic-economic and eco-friendly protocol for the preparation of CPs. C-H monomer with high reactivity and selectivity is crucial to the large-scale synthesis of CPs. Herein, we demonstrated that chlorination enables the efficient DAP of simply-synthesized thiophene derivatives, i.e., 3,3[*g*,4,4[*g*-tetrachloro-2,2[*g*-bithiophene (4CIBT) and (E)-1,2-bis(3,4-dichlorothiophen-2-yl)ethene (4CITVT). This finding allows the facile synthesis of high molecular weight CPs via DAP. When copolymerizing with diketopyrrolopyrrole derivatives, 4CITVT prepared the CP with electron mobility up to 1.44 cm²V⁻¹s⁻¹ via DAP. According to the 2D-GIWAXS pattern, the polymer exhibited edge-on packing mode. This work demonstrates that chlorinated thiophene derivatives are promising C-H monomers for large-scale synthesis of high mobility CPs via atom-economical and “green” method, i.e., DAP.

Soft x-ray studies of molecular nanoarchitectures

Jennifer MacLeod¹ |

¹ QUT

Corresponding Author(s): jennifer.macleod@qut.edu.au

One of the goals of nanoscience is achieving precise control over the structure and function of nanoscale architectures at surfaces. Bottom-up approaches using molecular building blocks present a flexible and intuitive approach to this challenge. Combining the Lego-like modularity of molecules with the epitaxial and reactive influences of surfaces creates a range of opportunities to build exciting new nanoarchitectures.

Our recent work has focused on studying the reactions of halogenated and carboxylated molecules at metal surfaces, where we investigate their adsorption, self-assembly, coupling reactions and the subsequent formation of oligomeric and polymeric structures. Understanding the on-surface behavior of the molecules is possible using a combination of scanning tunneling microscopy, photoelectron spectroscopy and near-edge x-ray absorption fine structure. We are particularly interested in looking at how the structure of these molecular systems affects their electronic properties, and I will discuss our progress in measuring both the filled and unfilled electronic states of these materials.

Soil carbon research from past, present and future using synchrotron-based techniques

Author(s): Han Weng¹

Co-author(s): Lukas Van Zwieten² ; Stephen Joseph³ ; Caixian Tang⁴ ; Roger Armstrong⁵ ; Peter M. Kopittke¹

1 The University of Queensland

2 NSW Department of Primary Industries; Southern Cross Plant Sciences

3 University of New South Wales, Sydney, Australia

4 Department of Animal, Plant and Soil Sciences, La Trobe University, Melbourne, Australia

5 Agriculture Victoria, Horsham, Australia

Corresponding Author(s): lukas.van.zwieten@dpi.nsw.gov.au, h.weng@uq.edu.au, c.tang@latrobe.edu.au, p.kopittke@uq.edu.au

Building and protecting soil carbon is critical to agricultural productivity, soil health and climate change mitigation. This study aims to answer new questions of the molecular scale mechanisms at the organo-mineral interfaces for building soil carbon in the past: Terra Preta Australis (ancient indigenous dark earth, dated back to 1600 years BP); present: the longest, continuous biochar field experiment in the world, located at Wollongbar, New South Wales (building new carbon over 14 years); future: the Australian Soil Free Air CO₂ Enrichment (SoilFACE) field facility at Horsham, Victoria (mimicking elevated CO₂ conditions in the field over 8.5 years in the Southern Hemisphere). Based upon synchrotron-based in situ spectromicroscopy, we reveal the functional complexity and spatial resolution of soil organic carbon under contrasting management practices, cropping histories and soil types over millennium. It will provide critical information to advance knowledge of building soil carbon for productive, sustainable and resilient cropping systems.

Solvent properties of protic ionic liquid-water mixtures, and their application to biological molecules

Qi (Hank) Han¹; Calum Drummond²; Tamar Greaves²

¹ RMIT University, College of Science, Engineering and Health

² RMIT University

Corresponding Author(s): tamar.greaves@rmit.edu.au, qi.han@rmit.edu.au, calum.drummond@rmit.edu.au

Protic ionic liquids (PILs) are cost efficient “designer” solvents which can be tailored to have properties suitable for a broad range of applications. PILs are also being combined with molecular solvents to enable more control over the solvent environment, driven by a need to reduce their cost and viscosity. However, there are relatively few structure-property studies which look at these more complex mixtures. We have explored the solvation properties of common PIL-molecular solvents using various techniques,[1] and have identified many interesting solvent properties of these solutions, and their interactions with solutes.

In this presentation I will discuss how we are using our understanding of PIL-water solvent properties to design and characterise solvents for biological molecules. In particular, we are targeting being able to control protein solubility and stability, which are critical for applications in bioprocessing, biocatalysis, protein crystallography and cryopreservation. We have explored lysozyme as a model protein in various PIL-water systems, predominantly using spectroscopic techniques and small angle x-ray scattering (SAXS).[2-3] From this we have been able to identify which PILs are more biocompatible, and to identify specific conformational changes of lysozyme due to the presence of PILs.[4] More recently, we have used protein crystallography to identify specific binding sites of the PIL ions and water to lysozyme.[4]

References

- Yalcin, D.; Drummond, C. J.; Greaves, T. L., High throughput approach to investigating ternary solvents of aqueous non-stoichiometric protic ionic liquids. *Phys. Chem. Chem. Phys.* 2019, 21, 6810-6827.
- Wijaya, E. C.; Separovic, F.; Drummond, C. J.; Greaves, T. L., Activity and conformation of lysozyme in molecular solvents, protic ionic liquids (PILs) and salt-water systems. *Phys. Chem. Chem. Phys.* 2016, 18, 25926-25936.
- Arunkumar, R.; Drummond, C. J.; Greaves, T. L., FTIR Spectroscopic Study of the Secondary Structure of Globular Proteins in Aqueous Protic Ionic Liquids. *Frontiers in Chemistry* 2019, 7, Article 74.
- Qi, H.; Smith, K. M.; Darmanin, C.; Ryan, T. M.; Drummond, C. J.; Greaves, T. L., Lysozyme conformational changes with ionic liquids: spectroscopic, small angle x-ray scattering and crystallographic study. *Journal of Colloid and Interface Science*, Accepted 8th October 2020.

Speckle-Based Dark-Field Tomography of a Phase Object

Author(s): Samantha Alloo

Co-author(s): Andrew Stevenson ¹ ; Anton Maksimenko ² ; Ben Kennedy ; David Paganin ³ ; Heyang (Thomas) Li; Joshua Bowden ; Konstantin Pavlov ⁴ ; Marcus Kitchen ⁵ ; Sherry Mayo ⁶ ; Timur Gureyev ⁷

1 Australian Synchrotron/ CSIRO

2 Australian Synchrotron

3 School of Physics and Astronomy, Monash University

4 University of Canterbury

5 Monash University

6 CSIRO

7 The University of Melbourne

Corresponding Author(s): timur.gureyev@unimelb.edu.au, anton.maksimenko@synchrotron.org.au, sherry.mayo@csiro.au, andrew.stevenson@synchrotron.org.au, samjanealoo@gmail.com, david.paganin@monash.edu, marcus.kitchen@monash.edu

Speckle-Based Dark-Field Tomography of a Phase Object

S.J. Alloo^(a), D.M. Paganin^(b), M.J. Kitchen^(b), A.W. Stevenson^(c), S.C. Mayo^(d), H.T. Li^(a,b), A. Maksimenko^(c), T.E. Gureyev^(e,f,g,b), J. Bowden^(d), B. Kennedy^(a), and K.M. Pavlov^(a,b,g).

(a) University of Canterbury, Christchurch 8041, New Zealand,

(b) Monash University, Clayton, Victoria 3800, Australia,

(c) Australian Synchrotron, ANSTO, Clayton, Victoria 3168, Australia,

(d) Commonwealth Scientific and Industrial Research Organisation, Clayton, Victoria 3168, Australia,

(e) The University of Melbourne, Parkville, Victoria 3010, Australia,

(f) The University of Sydney, Lidcombe, New South Wales 2141, Australia,

(g) University of New England, Armidale, New South Wales 2351, Australia.

Speckle imaging techniques have been utilised, in many forms over several decades, in a variety of optical contexts such as astronomy [1]. However, speckle-based X-ray imaging [2], [3] is a relatively recent field of phase-contrast imaging that utilises speckle-tracking to obtain microscopic sample information. Speckle-based imaging is an X-ray imaging technique that utilises a spatially random mask positioned between the X-ray source and sample. In this technique, the manner in which the illuminating speckles are modified, by the presence of the sample, are decoded to give position-sensitive information regarding that sample. One of the many applications is in failure prediction, e.g. in giving a method to identify microscopic cracks in composite structures [4].

X-ray imaging-techniques have limited spatial resolution due to the finite detector pixel size. Hence, nano and micro features within the sample often cannot be resolved in X-ray tomographic reconstructions. Dark-field (DF) tomographic images [5,6,7] are able to resolve these nano-features within samples as their contrast is related to the small-angle scattering of X-rays by features smaller than the detector pixel size. This study demonstrates how speckle-based imaging can be used to obtain a sample's DF image, via an approach that implicitly rather than explicitly analyses the speckles. Using Multimodal Intrinsic Speckle Tracking (MIST) [8], the speckle-based imaging projection data was used to retrieve a sample's DF image. The experimental data was collected at the Imaging and Medical Beamline at the Australian Synchrotron (proposal No 15230).

Compared to alternative techniques, this speckle-based DF imaging technique [8] only requires two sets of projection data for each tomographic view angle.

We obtain the first, to our knowledge, DF three-dimensional tomographic reconstructions (Fig. 1) using any form of speckle-based X-ray imaging technique. These reconstructions provide valuable complementary, and otherwise inaccessible, information to augment the information contained in phase-contrast images. The potential feasibility of clinical application of this imaging technique is supported by not only its simple experimental set-up, but also the low number of images required for each tomographic projection.

References:

- Horch, E. "Speckle Imaging in Astronomy". *International Journal of Imaging Systems and Technology*. Vol. 6(4). Pp. 295 - 417 (1995)
- Berujon, S., Ziegler, E., Cerbino, R., & Peverini, L. "Two-Dimensional X-Ray Beam Phase Sensing". *Physical Review Letters*. Vol. 108(15). 158102 (2012)
- Morgan, K.S., Paganin, D.M., & Siu, K. "X-ray phase imaging with a paper analyser". *Applied Physics Letters*. Vol. 100(12). 1241-2 – 124102-4. (2012)
- Fieres, J., Schumann, P., & Reinhart, C. "Predicting failure in additively manufactured parts using X-ray computed tomography and simulation". *Procedia Engineering*. Vol. 213. Pp. 69-78. (2018)
- Pfeiffer, F., Bech, M., Bunk, O., Donath, T., Henrich, B., Kraft, P., & David, C. "X-ray dark-field and phase-contrast imaging using a grating interferometer". *Journal of Applied Physics*. Vol. 105. 102006. (2009)
- Majidi, K., Brankov, J. G., & Wernick, M. N. "Sampling Strategies in Multiple-Image Radiography". *IEEE International Symposium on Biomedical Imaging*. Pp. 688-691. 10.1109/ISBI.2008.4541089. (2008)
- Ando, M., Sunaguchi, N., Shimao, D., Pan, A., Yuasa, T., Mori, K., Suzuki, Y., Jin, G., Kim, J., Lim, J., Seo, S., Ichihara, S., Ohura, N., & Gupta, R.. "Dark-Field Imaging: Recent developments and potential clinical applications." *Physica Medica*. Vol. 32, Pp. 1801-1812. (2016)
- Pavlov, K.M, Paganin, D.M, Heyang, L., Berujon, S., Rougé-Labriet, H., & Brun, E. "X-ray Multimodal Intrinsic-Speckle-Tracking (MIST)". *Journal of Optics*, in press. <https://arxiv.org/abs/1911.06814> (2019).

Spectroscopic Studies of Brain Zinc Homeostasis and Its Role During Cognitive Decline and Ageing

Ashley Hollings¹ ; Mark Hackett¹ ; Peter Kappen² ; John Mamo³ ; Ryu Takechi¹ ; Virgine Lam³ ; Cameron Kewish² ; Martin de Jonge² ; Nicholas Fimognari¹

1 Curtin University, Bentley Western Australia 6845, Australia

2 Australian Nuclear Science and Technology Organisation, 800 Blackburn Road, Clayton, VIC 3168, Australia

3 Curtin University, Bentley, Western Australia 6102, Australia

Corresponding Author(s): r.takechi@curtin.edu.au, peter.kappen@ansto.gov.au, j.mamo@curtin.edu.au, nicholas.fimognari@postgrad.curtin.edu.au, mark.j.hackett@curtin.edu.au, ashley.hollings@postgrad.curtin.edu.au, virginie.lam@curtin.edu.au, martind@ansto.gov.au, cameronk@ansto.gov.au

The greatest risk factor for dementia is ageing. With no cure or effective therapies to slow progression, and with an ageing population, dementia has reached crisis levels in Australia. The content and distribution of metals such as Fe, Cu, Zn is known to change in the ageing brain (metal dis-homeostasis)(1, 2), and thus, increased understanding of the mechanistic role of metal dis-homeostasis may illuminate new therapeutic strategies. Specifically, Zn homeostasis and dis-homeostasis appears to be a potent modulator of memory function (3-5), yet, the exact chemical form(s) of Zn that are vital to memory function are unknown (6,7). Development of new spectroscopic methods to image different chemical forms of Zn may help increase understanding of Zn-modulated memory function and dysfunction. There are currently no available imaging protocols to differentiate between different chemical forms of Zn, however, substantive evidence supports that X-ray absorption techniques could provide such capability (8-10). Recently, our group has utilised X-ray absorption spectroscopy (XAS) to build a spectroscopic library of Zn compounds that reflects the chemical forms of Zn likely to be present in the brain. Preliminary analysis has revealed that XAS is able to differentiate between multiple Zn compounds across anatomically separate brain regions (Figure 1). Future experiments hope to reveal which Zn compounds change, in which brain regions, during ageing or neurodegenerative disease. Such insights into whether specific types of zinc are affected with ageing may reveal mechanisms contributing to cognitive decline, in turn presenting potential pathways for targeted therapeutic interventions.

Zecca L, Zucca FA, Toscani M, Adorni F, Giaveri G, Rizzio E, et al. Iron, copper and their proteins in substantia nigra of human brain during aging. *Journal of Radioanalytical and Nuclear Chemistry*. 2005; 263(3):733-737.

Ramos P, Santos A, Pinto NR, Mendes R, Magalhães T, Almeida A. Anatomical Region Differences and Age-Related Changes in Copper, Zinc, and Manganese Levels in the Human Brain. *Biological Trace Element Research*. 2014; 161(2):190-201.

Takeda A. Significance of Zn²⁺ signaling in cognition: Insight from synaptic Zn²⁺ dyshomeostasis. *Journal of Trace Elements in Medicine and Biology*. 2014; 28(4):393-396.

Huang EP. Metal ions and synaptic transmission: Think zinc. *Proceedings of the National Academy of Sciences* [10.1073/pnas.94.25.13386]. 1997; 94(25):13386. Available from: <http://www.pnas.org/content/94/25/133>

Nakashima AS, Dyck RH. Enhanced Plasticity in Zincergic, Cortical Circuits after Exposure to Enriched Environments. *The Journal of Neuroscience* [10.1523/JNEUROSCI.4645-08.2008]. 2008; 28(51):13995. Available from: <http://www.jneurosci.org/content/28/51/13995.abstract>.

Sato S, Frazier J, Goldberg A. The distribution and binding of zinc in the hippocampus. *Journal of Neuroscience*. 1984; 4(6):1662-1670.

Frederickson C, Suh S, Silva D, Thompson R. Importance of Zinc in the Central Nervous System: The Zinc-Containing Neuron. *Journal of Nutrition*. 2000; 130(5):1471S-1483S.

Hackett M, Paterson P, Pickering I, George G. Imaging Taurine in the Central Nervous System Using Chemically Specific X-ray Fluorescence Imaging at the Sulfur K-Edge. *Analytical Chemistry* 18(22):10916-10924.

James SA, Roberts BR, Hare DJ, de Jonge MD, Birchall IE, Jenkins NL, et al. Direct in vivo imaging of ferrous iron dyshomeostasis in ageing *Caenorhabditis elegans*. *Chemical Science* [10.1039/C5SC00233H]. 2015; 6(5):2952-2962.

Salt DE, Prince RC, Baker AJM, Raskin I, Pickering IJ. Zinc Ligands in the Metal Hyperaccumulator *Thlaspi caerulescens* As Determined Using X-ray Absorption Spectroscopy. *Environmental Science & Technology*. 1999; 33(5):713-717.

Structural characterisation of influenza epitopes presented by dominant Indigenous Australian Human Leukocyte Antigens

Andrea Nguyen¹

1 Monash University

Corresponding Author(s): andrea.nguyen@monash.edu

Influenza is a highly infectious disease caused by the influenza virus. Previous research has shown that Indigenous Australians are at higher risk of developing severe cases of influenza infection than non-Indigenous Australians. In the event of a pandemic outbreak, Indigenous Australians are more likely (16%) to be hospitalised due to influenza infection than non-Indigenous Australians, despite only making up a small portion (2.5%) of the total population. The underlying immunological reason is still unclear but may be due to the distinct Human Leukocyte Antigen (HLA) profile of Indigenous Australians. The HLA type restricts the targets of anti-viral T cells, which play a critical role in the eradication of the virus.

We have focused our work on HLA-A24:02, a dominant HLA allele in the Indigenous Australian population. In order to understand the correlation between these distinct HLA molecules and severity of influenza infection, we have identified novel HLA-A24:02-restricted influenza-specific epitopes using immunopeptidomics and functional validation determined their structures using X-ray crystallography. Structural analyses of these HLA complexes with immunogenic epitopes provides insight into their ability to stimulate T cells.

For structural characterisation of the HLA-A*24:02-bound influenza epitopes, the HLA-peptide complexes are produced as pure protein and crystallised using the Monash university crystalmation platform. The crystals were then manually optimised to obtain large, good quality diffracting crystals that were used for X-ray diffraction at the Australian Synchrotron.

Structural characterisation of mitochondrial complex IV assembly factors

Shadi Maghool¹ ; Luke E. Formosa² ; N. Dinesha G. Cooray³ ; David A. Stroud³ ; David Aragão⁴ ; Michael T. Ryan²; Megan J. Maher¹

1 School of Chemistry and The Bio21 Molecular Science and Biotechnology Institute, The University of Melbourne, Parkville, Australia

2 Department of Biochemistry and Molecular Biology, Biomedicine Discovery Institute, Monash University, Clayton 3800, Australia

3 Department of Biochemistry and Genetics, La Trobe Institute for Molecular Science, La Trobe University, Melbourne 3086, Australia.

4 Diamond Light Source, Harwell Science and Innovation Campus, Didcot, UK

Corresponding Author(s): shadi.maghool@unimelb.edu.au

Cytochrome c oxidase or mitochondrial respiratory chain complex IV catalyses the transfer of electrons from cytochrome c in the intermembrane space, to molecular oxygen in the matrix and therefore contributes to the proton gradient that drives mitochondrial ATP synthesis. Complex IV dysfunction is a significant cause of human mitochondrial disease. Complex IV requires the incorporation of three copper ions, heme a and heme a₃ cofactors for the assembly and activity of the complex. Complex IV assembly factors are required for subunit maturation, co-factor incorporation and stabilization of intermediate assemblies of complex IV in humans. Loss-of-function mutations in several genes encoding complex IV assembly factors have been shown to result in diminished complex IV activity and severe pathologic conditions in affected infants [1].

Our study focuses on two mitochondrial complex IV assembly factors, Coa6 and Coa7, that are located in the intermembrane space of mitochondria and contain intramolecular disulfide bonds. Coa6 binds copper with femtomolar affinity and has been proposed to play a role in the biogenesis of the CuA site of complex IV [2,3]. The W59C pathogenic mutation in Coa6 does not affect copper binding or import of the protein into mitochondria but affects the maturation and stability of the protein [3,4]. The precise role of Coa7 in the biogenesis of complex IV is not completely understood. However, patients with Coa7 pathogenic mutations suffer from mitochondrial diseases owing to complex IV deficiency. This presentation will describe the crystal structures of the Coa7 and Coa6 (wild-type and the W59C mutant) proteins and implications for their roles in complex IV assembly and function. To elucidate the atomic structure of the WTCoa6, W59CCoa6 and WTCoa7 proteins, we crystallised and determined their structures to 1.65, 2.18 and 2.40 Å resolution, respectively by X-ray crystallography. Diffraction data were recorded at the Australian Synchrotron on beamline MX2. The crystal structure of WTCoa6 was determined by sulfur single-wavelength anomalous dispersion and the crystal structure of WTCoa7 and W59CCoa6 were solved by molecular replacement.

References:

- Timon-Gomez, A., Nyvltova, E., Abriata, L. A., Vila, A. J., Hosler, J., and Barrientos, A. (2018) Mitochondrial cytochrome c oxidase biogenesis: Recent developments, *Seminars in cell & developmental biology* 76, 163-178.
- Stroud, D. A., Maher, M. J., Lindau, C., Vögtle, F. N., Frazier, A. E., Surgenor, E., ... Ryan, M. T. (2015). COA6 is a mitochondrial complex IV assembly factor critical for biogenesis of mtDNA-encoded COX2. *Human molecular genetics*, 24(19), 5404–5415. doi:10.1093/hmg/ddv265
- Maghool, S., Cooray, N., Stroud, D. A., Aragão, D., Ryan, M. T., & Maher, M. J. (2019). Structural and functional characterization of the mitochondrial complex IV assembly factor Coa6. *Life science alliance*, 2(5), e201900458. doi:10.26508/lsa.2019004583.
- Maghool, S., Ryan, M. T., & Maher, M. J. (2020). What Role Does COA6 Play in Cytochrome C Oxidase Biogenesis: A Metallochaperone or Thiol Oxidoreductase, or Both?. *International journal of molecular sciences*, 21(19), E6983.

Structural plasticity between homo and heterodimeric IRF4-DNA Interactions

Srinivasan Sundararaj¹; Sandali Seneviratne¹; Simon J Williams¹; Anselm Enders¹; Marco G Casarotto¹

¹ Australian National University

Corresponding Author(s): simon.williams@anu.edu.au, srinivasan.sundararaj@anu.edu.au, marco.casarotto@anu.edu.au, sandali.seneviratne@anu.edu.au, anselm.enders@anu.edu.au

Interferon regulatory factor 4 (IRF4) is a transcription factor (TF) that regulates the gene expression of immune cells including T cells and B cells. Due to its critical role in B and T cell development, IRF4 is linked directly to numerous immune-related disease conditions including B cell-related chronic lymphocytic leukemia (CLL) and adult T cell leukemia (ATL) (1). Structurally, IRF4 consists of two conserved domains; an N-terminal DNA binding domain and the C-terminal IRF-association domain and binds the target DNA as either homo or heterodimer. Notably, it binds the canonical interferon-stimulated response elements (ISRE) DNA motif as a homodimer and regulates the expression of genes involved in interferon stimulation. Despite the significance of this association, the mechanistic basis underpinning this pivotal molecular interaction remains unknown. Through X-ray crystallography and surface plasmon resonance, we now provide the structural basis of this interaction. Our study has identified a head to tail orientation in IRF4-ISRE interaction, with each monomer docking the opposite face of the DNA. We also found a substantial bending in DNA to accommodate $\alpha 3$ recognition helix directly on the major groove with no observed intermolecular interaction between the bound monomers. This markedly contrasts heterodimeric form where DNA bound IRF4 is shown to physically interact with other TFs to regulate the target gene expression (2). Notably, we also identified that the disease-causing mutations (3,4) could bind directly to DNA as evidenced by their tighter binding affinities. Together, our study provides a structural snapshot of IRF4 homo and heterodimers and its role in regulating the target gene expression thereby providing insights into the basis of IRF4 mediated CLL and ATL pathogenesis.

References

- Hagman, J. (2017) Critical Functions of IRF4 in B and T Lymphocytes. *J Immunol* 199, 3715-3716
- Escalante, C. R., Brass, A. L., Pongubala, J. M., Shatova, E., Shen, L., Singh, H., and Aggarwal, A. K. (2002) Crystal structure of PU.1/IRF-4/DNA ternary complex. *Mol Cell* 10, 1097-1105
- Havelange, V., Pekarsky, Y., Nakamura, T., Palamarchuk, A., Alder, H., Rassenti, L., Kipps, T., and Croce, C. M. (2011) IRF4 mutations in chronic lymphocytic leukemia. *Blood* 118, 2827-2829
- Cherian, M. A., Olson, S., Sundaramoorthi, H., Cates, K., Cheng, X., Harding, J., Martens, A., Challen, G. A., Tyagi, M., Ratner, L., and Rauch, D. (2018) An activating mutation of interferon regulatory factor 4 (IRF4) in adult T-cell leukemia. *J Biol Chem* 293, 6844-6858

Structural studies of G protein-coupled receptors – implications for drug discovery

David Thal¹

¹ Monash Institute of Pharmaceutical Sciences

Corresponding Author(s): david.thal@monash.edu

G protein-coupled receptors (GPCRs) are key cell-surface proteins that transduce external environmental cues into biochemical signals across the cell membrane. They are the largest superfamily of cell-surface receptors encoded by the human genome and are also the largest class of FDA approved drug targets. The overarching goal of our lab is to understand the molecular basis of how GPCRs function and how this knowledge can be used to design new drug candidates. In particular, using lipidic cubic phase crystallography we have determined inactive state structures of the M4 and M5 muscarinic acetylcholine receptor (mAChR) subtypes, the A1 adenosine receptor (A1AR), and the neurokinin 1 receptor (NK1R). These GPCRs are important drug targets for neuropsychiatric diseases (mAChRs), cardiovascular disease (A1AR), and pain and inflammation (NK1R). In addition, using cryo-electron microscopy (cryo-EM) we have determined active state structures for several of these receptors. Collectively, the result of these structures has provided insight into how different classes of ligands bind to and modulate the structure and function of these receptors that we anticipate will aid future drug discovery efforts at these receptors.

Synchrotron Powder Diffraction to disclose effect of catalyst phase change on CO₂ reduction

Author(s): Jiajia Zhao¹

Co-author(s): Renata Lippi² ; Anita D'Angelo³ ; Rachel Caruso⁴ ; Ivan Cole⁴

1 RMIT University/CSIRO

2 CSIRO

3 Australian Synchrotron

4 RMIT University

Corresponding Author(s): zha319@csiro.au, renata.lippi@csiro.au, rachel.caruso@rmit.edu.au, ivan.cole@rmit.edu.au, anitad@ansto.gov.au

Current record-high CO₂ concentration in the atmosphere urges a shift into use of renewable fuels. CO₂ utilisation is one of strategies to mitigate this concern. One approach is CO₂ reduction, which can be driven by temperature or light to convert CO₂ and H₂ into the economically beneficial products – methane (CH₄) and methanol (CH₃OH). Cost-efficient implementation of this reaction is highly relied on the design of highly active and selective catalysts. The synergy among all the catalyst components depends on the structure. Disclosing this structure-activity relationship is crucial for rational design and optimisation of the catalysts. Catalyst design normal consists of two components: metal and support. The metals or their alloys normally work as active sites on the support surface, especially to facilitate H₂ dissociation to provide sufficient H to reduce CO₂. Ru, as one active plasmonic metals, has demonstrated enhanced catalytic activity due to the strong metal-support interaction. The supports are typically are stable metal oxides such as ZrO₂ that act as inert materials to provide absorption sites for CO₂ or intermediates. The controlled morphology of ZrO₂ (e.g. monoclinic or tetragonal phase, particle size, surface termination) can significantly affect catalytic activity. Hence, in this presentation, our efforts towards the controlled-morphology catalyst for CO₂ hydrogenation and the investigation on the structure-activity relationship will be discussed. A library of catalysts has been synthesised and characterised by ex situ PXRD. Using a high-throughput catalyst testing rig, catalysts were screened in parallel for their performance as catalyst for CO₂ hydrogenation. The results of this systematic investigation of the catalyst library together with insights recently obtained from in operando PXRD characterisation will be described.

Synchrotron macro ATR-FTIR: where we are and what's next for live-cell measurement

Author(s): Jitraporn (Pimm) Vongsvivut¹

Co-author(s): David Pérez-Guaita ² ; Leah Nankervis ¹ ; Adrian Massey ¹ ; Chris Ampt ¹ ; Jonathan McKinlay ¹ ; Christophe Sandt ³ ; Mark J. Tobin ¹

1 ANSTO - Australian Synchrotron

2 FOCAS Research Institute

3 SMIS beamline, SOLEIL synchrotron

Corresponding Author(s): christophe.sandt@synchrotron-soleil.fr, tobinm@ansto.gov.au, jitrapov@ansto.gov.au, jonathan.mckinlay@ansto.gov.au, amptc@ansto.gov.au, david.perezguaita@dit.ie, nankervl@ansto.gov.au, masseya@ansto.gov.au

This presentation aims to provide a summary on the recent applications of our synchrotron macro ATR-FTIR microspectroscopy, unique to the Australian Synchrotron's Infrared Microspectroscopy (IRM) beamline. The technique provides molecular information with sub-cellular resolution down to 1-2 μm beyond the resolution limit allowed for standard synchrotron-FTIR setups and further simplifies otherwise complicated sample preparation [1]. Since the technique was made available for users in 2016, this high-resolution chemical mapping capability has facilitated diverse experiments on the beamline expanding its applications into many new areas. Some of the recent examples include novel environmental sustainable geopolymer concretes [2,3], archaeological bones [4] and spider silk cross-sections [5].

The second part of the presentation will highlight further development of the macro ATR-FTIR technique specifically for live-cell measurement in an aqueous environment. Through the collaboration with the SMIS beamline at SOLEIL (France), we undertook a beamtime experiment using their inverted ATR-FTIR accessory to acquire spectra from live red blood cells. The experience and knowledge gained from this international beamtime experiment, together with the effort from our mechanical engineering team, have resulted in an optical design to be developed into the first prototype of ATR-FTIR setup for live-cell measurement.

Acknowledgement

We would like to acknowledge the financial support from International Synchrotron Access Program (ISAP No. AS/IA182/14167) to perform the live-cell ATR-FTIR experiment at SOLEIL's SMIS beamline (Proposal ID. 20180157).

References

- J. Vongsvivut, D. Pérez-Guaita, B. R. Wood, P. Heraud, K. Khambatta, D. Hartnell, M. J. Hackett, and M. J. Tobin, "Synchrotron Macro ATR-FTIR Microspectroscopy for High-Resolution Chemical Mapping of Single Cells," *Analyst* 144, 10, 3226-3238 (2019).
- A. Hajimohammadi, T. Ngo, J. L. Provis, T. Kim, and J. Vongsvivut, "High Strength/Density Ratio in a Syntactic Foam Made from One-Part Mix Geopolymer and Cenospheres," *Composites Part B*, 173, 106908 (2019).
- A. Hajimohammadi, T. Ngo, and J. Vongsvivut, "Interfacial Chemistry of a Fly Ash Geopolymer and Aggregates," *Journal of Cleaner Production*, 231, 980-989 (2019).

J. J. Miszkiewicz, C. Rider, S. Kealy, C. Vrahnas, N. A. Sims, J. Vongsvivut, M. J. Tobin, M. J. L. A. Bolunia, A. S. De Leon, A. L. Peñalosa, P. S. Pagulayan, A. V. Soriano, R. Page, and M. F. Oxenham, "Asymmetric Midshaft Femur Remodelling in an Adult Male with Left Sided Hip Joint Ankylosis, Metal Period Nagsabaran, Philippines," *International Journal of Palaeopathology*, 31, 14 (2020).

C. Haynl, J. Vongsvivut, K. R. H. Mayer, H. Bargel, V. J. Neubauer, M. J. Tobin, M. A. Elgar, and T. Scheibel, "Dimensional Stability of a Remarkable Spider Foraging Web Achieved by Synergistic Arrangement of Silk Fibers," accepted for publication in *Scientific Reports* (2020).

Synchrotron-based X-ray diffraction and spectroscopy for metal-ion battery material studies

Wei Kong Pang

Corresponding Author(s): wkpang@uow.edu.au

Institute for Superconducting and Electronic Materials, University of Wollongong, NSW 2500, Australia.

Email: wkpang@uow.edu.au

The commercialisation of lithium-ion batteries (LIBs) has gained huge success and LIBs are taking an important part of our daily modern life, as confirmed by the prestigious award of the 2019 Nobel Prize in Chemistry. Owing to the limited abundance of lithium, other metal-ion batteries (MIBs), such as zinc-, sodium-, and potassium-ion batteries, with similar working mechanism, have also been studied and developed as alternatives. Compared with other energy storages, MIBs are relatively less predictable due to the complex reactions occurred on the bulk and surface of electrodes, as well as other battery components, such as electrolyte, during electrochemical processes. During charge and discharge, the intercalation and de-intercalation processes of metal ions (i.e. lithium ions) happening in the electrodes are very complex, involving the evolutions of phase, structure, composition, as well as morphology, with these processes underpinning electrochemical function and performance of the battery. Therefore, a mechanistic understanding of the reaction pathways, i.e. the atomistic and molecular-scale origin of battery performance, will enable the rational improvement of electrode materials and pave the way for entirely new battery systems, and in-situ in-operando synchrotron-based X-ray powder diffraction (XRPD) with high brightness and tune-able wavelength is an extremely powerful tool to obtain this crucial understanding.

On the other hand, X-ray absorption spectroscopy (XAS) could be used to detect the electronic structure of certain ions within the active materials in the battery, especially helpful to investigate the elements with electrochemical activities. Transmission X-ray microscopy (TXM) can be employed to probe the electrode morphological changes during charge and discharge, linking to the electro-chemical performance of the materials. Infra-red microscopy (IRM) is also found to be a powerful analytical method, allowing the characterisation of the chemical information and their distribution of solid-electrolyte interphase formed on the electrode surface. By correlating the chemical information with data obtained from other techniques, additional insights into their mechanism, which is critical for further development, can be gained.

In this presentation, I will introduce the research work in our team and showcase some examples of these mechanistic and crystallographic research, demonstrating the important role of synchrotron-based X-ray scattering in battery research.

Synthesis and structure of ALaTiO_4 and $\text{A}_2\text{La}_2\text{Ti}_3\text{O}_{10}$ ($\text{A} = \text{Na}^{+}, \text{K}^{+}$) Ruddlesden-Popper type photocatalysts

Author(s): Junwei Li¹

Co-author(s): Brendan Kennedy²; Chris Ling³; Thomas Maschmeyer²

¹ the University of Sydney, School of Chemistry

² The University of Sydney

³ University of Sydney

Corresponding Author(s): thomas.maschmeyer@sydney.edu.au, junweibenli@gmail.com, chris.ling@sydney.edu.au, brendan.kennedy@sydney.edu.au

Global warming is a current hot topic due to its potential for irreversible environmental damage. Ambitions were made within the Paris agreement to limit the temperature rise to be below 1.5 °C pre-industrial level to minimise the impact of climate change. Therefore, alternative fuel sources are needed to replace fossil fuel, reducing the emission of greenhouse gases including CO₂. Hydrogen gas is one popular choice to replace fossil fuels, due to its high energy density per unit weight, with technologies utilising hydrogen as energy generator, such as hydrogen fuel cells, already existing. Hydrogen can be generated renewably by sunlight driven, photocatalytic water-splitting. Metal oxides, including those with a Ruddlesden-Popper type structures are being studied as potential photocatalysts. The structure contains multiple cationic sites, which allows for different combinations of metal cations that can be used to adjust the bandgap. The layered structuring also allows for the intercalation of different cations within the structure that allows for modifications post synthesis, therefore further optimising the photocatalyst. KLaTiO_4 is a $n=1$ Ruddlesden-Popper type layered perovskite. KLaTiO_4 can be used as a Hydrogen Evolution Catalyst (HEC), producing 9.540 μmol of H₂ gas per hour from 20 mg of catalyst, when using methanol as sacrificial electron donor and platinum co-catalyst.

KLaTiO_4 was prepared using traditional solid-state chemistry methods to provide a sample for both catalytic testing and structural studies using neutron diffraction. It was discovered that synthesis of KLaTiO_4 above 900 °C resulted in the presence of $\text{K}_2\text{La}_2\text{Ti}_3\text{O}_{10}$ impurity in the product. $\text{K}_2\text{La}_2\text{Ti}_3\text{O}_{10}$ is structurally similar to KLaTiO_4 , both being layered perovskite of the Ruddlesden-Popper type structure, with layers of TiO₆. The main difference between the two is KLaTiO_4 has 1-layer of perovskite-like TiO₆ blocks, while $\text{K}_2\text{La}_2\text{Ti}_3\text{O}_{10}$ has 3-layer perovskite slabs. The sodium analogues, NaLaTiO_4 and $\text{Na}_2\text{La}_2\text{Ti}_3\text{O}_{10}$ can also be made and these are isostructural to their potassium counterparts.

In this presentation, the two main factors important for the synthesis of ALaTiO_4 and $\text{A}_2\text{La}_2\text{Ti}_3\text{O}_{10}$ ($\text{A} = \text{Na}^+, \text{K}^+$) will be discussed. The first factor to consider is the volatility of alkaline metal ions at elevated temperatures.

Due to this volatility, excess Na or K needs to be included in the initial reagent mixture. Ex-situ X-ray diffraction measurements showed that if the excess of Na_2CO_3 was limited to 10% neither NaLaTiO_4 nor $\text{Na}_2\text{La}_2\text{Ti}_3\text{O}_{10}$ could be made. Successful synthesis of NaLaTiO_4 or $\text{Na}_2\text{La}_2\text{Ti}_3\text{O}_{10}$ required 50 % (minimum tested) alkaline metal reagent excess. The second factor to consider is related to sintering temperature. Multiple samples of NaLaTiO_4 or $\text{Na}_2\text{La}_2\text{Ti}_3\text{O}_{10}$ were made using traditional solid-state synthesis methods at temperature between 750 °C to 950 °C. Incomplete reaction was observed if the temperature was kept below 750 °C during the synthesis, XRD revealing unreacted La_2O_3 , as well as other unidentified impurities. It was also discovered that when reagents with the stoichiometry to make NaLaTiO_4 (with Na_2CO_3 excess) were sintered above 900 °C $\text{Na}_2\text{La}_2\text{Ti}_3\text{O}_{10}$ impurities were present, which is a lower temperature than most literature reports. Finally, $\text{Na}_2\text{La}_2\text{Ti}_3\text{O}_{10}$ was made at 800 °C, which is lower than other literature reports, and the temperature which NaLaTiO_4 was found to be made at good purity. The low synthesis temperature of $\text{Na}_2\text{La}_2\text{Ti}_3\text{O}_{10}$ suggests that care must be taken when synthesising and analysing NaLaTiO_4 to ensure no impurities are present in the sample. Details of the structures will be presented.

Synthesis of Single Atoms Metal Supported on Carbon Materials

ZHAO SHIYONG ¹

¹ Curtin University

Corresponding Author(s): shiyong.zhao@curtin.edu.au

The practical application of single atom catalysts (SACs) is constrained by the low achievable loading of single metal atoms. Here, nickel SACs stabilized on a nitrogen-doped carbon nanotube structure (NiSA-N-CNT) with ultrahigh Ni atomic loading up to 20.3 wt% have been successfully synthesized using a new one-pot pyrolysis method employing Ni acetylacetonate (Ni(acac)₂) and dicyandiamide (DCD) as precursors. The self-rolling-up mechanism has been proposed to explain the synthesis process. Furthermore, we have investigated the in-Situ stability of Ni, which confirms the significance of nitrogen to stabilize the single atom Ni. Besides CNTs, we also have achieved one unsaturated edge-anchored Ni single atoms of ~6.9% on porous microwave exfoliated graphene oxide through one feasible impregnation followed by annealing. Last but not least, we also will share our recent progress for SACs synthesis through firstly proposed hard-landing method.

Tableting of human milk and colostrum and its impact on digestion kinetics and lipid self-assembly during digestion

Author(s): Syaza Binte Abu Bakar¹

Co-author(s): Andrew Clulow ¹; Malinda Salim ²; Adrian Hawley ³; Donna Geddes ⁴; Kevin Nicholas ¹; Ben Boyd ²

1 Monash University

2 Monash Institute of Pharmaceutical Sciences

3 Australian Synchrotron

4 University of Western Australia

Corresponding Author(s): kevin.nicholas@monash.edu, donna.geddes@uwa.edu.au, syaza.binteabubakar@monash.edu, andrew.clulow@monash.edu, malinda.salim@monash.edu, ben.boyd@monash.edu, adrian.hawley@synchrotron.org.au

OBJECTIVES

Colostrum contains lipids and bioactive proteins that can stimulate the development of organs and reduce diseases in infants [1,2]. As a novel approach to nutrition especially for the developing world, we have been studying human milk and colostrum tablets. Surprisingly there have been no reports of human milk or colostrum being assessed in the context of lipid digestion, which is critical in the transport of lipophilic nutrients. This project aims to understand the digestion kinetics and structure formation during the digestion of colostrum before and after tableting and the differences between colostrum and human milk systems.

METHODS

Human milk/colostrum tablets were prepared by freeze-drying human milk/colostrum before directly compressing them into tablets. Human milk/colostrum samples were digested under intestinal conditions to understand the kinetics and extent of digestion. The in vitro digestion model was coupled to small-angle X-ray scattering at the Australian Synchrotron, enabling acquisition of the scattering patterns and access to structural changes during digestion [3].

RESULTS

Prior to digestion, peaks corresponding to a lamellar phase in non-pasteurised human milk (before and after tableting) were observed due to self-digestion by the breast milk's own bile salt-stimulated lipase (BSSL). This led to the formation of calcium soaps, which increasingly formed when human milk was digested under intestinal conditions leading to the appearance of persistent lamellar phase. Lamellar phase was evident in pasteurised human milk before digestion but this peak, which was at a different q value than that of in the non-pasteurised human milk, instead suggests interaction of medium-chain fatty acids with calcium.

In contrast, the absence of a lamellar phase in tableted pasteurised human milk before digestion indicates the effect of freeze-drying/compression step of tableting that might have caused the rearrangement of triglycerides in the milk fat globule. As the digestion progressed, non-lamellar phases were seen.

Analogous to the non-pasteurised human milk, the digestion of colostrum before and after tableting resulted in persistent lamellar phase due to calcium soaps.

CONCLUSION

In situ monitoring of the lipid liquid crystalline structures formed during the digestion of the dispersed tablets revealed that tableting induced minor changes in structure formation but additional phases were evident on the tableting of pasteurised human milk that were not evident on the digestion of non-pasteurised human milk nor colostrum formulations.

REFERENCES

- Yamashiro Y, Sato M, Shimizu T, Oguchi S, Maruyama K, Kitamura S. Possible Biological Growth Factors in Breast Milk and Postnatal Development of the Gastrointestinal Tract. *Pediatr. Int.* 1989, 31(4), 417-423.
- Delplanque B, Gibson R, Koletzko B, Lapillonne A, Strandvik B. Lipid Quality in Infant Nutrition: Current Knowledge and Future Opportunities. *J. Pediatr. Gastroenterol. Nutr.* 2015, 61(1), 8-17.
- Warren, D. B.; Anby, M. U.; Hawley, A.; Boyd, B. J. Real Time Evolution of Liquid Crystalline Nanostructure during the Digestion of Formulation Lipids Using Synchrotron Small-Angle X-ray Scattering. *Langmuir.* 2011, 27 (15), 9528-9534.

The Evolution of Electronic Complexity in Biology: 2p3d and 1s3p RIXS of Iron-Sulfur Clusters

Serena DeBeer

Corresponding Author(s): serena.debeer@cec.mpg.de

The Evolution of Electronic Complexity in Biology: 2p3d and 1s3p RIXS of Iron-Sulfur Clusters Serena DeBeer*¹

1 Max Planck Institute for Chemical Energy Conversion, Stiftstr. 34-36, Mülheim an der Ruhr, D- 45470, Germany

*e-mail: serena.debeer@cec.mpg.de

Iron sulfur proteins are ubiquitous in nature, performing essential roles in electron transfer processes, redox chemistry, regulatory sensing and catalysis. The metal active sites of these proteins range from simple single iron sites to complex eight iron clusters. Perhaps the most complex iron sulfur cluster that has been identified to date is the iron molybdenum cofactor (or FeMoco) of nitrogenase, which is capable of cleaving the strong triple bond of dinitrogen. The fundamental question that arises is how does nature evolve complexity in order to enable challenging transformations? In our view, a deeper understanding of the complex geometric and electronic structure of iron sulfur clusters requires the pursuit of novel experimental approaches for integrating their electronic structure in a detailed and quantitative fashion. To this end, we are applying both 2p3d and 1s3p resonant inelastic X-ray scattering (2p3d RIXS), in order to obtain deeper insights into the electronic structure of these important clusters. These data provide an experimental measure of the d-d transitions and allow for more detailed insights into the nature of the multiplet structure. The utility of these methods for understanding the electronic structure of nitrogenase will be highlighted. The challenges that RIXS spectroscopy presents for theoretical modeling will also be discussed.

The Structure and Air Stability of Calcium and Magnesium Intercalated Graphene on 6H-SiC(0001)

Author(s): Jimmy Kotsakidis¹

Co-author(s): Antonija Grubisic-Cabo¹; Yuefeng Yin²; Anton Tadich; Rachael Myers-Ward³; Matt Dejarld³; Shojan Pavunny³; Marc Currie³; Kevin Daniels⁴; Chang Liu⁵; Mark Edmonds¹; Nikhil Medhekar⁶; Kurt Gaskill⁷; Amadeo Vazquez de Parga⁸; Michael Fuhrer⁹

1 Monash University

2 Monash University

3 U.S. Naval Research Laboratory

4 Institute for Research in Electronics and Applied Physics, University of Maryland

5 School of Physics and Astronomy, Monash University

6 Department of Materials Science and Engineering, Monash University

7 U.S. Naval Research Laboratory

8 Autonomous University of Madrid

9 School of Physics and Astronomy, Monash University, Clayton VIC 3800, Australia

Corresponding Author(s): jckot1@student.monash.edu, matt.dejarld@nrl.navy.mil, yuefeng.yin@monash.edu, anton.tadich@synchrotron.org.au, al.vazquezdeparga@uam.es, mark.edmonds@monash.edu, kurt.gaskill@nrl.navy.mil, antonija.grubisic-cabo@monash.edu, danielkm@umd.edu, nikhil.medhekar@monash.edu

Calcium intercalated graphene has been shown to exhibit superconductivity below 2 K, yet its structure has remained elusive in the literature to date. Furthermore, the intercalation of Mg underneath epitaxial graphene on SiC(0001) has not been reported. In this talk, epitaxial monolayer graphene samples synthesised on 6H-SiC(0001) are utilised to investigate calcium and magnesium intercalated graphene. By making use of low energy electron diffraction, X-ray photoelectron spectroscopy and secondary electron cut-off photoemission techniques available at the Australian Synchrotron Soft X-ray Beamline, and the scanning tunnelling microscope at Monash University, we are able to elucidate the structure of these intercalated systems.

We find that Ca intercalates underneath the buffer layer and bonds to the Si-terminated SiC surface, breaking the C–Si bonds of the buffer layer, i.e., “freestanding” the buffer layer to form Ca- intercalated quasi-freestanding bilayer graphene (Ca-QFSBLG). The situation is similar for the Mg-intercalation of epitaxial graphene on SiC(0001), where an ordered Mg-terminated reconstruction at the SiC surface is formed and Mg bonds to the Si-terminated SiC surface are found, resulting in Mg-intercalated quasi-freestanding bilayer graphene (Mg-QFSBLG). Ca-intercalation underneath the buffer layer has not been considered in previous studies of Ca-intercalated epitaxial graphene.

Furthermore, we find no evidence that either Ca or Mg intercalates between graphene layers. However, we do find that both Ca-QFSBLG and Mg-QFSBLG exhibit very low work functions of 3.68 and 3.78 eV, respectively, indicating high n-type doping. Upon exposure to ambient conditions, we find Ca-QFSBLG degrades rapidly, whereas Mg-QFSBLG remains remarkably stable.

The design of Metal-Organic Frameworks using flexible and extendable tetra-carboxylic acid linkers enriched with embedded cyclohexyldiamine

Ali Chahine¹

¹ PhD student

Corresponding Author(s): ali.chahine@monash.edu

Carbon dioxide presents one of the main anthropogenic greenhouse gases which has a significant impact on global warming and climate change. One method to mitigate the CO₂ emissions, which is currently implemented, is the use of liquid amines to capture CO₂ through post-combustion chemical sorption process. This process is accompanied with high regeneration cost and high corrosive hazard. An alternative class of materials is denoted as metal-organic frameworks or porous coordination polymers represents a class of crystalline porous materials which are highly stable, porous and capable of capturing CO₂ selectively through incorporating amines into their structure; that is achieved through one of the three methods: (a) post-synthetic grafting into open metal sites; secondly, (b) use of linkers with pendant amines and (c) use of linkers with embedded amines into their backbone.¹ These materials are less corrosive and have a low generation cost. This work explore the design of amine-rich MOFs containing tetracarboxylate ligands with cyclohexyldiamine embedded into their backbone and have increased length which increased the pores size as anticipated towards increased and selective CO₂ uptake application.

The effect of fat content on the solubilization of halofantrine in infant formula during in vitro intestinal digestion

Thomas Eason¹ ; Malinda Salim² ; Ben Boyd²

1 Monash University

2 Monash Institute of Pharmaceutical Sciences

Corresponding Author(s): ben.boyd@monash.edu, taeas2@student.monash.edu, malinda.salim@monash.edu

ABSTRACT SUMMARY

The solubilization of the poorly water-soluble drug halofantrine in infant formula during simulated intestinal digestion was measured using small-angle x-ray scattering. Halofantrine was well solubilized during digestion in infant formula at 3.8%, 1.9% and 0.95% fat content, demonstrating that halofantrine has a very high affinity for the fatty acids produced during the digestion of fats in infant formula.

INTRODUCTION

Drug solubility is a major obstacle to the absorption of drugs in the gastrointestinal tract. Increasing the solubility of poorly water-soluble drugs is therefore an area of interest to pharmaceutical formulators (1). One common formulation approach is to administer the drug in a mixture of pharmaceutical-grade fats known as a lipid-based formulation (LBF) (2). Fats are digested in the small intestine and their digestion products have been shown to solubilize poorly water-soluble drugs. Recent research has shown that administering poorly water-soluble drugs with infant formula improves drug solubilization in the same manner as a lipid-based formulation (3, 4). These studies have not investigated the effect of fat content on the solubilization of drugs.

EXPERIMENTAL METHODS

50 mg of halofantrine was mixed with 18 mL of reconstituted infant formula to form a suspension. The suspension was stirred in a temperature-controlled vessel and porcine pancreatin (containing lipase) was introduced to digest the fat contained in the infant formula. The presence of crystalline halofantrine during this simulated digestion was monitored in real time using small-angle x-ray scattering. The SAXS peak corresponding to crystalline halofantrine was integrated to quantify the amount of crystalline halofantrine remaining in the digestion media. Any reduction in the peak area was interpreted as solubilization of halofantrine. This method was carried out with infant formula reconstituted at 3.8%, 1.9% and 0.95% fat contents to assess the effect of fat content on halofantrine solubilization.

RESULTS AND DISCUSSION

Halofantrine was not solubilized significantly in infant formula prior to the onset of lipid digestion. The onset of digestion triggered a rapid decrease in crystalline halofantrine over the first 10-15 minutes before plateauing over the remainder of the digestion. The amount of fat in the reconstituted infant formula did not significantly affect the extent of halofantrine solubilisation. Our group previously showed that halofantrine is only partially solubilized (~50%) when administered with 1.3% milk, whereas it is fully solubilized when administered with 3.8% milk. This is because halofantrine is solubilized in fatty acid colloidal structures produced during lipid digestion. Reducing the fat content reduced the amount of fatty acids produced, therefore reducing the solubilization capacity of the colloids. In this study however, no decrease in solubilization was observed. The likely reason for this is that halofantrine is highly soluble in the fatty acids produced upon digestion of infant formula. Even the lowest fat content formula used in this study (0.95%) produced a sufficient quantity of fatty acids upon digestion to solubilize 50 mg of halofantrine. This information could aid in the future development of infant formula as a formulation.

REFERENCES

- Williams HD, Trevaskis NL, Charman SA, Shanker RM, Charman WN, Pouton CW, et al. Strategies to address low drug solubility in discovery and development. *Pharmacological reviews*. 2013;65(1):315.
- Feeneya O, Cruma M, McEvoya C, Trevaskis N, Williams H, Pouton C, et al. 50 years of oral lipid-based formulations: Provenance, progress and future perspectives. *Advanced Drug Delivery Reviews*. 2016;101:167-94.
- Salim M, Ramirez G, Peng K-Y, Clulow AJ, Hawley A, Ramachandruni H, et al. Lipid Compositions in Infant Formulas Affect the Solubilization of Antimalarial Drugs Artefenomel (OZ439) and Ferroquine during Digestion. *Molecular Pharmaceutics*. 2020;17(7):2749-59.
- Salim M, Fraser-Miller SJ, Bērziņš Kr, Sutton JJ, Ramirez G, Clulow AJ, et al. Low-Frequency Raman Scattering Spectroscopy as an Accessible Approach to Understand Drug Solubilization in Milk-Based Formulations during Digestion. *Molecular Pharmaceutics*. 2020;17(3):885-99.

ACKNOWLEDGMENTS

The SAXS experiments for this work were conducted on the SAXS/WAXS beamline of the Australian Synchrotron, part of ANSTO.

The effect of surfactant type on the secondary crystallisation of milk fat at the oil-water interface

Author(s): Damien Sebben¹ ; Stephanie Macwilliams¹

Co-author(s): Andrew Clulow² ; James Ferri³ ; Graeme Gillies⁴ ; Matt Golding⁵ ; Ben Boyd² ; David Beattie¹ ; Marta Krasowska¹

1 University of South Australia

2 Monash University

3 Virginia Commonwealth University

4 Fonterra Co-Operative Group

5 Massey University

The crystallisation of lipids within a dispersed oil phase has the potential to stabilise or destabilise the system, depending on the size and position of the crystals. Interfacial crystallisation within dairy emulsions is of particular interest owing to the role of lipid crystals in partial coalescence, an essential process in the stabilisation of products such as whipped creams. Despite the critical importance of lipid crystallisation at droplet interfaces, little is known about this phenomenon. Our work utilises two complementary techniques to analyse the effect of thermal cycling on interfacial crystallisation within a simulated milk system. Profile analysis tensiometry (PAT) allows us to monitor the kinetics of interfacial lipid crystallisation by tracking the interfacial tension of a single droplet as a function of time and temperature. PAT analysis enabled determination of the temperature at which interfacially-active crystals affect the interfacial properties and highlighted the differences in behaviour of these lipid crystals due to the presence of an emulsifier. Additionally, the effect of emulsifier type was studied using both a protein and non-ionic emulsifier. We found that the presence of emulsifiers delays the effect of interfacial crystals on the interfacial tension, as well as altering the rates of change in interfacial tension. Synchrotron small angle X-ray scattering (SAXS) was conducted on emulsion systems (for the same composition as in PAT experiments) to study the formation, growth and structure of lipid crystals, following a similar temperature cycling regime to that of the PAT experiments. The SAXS results also indicated a suppression of interfacial crystallisation in the presence of emulsifiers, and a difference in the degree of suppression due to the type of emulsifier used.

The impact of microbeam irradiation on spinal cord function

Author(s): Elette EngelsNone

Co-author(s): Felix Jaekel; Jason Paino ¹; Micah Barnes ²; Mitzi Klein ³; Chris Hall ⁴; Daniel Hausermann ³; Michael Lerch ⁵; Elisabeth Schultke

1 UOW

2 Royal Melbourne Institute of Technology, Applied Physics, Melbourne, Australia

3 ANSTO

4 Australian Synchrotron

5 University of Wollongong

Corresponding Author(s): danielh@ansto.gov.au, christoh@ansto.gov.au, micah.barnes@student.rmit.edu.au, ee215@uowmail.edu.au, elisabeth.schultke@med.uni-rostock.de, mierch@uow.edu.au, mitzik@ansto.gov.au, jrp933@uowmail.edu.au

Non-small-cell lung carcinoma (NSCLC) is considered to be highly radioresistant in clinical radiotherapy. The therapeutic dose is limited by the normal tissue tolerance in the organs at risk. The spinal cord is one of the most important organs at risk during radiotherapy of the thoracic cavity. Microbeam Radiation Therapy (MRT) has a remarkably high normal tissue tolerance and allows delivery of extremely high irradiation doses. MRT may therefore be a potential alternative for NSCLC treatment, however, the spinal cord tolerance to MRT must first be established.

The in vivo study was performed in Hutch 2B of the Imaging and Medical Beam Line at the Australian Synchrotron. The acute (up to 3 days post irradiation) and subacute (6 days post irradiation) response of the spinal cord to MRT was tested for peak doses up to 800 Gy. Electrophysiology measurements and motor and sensory function tests (including Rotarod, gait analysis, von Frey filaments) were used to determine spinal cord function in adult Wistar rats before and after MRT.

No neurologic deficits or loss in motoric abilities was observed up to peak doses of 400 Gy. Reversible neurologic deficits occurred at 450 Gy, and non-reversible neurologic deficits developed with peak doses above 450 Gy.

These results demonstrate a remarkable spinal tissue tolerance towards microbeam radiation doses, and are significant for any MRT irradiation of the spinal cord and thoracic cavity.

The use of synchrotron X-ray fluorescence microscopy to study the “battle for nutrients” between plant and pathogen

Author(s): Fatima Naim¹

Co-author(s): Karina Khambatta ² ; Lilian Sanglard ¹ ; Georgina Sauzier ³ ; Juliane Reinhardt ⁴ ; David Paterson ⁴ ; Ayalsew Zerihun ¹ ; Mark Hackett ³ ; Mark Gibberd ¹

1 Centre for Crop and Disease Management, School of Molecular and Life Sciences, Curtin University, Bentley, Western Australia 6102, Australia

2 School of Molecular and Life Sciences, Curtin University, Bentley, Western Australia 6102, Australia

3 School of Molecular and Life Sciences, Curtin University, Bentley, Western Australia 6102, Australia

4 The Australian Synchrotron, Clayton, Victoria 3168, Australia

Corresponding Author(s): fatima.naim@curtin.edu.au

Metal homeostasis is essential to normal plant growth and development. The balance is potentially impacted during plant-pathogen interactions as the host and pathogen compete for the same nutrients. Our knowledge of outcome of the interaction in terms of metal homeostasis is still limited. Here, we visualise and analyse the fate of nutrients in wheat leaves infected with a devastating pathogen, by high-resolution X-ray fluorescence microscopy (XFM). We employed XFM, at the ANSTO Australian synchrotron, for a detailed time-course of nutrient re-distribution in wheat leaves infected with *Pyrenophora tritici-repentis* (Ptr) to (i) evaluate the utility of XFM for spatially mapping the essential mineral nutrients in wheat leaves at sub-micron level, and (ii) examine the spatiotemporal impact of a necrotrophic fungus on nutrient re-distribution in wheat leaves. The XFM maps of K, Ca, Fe, Cu, Mn, and Zn revealed substantial hyperaccumulation and depletion within and around the infected region relative to uninfected control leaf tissue. We were able to visualise fungal mycelia as threadlike structures in the Cu and Zn maps. The hyperaccumulation of Mn in the lesion and localised depletion in asymptomatic tissue surrounding the lesion was particularly striking. Interestingly, Ca accumulated within and closer to the periphery of symptomatic region, often observed as micro-accumulations aligning with fungal mycelia. These disruptions may reflect secondary strategies used by the fungus to induce cell death, localised defence mechanisms used by the plant or wound responses. Collectively, our results highlight that synchrotron-based XFM imaging provides capability for high resolution mapping of elements for probing nutrient distribution in hydrated diseased leaves in situ.

Towards Personalized Microbeam Radiation Therapy for Brain Cancer Treatment

Author(s): Elette Engels¹

Co-author(s): Nan Li ² ; Jeremy Davis ¹ ; Jason Paino ³ ; Matthew Cameron ⁴ ; Andrew Dipuglia ¹ ; Sarah Vogel ¹ ; Michael Valceski ¹ ; Abass Khochaiche ; Alice O'Keefe ¹ ; Micah Barnes ⁵ ; Ashley Cullen ⁶ ; Andrew Stevenson ⁷ ; Anatoly Rosenfeld ¹ ; Michael Lerch ¹ ; Stephanie Corde ⁸ ; Moeava Tehei ²

1 University of Wollongong

2 University of Wollongong, Centre for Medical Radiation Physics, Wollongong, Australia

3 UOW

4 CMRP University of Wollongong

5 Royal Melbourne Institute of Technology, Applied Physics, Melbourne, Australia

6 Centre for Medical Radiation Physics

7 Australian Synchrotron/ CSIRO

8 Prince of Wales Hospital, Radiation Oncology Department, Randwick, Australia

Corresponding Author(s): ashley.cullen@health.nsw.gov.au, nli@uow.edu.au, ad150@uowmail.edu.au, mierch@uow.edu.au, andrew.stevenson@synchrotron.org.au, moeava@uow.edu.au, micah.barnes@student.rmit.edu.au, anatoly@uow.edu.au, jeremyd@uow.edu.au, jrp933@uowmail.edu.au, ellette@uow.edu.au, mc815@uowmail.edu.au, stephanie.cordetehei@health.nsw.gov.au, ak049@uowmail.edu.au

Brain cancer is a detrimental disease with poor long term prognosis. The most common type of brain cancer, glioblastoma, has an associated 5 year survival of only 5% in Australia [1]. New treatments are therefore highly sought after to overcome the glioblastoma resistance to radiation and chemotherapy. Microbeam Radiation Therapy (MRT) at the Imaging and Medical Beam Line (IMBL) of the Australian Synchrotron implements ultra-fast radiosurgical cancer treatment with 50 μm microbeams spaced 400 μm apart [2].

This study reports the brain cancer treatment efficacy of individualized MRT at the IMBL delivered in a single fraction with results from the first long-term MRT pre-clinical trial in Australia. The personalized treatment approach used state of the art dosimetry, new image alignment systems, cell studies and preclinical treatments performed at the IMBL. A 9L gliosarcoma brain cancer model was investigated in vitro with MRT and synchrotron broad beam to understand the cell response to the ultra-fast X-ray treatment. Following this, juvenile (8-week old) male Fischer rats were injected with intracerebral 9L gliosarcoma cells. Twelve days later, the rats received MRT following individualized image alignment based on individual tumours imaged on day 11 performed at Monash Biomedical Imaging. Treatment efficacy was evaluated in terms of in vitro cell survival, long term preclinical survival, histological brain and tumour morphology, and a pioneering assessment of the individual MRT tumour dose-coverage (Figure 1).

The results of our study reveal the relationships between the in vitro cell response, tumour dose- volume coverage and survival post MRT irradiation of a radioresistant brain cancer in a rodent model. The synchrotron radiation therapy (both MRT and broad beam) showed improvements over the conventional (low dose rate) treatment of 9L cells, providing evidence for an in vitro dose rate dependence and FLASH effect. Preclinical studies showed that MRT increased the mean lifespan of rats by 570% compared to unirradiated controls. Individuals responded to MRT based on their tumour dose coverage with depth and tumour size (Figure 1).

This innovative and interdisciplinary approach provides an in-depth understanding of brain cancer treatment using MRT at the Australian Synchrotron. The developments made in this work are the first steps towards personalized clinical strategies using MRT. The extension of this work to larger animals is required, but may ultimately improve the outcome for young patients with brain cancer.

We acknowledge time and access to the Illawarra Health and Medical Research Institute (IHMRI), Wollongong, Australia, the Australian Synchrotron, and Monash Biomedical Imaging, Melbourne, Australia, the Australian Nuclear Science and Technology Organisation (ANSTO), and the University of Wollongong (UOW) Animal House. We are grateful to all assisting personnel including IMBL staff, Beamline Veterinary Scientist Mitzi Klein, UOW animal research staff, and UOW Animal Welfare Officer Dr Sarah Toole. We acknowledge the support of the Monash, Australian Synchrotron and UOW Animal Ethics Committees. We acknowledge the financial support of the Australian Government Research Training Program Scholarship, and Australian National Health & Medical Research Council (APP1084994 and APP1093256).

References

Australian Institute of Health and Welfare 2017. Brain and other central nervous system cancers. Cat. no. CAN 106. Canberra: AIHW.

Engels, E., Li, N., Davis, J. et al. Toward personalized synchrotron microbeam radiation therapy. *Sci Rep* 10, 8833 (2020).

Trace element distributions in Al-Zn based coating alloys on steel substrates investigated by synchrotron XFM

Dongdong Qu¹ ; Matthew Gear² ; Nega Setargew³ ; Wayne Renshaw³ ; Stuart McDonald¹ ; David StJohn¹ ; David Paterson⁴ ; Kazuhiro Nogita¹

1 The University of Queensland

2 University of Queensland

3 Product Innovation and Technology, Bluescope Ltd

4 The Australian Synchrotron, Clayton, Victoria 3168, Australia

Corresponding Author(s): k.nogita@uq.edu.au, s.mcdonald1@uq.edu.au, waynewawa.renshaw@bluescopesteel.com, d.stjohn@uq.edu.au, nega.setargew@bluescopesteel.com, d.qu1@uq.edu.au, matthew.gear@uqconnect.edu.au

The 55Al-Zn-1.6Si alloy is widely used in hot-dip galvanizing to coat steel and displays a multilayered microstructure (steel substrate/intermetallic compound (IMC) layer/coating overlay) that offers protection from corrosion. Trace level (less than a few tens of ppm) V and Cr are hypothesized to influence the corrosion performance of the coated steel via localized segregation. This work investigates the distribution of trace V and Cr using synchrotron X-ray fluorescence microscopy (XFM) and scanning transmission electron microscopy (STEM), and discusses the mechanism of trace V and Cr distribution during coating formation.

Tracks, Pores, Cylinders and Cones: SAXS as a tool to study high-energy ion modified materials

Patrick Kluth¹

1 Australian National University

Corresponding Author(s): patrick.kluth@anu.edu.au

Heavy ions with MeV to GeV energies (also termed 'swift heavy ions') interact predominately through inelastic interactions with the target electrons when penetrating a material. The resulting intense electronic excitation can produce narrow trails of permanent damage along the ion paths, so called 'ion tracks'. Ion tracks are generally between 5-20 nm in diameter, tens of micrometers long and have been observed in many materials. They have numerous applications across a variety of scientific areas such as materials science and engineering, nanotechnology, geology, archaeology, nuclear physics, and interplanetary science. For example, nanopores in polymer membranes are commercially produced using ion tracks by preferential chemical etching of the damaged material in the tracks. Tracks also naturally occur in minerals such as apatite and are widely used to determine the age and thermal history of geological sites.

Small angle x-ray scattering (SAXS) provides a powerful tool for characterizing both ion tracks and track etched nano-pores and enables in situ measurements in high-temperature, high-pressure and corrosive environments. Over the last decade we have developed a number of SAXS experiments and analytical methods to characterize ion tracks and track etched nano-pores with unprecedented precision. The presentation will give an overview over some of the developments including in situ nanopore etching in polymers, temperature induced track recovery in minerals under high-pressure and the temperature dependent elastic response of cylindrical tracks in silica.

Trindex: A complimentary grain mapping technique using neutron imaging

Author(s): Patrick Tung¹

Co-author(s): Stavros Samothrakitis ² ; Camilla Larsen ² ; Nancy Elewa ² ; Ryoji Kiyonagi ³ ; Takenao Shinohara ⁴ ; Robin Woracek ⁵ ; Luise Theil Kuhn ⁶ ; Markus Strobl ⁷ ; Petr Sittner ⁸ ; Soren Schmidt ⁵

1 UNSW

2 Nuclear Physics Institute

3 Japan Accelerator Proton Research Complex 4 Japan Proton Accelerator Research Complex 5 European Spallation Source

6 Danish Technical University

7 Paul Scherrer Institute

8 Institute of Physics

Corresponding Author(s): patrick.tung@unsw.edu.au

The mechanical and functional properties of polycrystalline materials have significant contributions from the 3D interaction of grains that form their micro-structure. Such grain maps can be extracted from existing characterisation techniques that utilise synchrotron radiation. However, complimentary techniques using neutrons have not yet developed to maturity. Furthermore, neutrons provide different capabilities where, due to the lower attenuation, larger materials can be analysed, such as real-world engineering materials.

Here, a novel 3D grain mapping methodology, known as Trindex, has been demonstrated to re-veal the micro-structure of a prototypical cylindrical iron material. While there already exist several methods on grain mapping with neutron imaging [1,2], Trindex provides a robust and relatively straightforward approach. Trindex is a pixel-by-pixel neutron time-of-flight reconstruction method which extracts the morphology of grains throughout the sample, in addition to their pseudo-orientations.

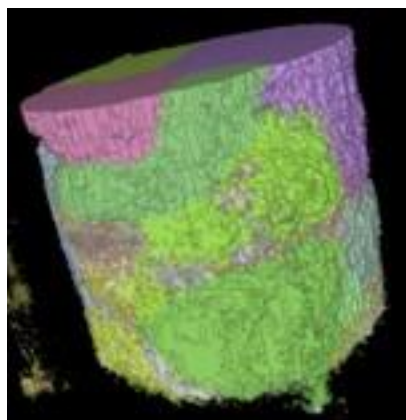


[Figure 1: 3D reconstruction of grain map from a prototypical Fe sample. Colours represent different grain orientations. Sample height of approx. 4 mm.](#)

Experiments were performed at the SENJU diffractometer beamline of the Japan Proton Acceleration Research Complex (J-PARC). For the setup, an imaging detector was installed behind the sample with diffraction detectors simultaneously collecting the backscattering from the sample. Such diffraction will be used to confirm grain orientations. The method will add to the suite of microstructural analysis techniques available at large-scale synchrotron and neutron facilities. Details of the methodology and the resulting 3D grain maps of materials will be presented.

Cereser, A., et al. "Time-of-flight three dimensional neutron diffraction in transmission mode for mapping crystal grain structures." *Scientific reports* 7.1 (2017): 1-11.

Peetermans, S., et al. "Cold neutron diffraction contrast tomography of polycrystalline material." *Analyst* 139.22 (2014): 5765-5771.

Using Synchrotron Radiation to Map the Metallo-maze to Memory Loss

Mark J. Hackett¹

1 School of Molecular and Life Sciences, Curtin University

Corresponding Author(s): markjhackett.curtin@gmail.com

Transition metals such as Fe, Cu, Zn are essential for brain function, because they enable energy production, metabolism, and neurotransmitter synthesis. Disturbed brain metal homeostasis has been observed in the ageing and degenerating brain (e.g., Alzheimer's disease). Elevated levels of Fe, Cu, Zn are frequently observed in to spatially associate with markers of brain pathology (e.g. elevated metal content within amyloid plaques). Due to the redox active nature of Fe and Cu (e.g., classic Fenton Chemistry pathways) there is much interest in the role metal ion catalyzed free radical production and oxidative stress may hold in driving cognitive decline.

There is extensive literature studying possible roles for Fe and Cu overload during natural ageing and neurodegeneration; yet in our studies at the XFM beamline of the Australian Synchrotron we have not observed any direct increase in Fe or Cu concentration within hippocampal neurons, in rodent models of natural ageing or dementia. Indeed, under certain conditions we have observed apparent decreases in neuronal metal ion concentration during ageing or neurodegeneration. This finding has led our research group to investigate differences in the sensitivity and specificity of direct elemental mapping techniques compared to histochemical methods to detect metal ions in brain tissue (e.g., Perl's Fe stain). We have also examined at length, how multiple aspects of sample preparation may affect the metal ion concentration, distribution, and chemical form in brain tissue.

Our findings appear to indicate that there are unique differences in the handling of metal ions by different brain cells. Specifically, brain cells of glial lineage (oligodendrocytes, macrophages, astrocytes) appear to be capable of accumulating Fe and Cu metal ions, while concomitantly neurons may become metal ion deficient. On the basis of our results, we suggest that neuronal metal ion deficiency may occur in the ageing and degenerating brain, possibly as a result of excessive metal ion accumulation in glia. If this is correct, metal ion deficiency would result in impaired energy metabolism and reduced neurotransmitter synthesis, which could be a potent driver of cognitive decline and memory loss. Our results suggest that future studies are needed to specifically investigate the mechanisms through which neuronal metal ion deficiency can occur, which may identify new opportunities for therapeutic intervention.

Understanding disorder in the $\text{Y}_2\text{Sn}_{2-x}\text{Zr}_x\text{O}_7$ pyrochlore oxides

Chris Ling¹; Brendan Kennedy²; Zhaoming Zhang³; Frederick Marlton¹

1 University of Sydney

2 The University of Sydney

3 ANSTO

Corresponding Author(s): chris.ling@sydney.edu.au, zhaoming.zhang@ansto.gov.au, frederick.marlton@sydney.edu.au, brendan.kennedy@sydney.edu.au

Solid oxide fuel cells (SOFCs) offer clean alternatives to current carbon emitting energy sources; however, reducing their operation temperature is a major challenge for widespread application. Hence, the development of novel electrolyte materials with high room temperature ionic conductivity is crucial. Pyrochlore oxides, of the general chemical formula $\text{A}_2\text{B}_2\text{O}_7$, exhibit chemical and structural flexibility, resulting in a diverse range of physical properties and technological applications, such as host matrices in the immobilization of actinide-rich nuclear wastes. In particular, they have gained interest as fast-ion conductors for electrolytes in SOFCs.

The pyrochlore structure is highly ordered, which limits long-range oxygen diffusion. This can be altered via disordering, which results in the formation of oxygen Frenkel pairs that improve conductivity. The pyrochlore structure can adopt the disordered-fluorite structure via changes in composition, temperature, pressure and radiation. The disordered-fluorite exhibits lower formation energy of the Frenkel defect; however, this increase in structural disorder can increase the activation energies needed for long-range migration, which results in optimal conductivity occurring in partially disordered materials. Hence, the interplay between disorder and order in the atomic structure is key to the physical properties of these materials.

There have been many studies dedicated to understanding the structural order and disorder in pyrochlore and disordered-fluorite oxides, with a recent study claiming the local structure of the disordered-fluorite to be weberite. It was proposed that the overall structure of a disordered-fluorite consists of randomly arranged orthorhombic weberite domains that result in the long-range cubic disordered-fluorite.

In this study we use low temperature (15 K) neutron pair distribution function (PDF) and big box modelling to understand the local-scale structure of the $\text{Y}_2\text{Sn}_{2-x}\text{Zr}_x\text{O}_7$ system. We show that the local structure of the $\text{Y}_2\text{Zr}_2\text{O}_7$ disordered fluorite does not contain ordered weberite domains, which emphasizes the importance of low temperature measurements in the local structure analysis of disordered oxide materials.

Our analysis of the $\text{Y}_2\text{Sn}_{2-x}\text{Zr}_x\text{O}_7$ series serves as a direct method for quantifying disorder and Frenkel defects. Understanding and quantifying these atomic-scale distortions is essential in simulations and design as it directly influences the energy landscape for anion mobility. These techniques can be used in the development and engineering of novel and advanced electrolyte materials for SOFCs.

Understanding the Mechanisms Bending in Flexible Crystals

Jack Clegg¹

¹ The University of Queensland

Corresponding Author(s): j.clegg@uq.edu.au

Amy J. Thompson, ^a Anna Worthy, ^b Arnaud Grosjean^a Jason R. Price,^c John C. McMurtrie, ^b and Jack K. Clegg^{*a}

^a School of Chemistry and Molecular Biosciences, The University of Queensland, Brisbane St Lucia, QLD, Australia, 4072

^b School of Chemistry, Physics and Mechanical Engineering, Queensland University of Technology, Brisbane 4001, Australia

^c ANSTO Melbourne, The Australian Synchrotron, 800 Blackburn Rd, Clayton, Vic 3168, Australia.

E-mail: j.clegg@uq.edu.au

A crystal is normally thought of as a homogenous solid formed by a periodically repeating, three- dimensional pattern of atoms, ions, or molecules. Indeed, the regular arrangement of molecules, in a single crystal lead to many useful characteristics (in addition to diffraction!) including unique optical and electrical properties, however, molecular crystals are not typically mechanically robust, particularly compared to crystals of network solids like diamond. Upon the application of stress or strain, these crystals generally irreversibly deform, crack or break resulting in the loss of single crystallinity.

We have recently discovered a class of crystalline compounds that display the intriguing property of elastic flexibility – that is they are capable of reversibly bending without deforming, cracking or losing crystallinity. A number of these crystals are flexible enough to be tied into a knot! (See Figure 1). We have developed a unique approach to determine the atomic-scale mechanism that allows the bending to occur which employs mapping changes in crystal structure using micro-focused synchrotron radiation. We have applied this technique to understand the deformation in both elastically¹ and plastically² flexible crystals. Most recently we have used it to show that previous theories regarding the requirement of “interlocked” crystal packing for flexibility is incorrect.

Figure 1: A crystal of [Cu(acac)₂] showing elastic flexibility.

A. Worthy, A. Grosjean, M. Pfrunder, Y. Xu, C. Yan, G. Edwards, J. K. Clegg and J. C. McMurtrie, “Atomic Resolution of Structural Changes in Elastic Crystals of Copper(II) acetylacetonate”, *Nature Chemistry*, 2018, 65-69.

S. Bhandary, A. J. Thompson, J. C. McMurtrie, J. K. Clegg, P. Ghosh, S. R. N. K. Mangalampalli,

S. Takamizawa, and D. Chopra, “The mechanism of bending in a plastically flexible crystal.” *Chem. Commun.*, 2020, 12841-12844.

Unexpected Structural Properties in 4d and 5d Metal Oxides

Bryce Mullens¹ ; Brendan Kennedy² ; Helen Brand³ ; Maxim Avdeev⁴ ; Garapathy Vaitheeswaran⁵

1 University of Sydney

2 The University of Sydney

3 Australian Synchrotron

4 ANSTO

5 University of Hyderabad

Corresponding Author(s): helen.brand@synchrotron.org.au, brendan.kennedy@sydney.edu.au, bmul2806@uni.sydney.edu.au

Carbon-neutral energy-generation is being developed in Australia in order to combat climate change. One such technology is the development of next-generation ion conductors for solid-oxide fuel cells. However, a bottleneck to the large-scale uptake of solid-oxide fuel cells is the poor performance of the proton-conducting electrolytes that separate the anode from the cathode. Various lanthanoid Fergusonite structures (LnBO₄) have recently been proposed as potential solid electrolytes in solid- oxide fuel cells, with high-temperature proton conductivity being measured in chemically doped lanthanum orthoniobates (LaNbO₄) [1](#).

In order to understand the effects of chemical doping on the structure and electrochemical properties of these Fergusonite structures, substitutions into the LnBO₄ Fergusonites have been investigated [2-3]. Of interest is the substitution of Nb for Ta on the B-site, which has shown a decrease in the unit cell volume of the structure [4]. This is particularly remarkable, given the two metal cations have the same ionic radius and Ta has an extra 5d valence shell compared to the 4d shell of Nb.

Two solid-solution series – Sm(Nb_{1-x}Ta_x)O₄ and Ho(Nb_{1-x}Ta_x)O₄ with $x = 0.0 - 1.0$ – have been synthesised using conventional solid-state methods. Both synchrotron X-ray diffraction and neutron powder diffraction have been used to investigate their structures in order to determine the role of the B–O bonds on both the unit cell volume and the observed first-order phase transitions. The experimental data has been further reinforced by ground state energy calculations performed using density functional theory.

These results will be presented, along with a judgement as to whether inducing chemical doping into the LnBO₄ Fergusonite structures may lead to them being viable candidates for solid electrolytes in solid-oxide fuel cells.

[1](#) - Cao, Y.; Duan, N.; Yan, D.; Chi, B.; Pu, J.; Jian, L.; Enhanced Electrical Conductivity of LaNbO₄ by A-Site Substitution. Int. J. Hydrogen Energy, 2016, 41 (45), 20633-20639.

- Arulnesan, S. W.; Kayser, P.; Kimpton, J. A.; Kennedy, B. J.; Studies of the Fergusonite to Scheelite Phase Transition in LnNbO_4 Orthoniobates. *J. Solid State Chem.*, 2019, 277, 229-239.
- Ivanova, M.; Ricote, S.; Meulenberg, W. A.; Haugsrud, R.; Ziegner, M.; Effects of A- and B-Site (Co-)Acceptor Doping on the Structure and Proton Conductivity of LaNbO_4 . *Solid State Ionics*, 2012, 213, 45-52.
- Mullens, B. G.; Avdeev, M.; Brand, H. E. A.; Vaitheeswaran, G.; Kennedy, B. J.; Solid Solubility in $\text{SmNb}_{1-x}\text{Ta}_x\text{O}_4$ and $\text{HoNb}_{1-x}\text{Ta}_x\text{O}_4$. In preparation.

Using Synchrotron Sourced Microscopy to Explore Fingerprint Chemistry

Author(s): Rhiannon Boseley¹

Co-author(s): Buddhika N. Dorakumbura²; Daryl Howard³; Jitraporn (Pimm) Vongsivut³; Mark J. Hackett²; Mark J. Tobin³; Martin de Jonge⁴; Simon Lewis²; Wilhelm van Bronswijk²

1 Curtin University

2 School of Molecular and Life Sciences, Curtin University

3 Australian Synchrotron

4 Australian Nuclear Science and Technology Organisation, 800 Blackburn Road, Clayton, VIC 3168, Australia

Corresponding Author(s): rhiannon.boseley@student.curtin.edu.au, darylh@ansto.gov.au, jitrapov@ansto.gov.au, tobinm@ansto.gov.au, martind@ansto.gov.au, markjhackett.curtin@gmail.com

The successful detection of latent fingerprints is crucial to forensic investigations, however detection methods can be hindered by variation in response or lack of robustness. Despite ongoing research into fingerprint development, many remain undetected(1). A fundamental understanding of fingerprint chemistry can provide explanations for the effectiveness or lack thereof for current detection methods and drive development of improved techniques.

We have combined synchrotron sourced Fourier Transform Infrared (FTIR) and X-ray Fluorescence Microscopy (XFM) to reveal the spatial distribution of the molecular and elemental components within latent fingerprints. FTIR showed that fingerprints have a complex heterogeneous distribution of organic material, our research focussing primarily on visualising the lipid and amino acid distribution at the sub-micron scale (2). Recent time-course studies have imaged the rate which freshly deposited fingerprints dry, with the results reinforcing the chemical heterogeneity of latent fingerprints and demonstrate how differences in composition appear to influence drying rates and redistribution of lipid material during drying.

We used XFM to explore the inorganic components within fingerprint residue. The distribution of trace metals including endogenous trace metals (Fe, Cu, Zn), diffusible ions (Cl⁻, K⁺, Ca²⁺), and exogenous metals (Ni, Ti) have been imaged across multiple donors (see Figure 1) (3). Further experiments have explored the effects of the external environment on these metals post deposition, and the transfer of exogenous metals prior to deposition.

With these techniques, we have begun to have a better understanding of the chemical complexity and transfer processes associated with latent fingerprints, thus providing the essential fundamental underpinning for the development of improved detection methods.

B. N. Dorakumbura, R. E. Boseley, T. Becker, D. E. Martin, A. Richter, M. J. Tobin, W. van Bronswijk, J. Vongsvivut, M. J. Hackett and S. W. Lewis, *Analyst*, 2018, 143, 4027-4039.

R. E. Boseley, B. N. Dorakumbura, D. L. Howard, M. D. de Jonge, M. J. Tobin, J. Vongsvivut, T. T. M. Ho, W. van Bronswijk, M. J. Hackett and S. W. Lewis, *Analytical Chemistry*, 2019, 91, 10622-10630.

Using synchrotron XFM, LA-ICP-MS and stable isotopes to identify an intense wildfire event recorded in a speleothem

Liza McDonough¹ ; Pauline Treble¹ ; Andy Baker² ; Gurinder Nagra³ ; Andrea Borsato⁴ ; Silvia Frisia⁴ ; Martin de Jonge¹ ; David Paterson¹ ; Sirine Fakra⁵

1 Australian Nuclear Science and Technology Organisation (ANSTO)

2 School of Biological, Earth and Environmental Sciences, UNSW Sydney

3 School of Earth, Energy and Environmental Sciences, Stanford University

4 School of Environmental and Life Sciences, University of Newcastle

5 Advanced Light Source, Lawrence Berkeley National Laboratory

Corresponding Author(s): davidp@ansto.gov.au, martind@ansto.gov.au, sfakra@lbl.gov, a.baker@unsw.edu.au, silvia.frisia@newcastle.edu.au, andrea.borsato@newcastle.edu.au, ptr@ansto.gov.au, lizam@ansto.gov.au, gnagra@stanford.edu

Wildfires are becoming progressively more extreme in some regions as a result of climate and land use changes. However, little is known as yet about their impacts on karst systems. Cave speleothems (stalagmites, stalactites and flowstones) provide long-term records of changes of the surface environment, and have the potential to capture information relating to environmental impacts from fires. Here, we use X-ray Fluorescence Microscopy (XFM) chemical mapping from ANSTO's Australian Synchrotron and the Lawrence Berkeley National Laboratory's Advanced Light Source, coupled with Laser Ablation Inductively Coupled Plasma Mass Spectrometry (LA-ICP-MS) trace element tracts and stable isotope (^{13}C and ^{18}O) ratios to pinpoint a fire event that occurred during a dry season in the late 1800s recorded in a speleothem from Western Australia. An age-depth model was constructed using annual lamina visible on both thin section and strontium maps (and scans), which allowed us to identify the timing of the fire event and develop time-series data. Principal Component Analysis (PCA) of time-series data was then used to reconstruct long-term changes in surface-cave hydrology and water-rock interactions resulting from the post-fire modifications in the soil zone and aquifer. These results show the potential for speleothems to provide records of fire recurrence intervals, which can be used to better understand the fire-climate relationship.

Using synchrotron infrared micro-spectroscopy to monitor the electrochemical processes of non-flammable electrolytes on the electrode surface

SAILIN LIU¹ ; Wei Kong Pang¹ ; Jitraporn Pimm Vongsvivut² ; Zaiping Guo¹

1 University of Wollongong

2 Australian Synchrotron

Corresponding Author(s): sl329@uowmail.edu.au

In all battery systems, electrolyte plays a vital role in determining the stability of the electrodes, as well as the safety of the battery uses. Due to the frequently reported thermal runaway accidents in batteries [1, 2], the key criteria for selecting the electrode materials for industrial production purposes must focus not only on providing high energy density but also on their long term stability and safety of the consumers.

In most batteries, solid electrolyte interface (SEI), which is formed by the decomposition of the electrolyte during charging/discharging cycles, is a critical factor that influences both the stability of the electrode and the performance of the battery [3]. A good SEI protective layer should be formed at the 1st cycling process of the battery, rather than continually accumulating on the electrode surface, and is not dissoluble in electrolytes, making its properties highly dependent on the chemical structure [4]. Therefore further development of safe battery technology strongly requires a better understanding of the chemistry and formation mechanism of the SEI, which still remains largely unknown due to their complex structure and a lack of reliable in situ experimental techniques. Accordingly, our aim is to implement an analytical approach based on S-FTIR micro-spectroscopy for in situ monitoring of the SEI formation during the cycling process. Changes in functional groups and their chemical distribution on the electrode surface observed through the S-FTIR spectra will be used to identify the formation mechanisms in different combinations of electrolyte ingredients.

¹E. P. Roth, C. J. Orendorff, *The Electrochemical Society Interface* 2012, 21, 45.

X. Feng, M. Ouyang, X. Liu, L. Lu, Y. Xia, X. He, *Energy Storage Materials* 2018, 10, 246.

E. Peled, S. Menkin, *J. Electrochem. Soc.* 2017, 164, A1703.

A. Wang, S. Kadam, H. Li, S. Shi, Y. Qi, *npj Computational Materials* 2018, 4, 15.

Using the Imaging and Medical Beamline (IMBL) as a novel method to investigate structures and processes of lead-acid batteries

Chad Stone¹ ; Peter Mahon¹ ; Rosalie Hocking¹ ; Tony Hollenkamp² ; Russell Newnham³ ; Chris Hall⁴

1 Swinburne University of Technology

2 CSIRO

3 Electric Applications Inc.

4 Australian Synchrotron

Corresponding Author(s): tony.hollenkamp@csiro.au, chris.hall@synchrotron.org.au, rhocking@swin.edu.au, rnewnham@electric-applications.com, cstone@swin.edu.au, pmahon@swin.edu.au

Despite its age, the lead-acid battery is one of the most widely used electrochemical energy storage devices in the world. It is used in uninterruptible power supplies, small vehicles such as forklifts and submarines. The benefits of using lead-acid batteries are its low cost and very high recyclability relative to other battery chemistries. In recent years, hybrid electric vehicles have grown in popularity as consumers seek to reduce fuel consumption and greenhouse gas emissions. Research into the suitability of lead-acid batteries for operation in Micro-HEVs has shown that the batteries suffer from premature capacity loss leading to early failure. Breakdown analysis shows that premature capacity loss is related to the formation of a layer of lead sulfate on the surface of the negative electrode, which cannot be recharged easily. Investigators have also shown that small amounts of conductive carbon added to the negative electrode has a highly beneficial effect. However, the cause for the accumulation of lead sulfate and how carbon is able to alleviate this has yet to be found. It is suspected that the cause is related to the morphology of the negative electrode, but analytical tools used so far have not been able to confirm this. Often the tools used cannot observe the negative electrode in-situ whilst it is operating and/or it cannot achieve the required resolution.

This project aimed to determine the suitability of the IMBL to analyse the structure and processes of the lead-acid battery. A 3D model was constructed of electrodes from a failed Yuasa model NP 1.2-6 absorptive glass matt battery from a CT scan at the IMBL. Structures associated with ageing could be identified such as dendrites and positive active material shedding.

Another small lead-acid cell was constructed on-site to observe cycling processing in-situ. Whilst the small cell was charging, hydrogen gas bubbles were observed to generate from the surface of the negative electrode.

The IMBL was found to be a potentially very powerful tool to observe the lead-acid battery, capable of generating new knowledge and improve the current understanding of the lead-acid battery. Future projects may be able to utilize the IMBL to find the cause of the accumulation of lead sulfate and determine why carbon delays this process.

Using the Pair Angle Distribution Function for Analysing Protein Structure

Author(s): Patrick Adams¹

Co-author(s): Jack Binns ¹ ; Tamar Greaves ¹ ; Andrew Martin ¹

¹ RMIT University

Corresponding Author(s): andrew.martin@rmit.edu.au, tamar.greaves@rmit.edu.au, jack.binns@rmit.edu.au, s3826109@student.rm

X-Ray Free Electron Lasers provide a means of conducting crystallography experiments with remarkable time and spatial resolution. These methods can directly recover the electron density of the materials analysed, however, stringent requirements such as crystal size, number density per exposure, and the crystal order can compromise data quality. Membrane proteins, which do not readily crystallise or meet these requirements ¹, are particularly interesting to study as they comprise up to 50% of drug targets [2], but less than 10% of the protein structures in the Protein Data Bank [3]. The Pair Angle Distribution Function (PADF) describes the three and four body correlations of the electron density in a sample, and can be recovered from X-ray angular cross-correlation analysis [4]. Although it does not recover the electron density directly, it still contains significant information about the local three dimensional structure of the material. PADF analysis also has the potential to relax the stringent crystal requirements imposed by current XFEL experiments. We discuss the sensitivity of the PADF to different protein structures [5], and the correlations generated at different length scales; from atomic bonding to tertiary structure. Our aim is to develop PADF analysis to be used complementarily with conventional crystallography analysis, and to use changing angular correlations to measure conformational changes in proteins.

¹Johansson, L.C. et al. Lipidic phase membrane protein serial femtosecond crystallography. Nat. Methods 2012, 9, 263–265.

Cournia, Z. et al. Membrane protein structure, function, and dynamics: A perspective from experiments and theory. J. Membr. Biol. 2015, 248, 611–640.

Berman, H.M. et al. The Protein Data Bank. Acta Crystallogr. Sect. D Biol. Crystallogr. 2002, 58, 899–907.

Martin, A.V. Orientational order of liquids and glasses via fluctuation diffraction. IUCrJ 2017, 4, 24–36.

Adams, Patrick, et al. "The Sensitivity of the Pair-Angle Distribution Function to Protein Structure." Crystals 10.9 (2020): 724.

Visualisation of the rapid Cu₆Sn₅ lithium-ion battery anode fabrication process via real-time X-ray imaging

Xin Fu Tan¹ ; Hideyuki Yasuda² ; Stuart McDonald³ ; Kazuhiro Nogita³

1 University of Queensland

2 Kyoto University

3 The University of Queensland

Corresponding Author(s): k.nogita@uq.edu.au, yasuda.hideyuki.6s@kyoto-u.ac.jp, xin.tan@uq.edu.au, s.mcdonald1@uq.edu.au

Under the sponsorship of the Australian Synchrotron International Synchrotron Access Program (ISAP), real-time X-ray imaging was conducted at the SPring-8 synchrotron BL20XU beamline to visualise the rapid formation of Cu₆Sn₅ for lithium-ion battery anode applications. This presentation describes the experimental setup employed at the BL20XU beamline, and shares the results obtained. Lithium-ion batteries have found numerous applications in modern technologies, especially in portable devices, and increasingly in electric vehicles and renewable energy storage applications. Sn-based lithium-ion battery anodes have a higher theoretical storage capacity of 993 mAh g⁻¹ vs. 372 mAh g⁻¹ compared to commercial carbon-based anodes. Their better safety profile due to a lower risk of lithium dendrite formation compared to the carbon-based anodes is also desirable. However, Sn-based anodes suffer from inferior cycling performance due to the enormous stresses during the lithiation and delithiation process. Alloying Sn with Cu can reduce the reaction stresses in the anode, as Cu does not react with Li, and acts as a stress buffer. Cu₆Sn₅ is therefore a promising candidate material to replace carbon-based anodes. Traditionally, anode fabrication is a multi-step process where the active materials are first fabricated, and then mixed with binders and conductive materials, followed by slip casting the resultant slurry on to a current collector and dried. To simplify this fabrication process, a simple method involving direct growth of Cu₆Sn₅ on a Cu current collector is proposed. Yet, the growth rate of Cu₆Sn₅ is limited by the inter-diffusion of Cu and Sn, restricting the potential of this method for large scale production. This study proposes a method to accelerate the growth rate of Cu₆Sn₅ by alloying Ni to the Cu current collector. A maximum growth rate is found when 6 wt% of Ni is present in the Cu current collector, where a growth rate of up to 50x faster compared to the growth rate on a pure Cu current collector is observed. Visualisation of the fabrication process via real-time synchrotron X-ray imaging allowed the kinetics and mechanisms of the rapid Cu₆Sn₅ growth to be characterised.

X-ray absorption spectroscopy studies of mixed metal-antimony oxide water oxidation catalysts: Studies comparing Sb, Mn, Co, and Ru edges

Author(s): Brittany Kerr¹ ; Rosalie Hocking¹

Co-author(s): Manjunath Chatti² ; Bernt Johannessen³ ; Daniel Eldridge¹ ; Alexandr Simonov²

1 Swinburne University of Technology

2 Monash University

3 Australian Synchrotron

Corresponding Author(s): bernt.j@synchrotron.org.au, alexandr.simonov@monash.edu, bvkerr@swin.edu.au, deldridge@swin.edu.au, rhocking@swin.edu.au

Electrochemical water splitting with a proton-exchange membrane electrolyte provides many advantages for the energy-efficient production of high-purity dihydrogen in a sustainable manner, but the current technology relies on high loadings of expensive and scarce iridium at the anodes, which are also often insufficiently stable in operation.

Improvements at low pH have been found in mixed metal oxides based on SbOx materials with Ru, Mn and Co dopants. This study explores the characterisation of these materials by X-ray absorption spectroscopy (XAS) and the effect that structural elements such as disorder, or non-crystallinity, can have on XAS spectra and the interpretation of how a material functions as a catalyst.

XFM analysis of marsupial teeth - insights into life, growth and reproduction

William Parker¹ ; Justin Adams² ; Alistair Evans³

1 School Of Biological Sciences, Monash University, Melbourne, Victoria, Australia

2 Department of Anatomy and Developmental Biology, Monash University

3 Monash University

Corresponding Author(s): justin.adams@monash.edu, arevans@fastmail.fm, william.parker@monash.edu

Mammal species vary in how much time and energy they invest in growth, reproduction and development throughout their lifetime, summarised collectively as their 'life history'. Knowledge of such differences among species helps us understand how they trade off these factors of their life history, yet, due to variability between populations, the logistical challenge of multi-year observational studies and extinction these data can be very difficult or impossible to collect. Elemental indicators of life history, environment and diet are mineralised into an animal's hard tissues as they develop incrementally. Our research, using the X-Ray Fluorescence Microscopy (XFM) beamline of the Australian Synchrotron, focuses on unlocking biological information from the teeth of Australian marsupials. We have analysed the sectioned teeth of a range of living (e.g. *Macropus giganteus*, *Notamacropus eugenii* & *Vombatus ursinus*) and extinct (e.g. *Macropus giganteus titan* & *Diprotodon optatum*) marsupials. Our novel results indicate that strontium is a particularly powerful indicator of life history in marsupials. A gradual rise in strontium concentration tracks the progression of weaning, with subsequent oscillations following a likely seasonal dietary signal. Furthermore, calcium reflects the varying degree of mineralisation of tooth enamel and dentine, while zinc is preferentially deposited in the outer enamel layers. These results, applicable to both living and extinct marsupials, indicate that trace element mapping can provide unique insights into the life history of Australia's living marsupials and extinct marsupial megafauna.

Presentation 19 / 169

Session 12 - Earth, Atmosphere and Environment / 191

“Wax On – Wax Off” Using Infrared Reflectance for minimally invasive in vivo monitoring of changes in leaf epicuticular waxes

Author(s): Karina Khambatta¹

Co-author(s): Mark J. Hackett² ; Fatima Naim³

1 School of Molecular and Life Sciences, Curtin University, Bentley, Western Australia 6102, Australia

2 School of Molecular and Life Sciences, Curtin University

3 Curtin University

Corresponding Author(s): fatima.naim@curtin.edu.au, markjhackett.curtin@gmail.com

With increasing global populations and rising temperatures associated with climate change it is important to monitor and mitigate the effects of environmental stress on both native flora and agri- cultural crops. Epicuticular waxes on the surface of plant leaves play essential roles in sustaining plant health. Such roles include; minimising water loss, protection against UV and diseases, as well as acting as an antifeedent. Studying the composition and distribution of epicuticular waxes on the surface of plant leaves can therefore, provide a valuable window-of-insight into plant fitness and the presence of environmental stressors.

Current methods to study plant waxes require extraction of the wax from the leaf surface. This approach reveals substantial insight into chemical composition of plant waxes but, destroys valuable information relating to the spatial distribution of waxes on the leaf surface. Few methods exist that are capable of imaging the wax distribution in situ across anatomical components of the leaf surface, and a gap exists for non-destructive macro-scale imaging in vivo. In this presentation I will describe the development of FTIR micro-spectroscopy to non-destructively image in vivo wax distribution across the leaf surface of native flora and an important agriculture crop (wheat). The method is underpinned by apparent strong specular reflection that comes from the thin, highly ordered wax layers on leaf surfaces. To the best of our knowledge, this is the first report of in vivo monitoring of changes in leaf epicuticular waxes in response to environmental stressors. This new analytical capability could now enable in vivo studies of plants to provide insights into physiological responses of plants to environmental stresses such as disease, soil contamination, drought, soil acidity and/or climate change

Evaluation of bone microstructure of distal radius and distal tibia on human objects using phase-contrast synchrotron radiation computed tomography